AN INSIGHT INTO THE PARAMETRIC EVALUATION OF: SOIL STRUCTURE INTERACTION ANALYSIS

Dr. Eng. Niyazi Özgür BEZGİN

İSTANBUL
January 2010

TABLE OF CONTENTS

PARAMETRIC ANALYSIS

1.1 Introduction

This chapter summarizes the effect of various parameters that influence the response of SSI system under lateral loads. The FE models will be used to analyze the effect of these parameters on the response quantities (displacement, bending moment, and shear) of the drilled shaft. The quantitative parameters analyzed in this chapter that are related to soil, shaft, interface and loading include the following:

1. Interface friction between the shaft and soil surfaces.
2. Soil Poissons ratio.
3. Soil weight.
4. Soil elastic modulus.
5. Shaft elastic modulus.
6. Shaft diameter.
7. Column height.
8. Lateral load.

The qualitative parameters analyzed include the following

1. Effect of the boundary conditions on the response of the shaft.
2. Assessment of foundation capacity reduction due to interface separations.
3. Effect of soil strength changes due to soil disturbance.

1.2 Effect of Friction at the Soil-Shaft Interface

The friction forces that develop at the soil-shaft interface due to deformations are dependent on the contact pressure and the surface properties. The effect of this shear force is also related to shaft slenderness and boundary conditions at the

bottom of the shaft. To evaluate the response of the shaft under the influence of surface friction, a 6 ft diameter shaft and 20ft column height was selected with varying shaft depths of 30ft, 40ft, 50ft and 100ft. The applied lateral load was 50 kips. There are two types of friction forces: 1) static friction force, which is effective prior to relative movement, and 2) kinetic friction force, which acts after the movement takes place. The kinetic friction is always smaller than static friction. In this analysis, kinetic friction was used. The following kinetic friction coefficients μ_k were used: 0, 0.2, 0.5 and 0.9. Figure 4.1 shows the variation of displacements for various friction coefficients for 100ft, 50ft, 40ft and 30ft shaft depths and figure 1.2 shows the moment and shear variation for 100ft and 50ft deep shafts with varying friction coefficients. Figure 1.3 shows the moment and shear variation for 40ft and 30ft shafts with varying friction coefficients. The variation in displacement for different depth to diameter ratios is shown in figure 1.4. The variation in the maximum moment and shear values versus the depth to diameter ratio of the shaft is presented in figures 1.5 and 1.6.

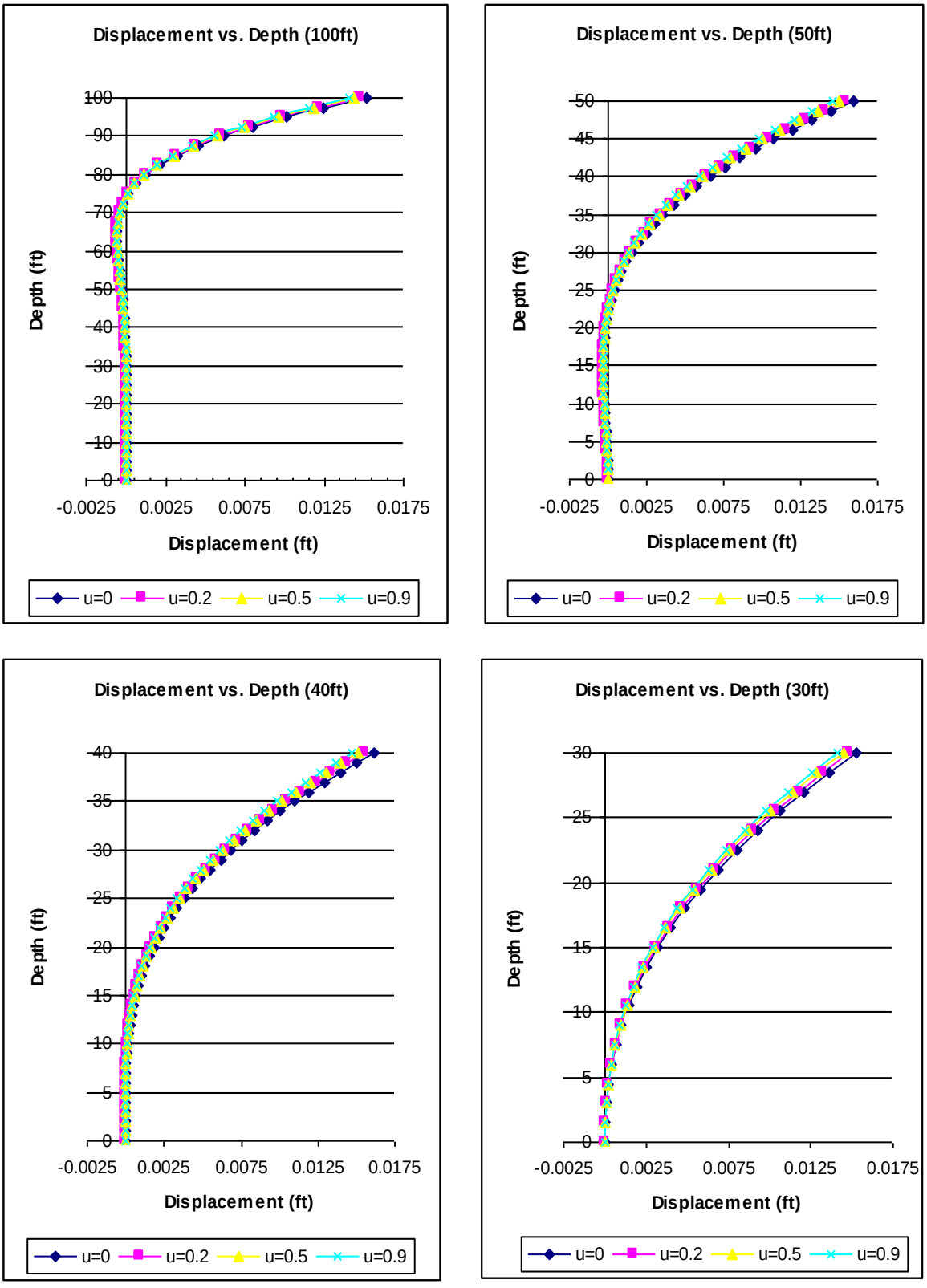

Figure 1.1 – Variation of shaft displacements for 100ft, 50ft, 40ft,and 30ft deep shafts.

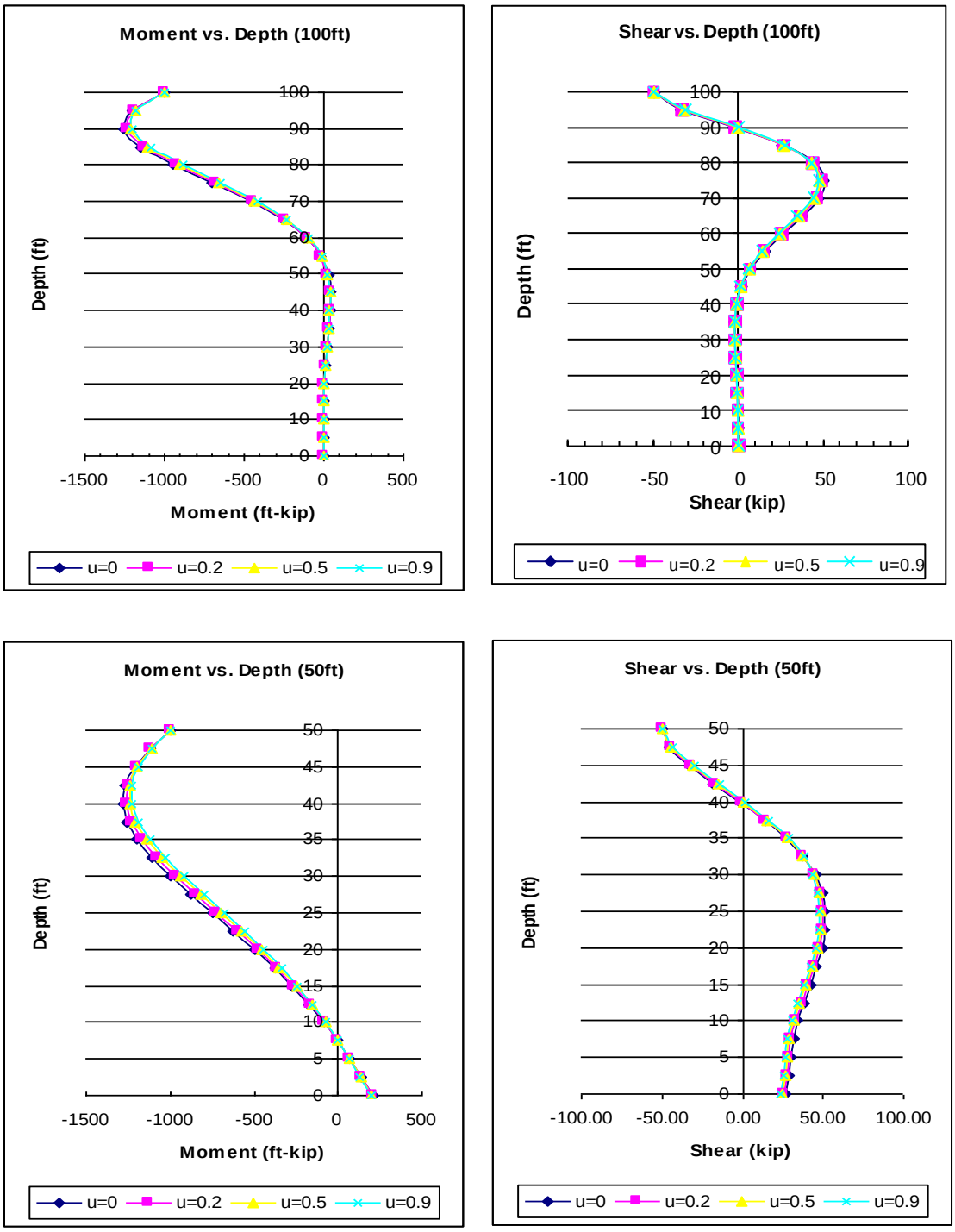

Figure 1.2 – Variation of moment and shear along the shaft depth for 100ft and 50ft shafts.

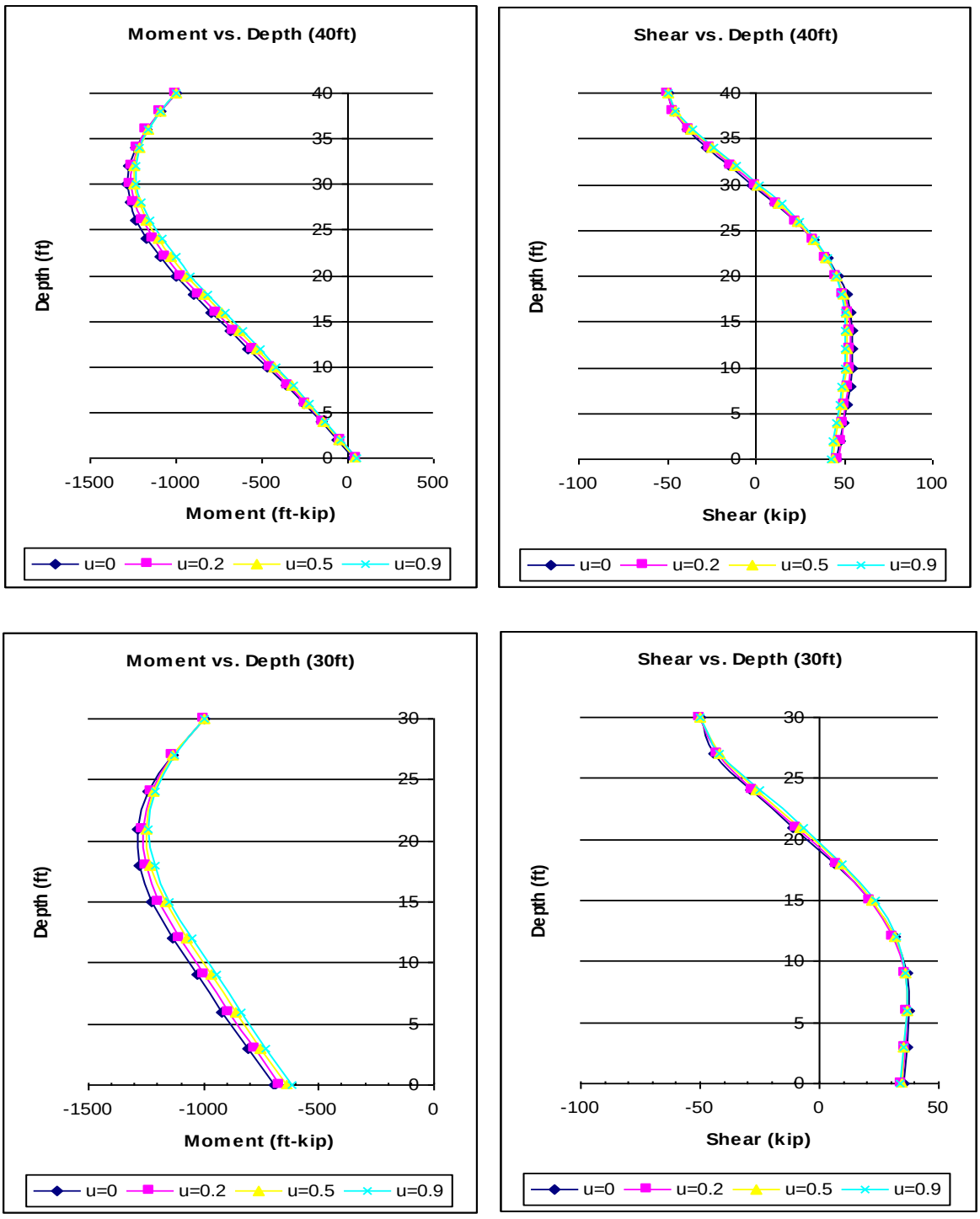

Figure 1.3 – Variation of moment and shear along the shaft depth for 40ft and 30ft shafts.

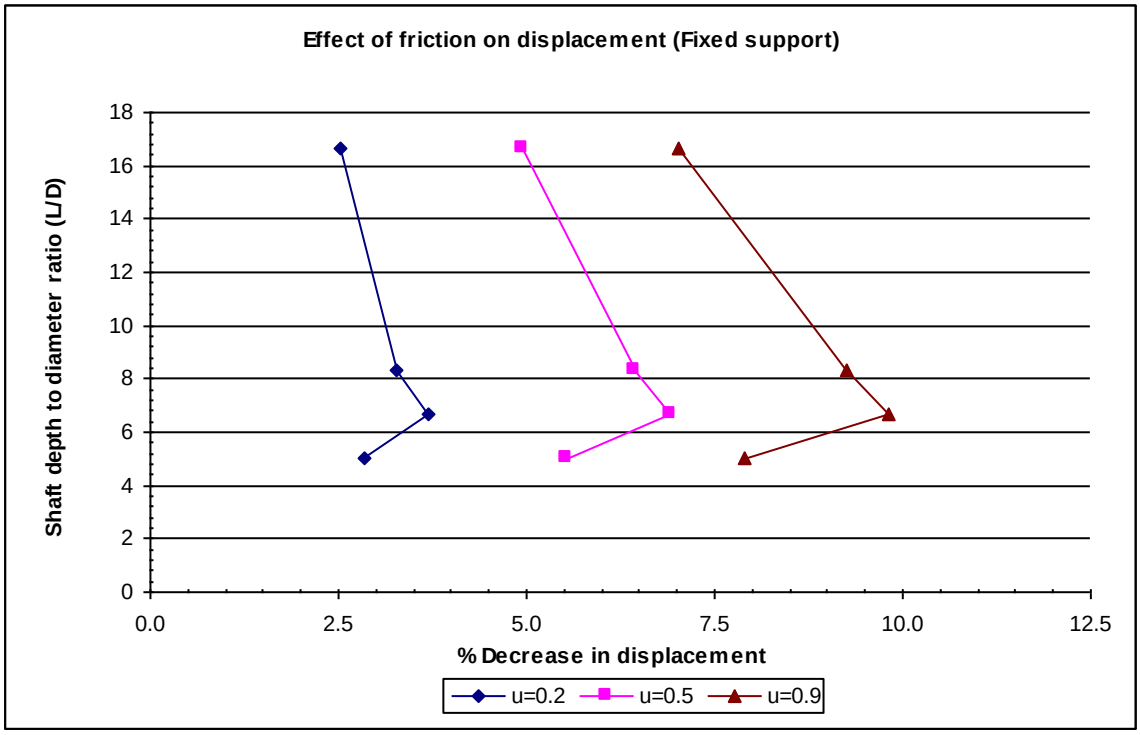

Figure 1.4 – Effect of friction on displacements for shafts, with fixed support.

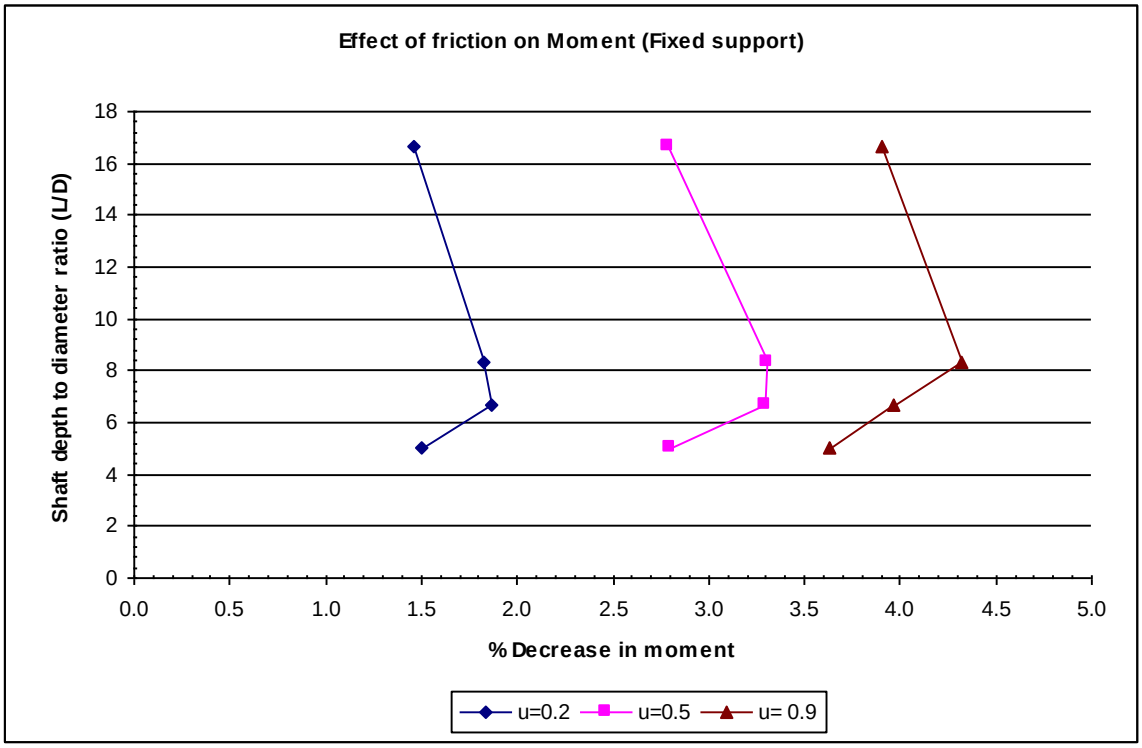

Figure 1.5 – Effect of friction on moment for shafts, with fixed support.

Figure 1.4 and figure 1.5 shows that the displacements and the moments decrease as the friction between the shaft and soil increase. These two figures also show that the effect of friction is less for shafts with higher depth to diameter ratios. Figure 1.6 shows the change in shear for different friction coefficients. Variations in shear are similar to those of displacements and moments shown in figures 1.4 and 1.5.

However, in figures 1.4, 1.5 and 1.6, it seen that below certain shaft depth to diameter ratio (L/D), the increasing trend in the percentage variations tends to decrease. This is the point where the support conditions start to influence the shaft behavior. It will be shown in the following chapters that for slender shafts below a certain depth, the support conditions do not influence the behavior of deep shafts under lateral loading, (i.e. no moment or shear is generated at the support). However, as the flexural stiffness of the shaft increase (smaller shaft depth) and as the soil stiffness decrease (smaller soil depth), the moment at the shaft support becomes significant. When the shaft is socketed into rock, it is valid to assume that the shaft is fixed at the bottom. However, if the shaft is not socketed but merely resting on the rigid surface, or embedded into stiff soil; the only support to the shaft is the normal support provided by the bottom surface and the friction forces between the bottom shaft surface and the rigid surface. The shaft stiffness tends to dominate the overall SSI system stiffness as the depths become shallower for the fixed supported case. The effect of friction, which is related to the relative movement, becomes lower i.e. the displacement of the shaft is more dependent on the shaft stiffness itself rather than the interaction of the shaft with the surrounding.

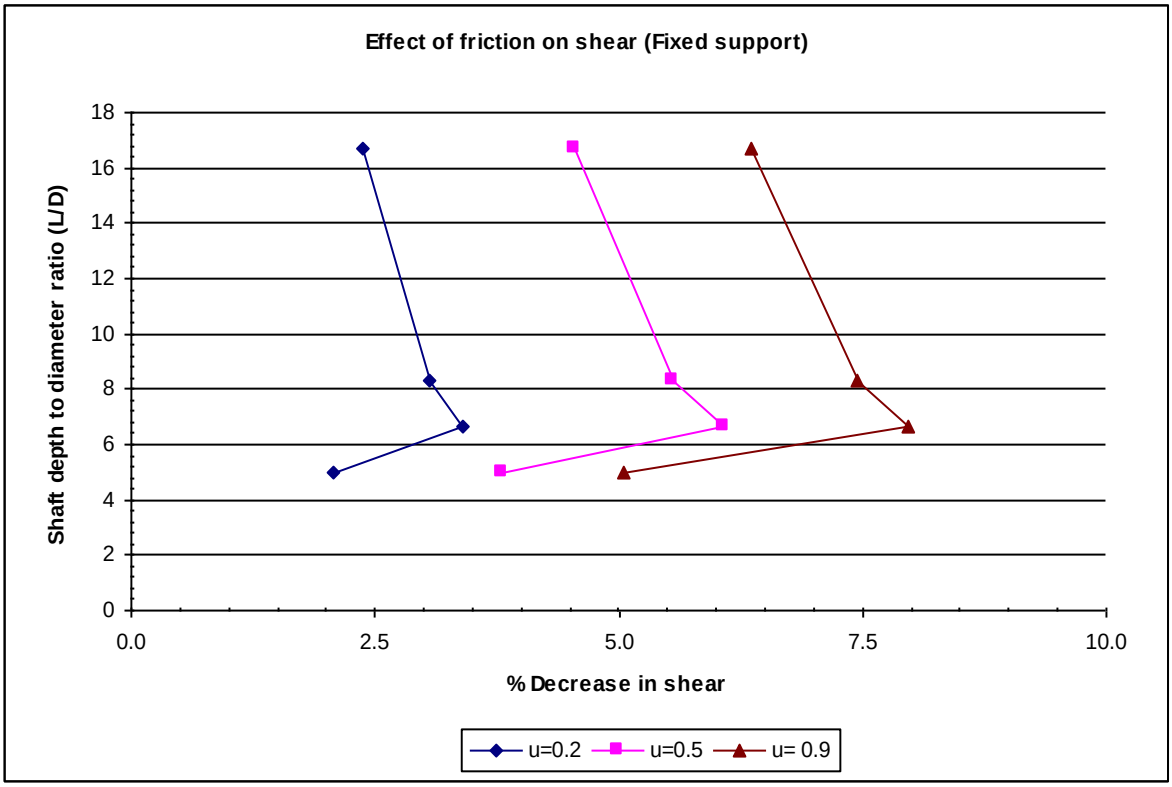

Figure 1.6 – Effect of friction on shear for shafts, with fixed supports.

To investigate the effect of support conditions for variable friction conditions between shaft and soil, lateral load analysis was conducted for shaft depths of 50ft, 40ft and 30ft with soil support instead of fixed support, where the only forces provided by the soil surface are normal forces. The friction between the shaft bottom surface and the bottom soil surface was not included in order to isolate its effect. Individual displacement, moment and shear diagrams will not be presented. Instead, the plots will show the effect of the friction on shaft response versus depth to diameter ratios of the shafts.

Figures 1.7, 1.8, and 1.9 are similar to figure 1.4, 1.5, and 1.6 except for shaft support conditions at the bottom. Note in these figures the difference in the response below slenderness ratios of 8. Figure 1.7 shows the variation in displacements. The percentage increase in the displacement becomes larger as the depth to diameter ratio of the shaft becomes smaller. This is because the shaft

is not fixed and the soil resistance is low (due to lower depth). The shaft movements as well as the ratio of the displaced depth of the shaft to the overall depth are higher. Both these factors increase the effect of friction forces on the reduction of displacement for lower slenderness ratios.

The variation of moment and shear along the shaft with the shaft slenderness values are shown in figures 1.8 and 1.9. The lack of fixed support reduces the stiffness and increases the mobility of the shaft. Unlike the fixed support case, the variation of moment and shear with decreasing shaft depth increases due to higher mobility of the shaft.

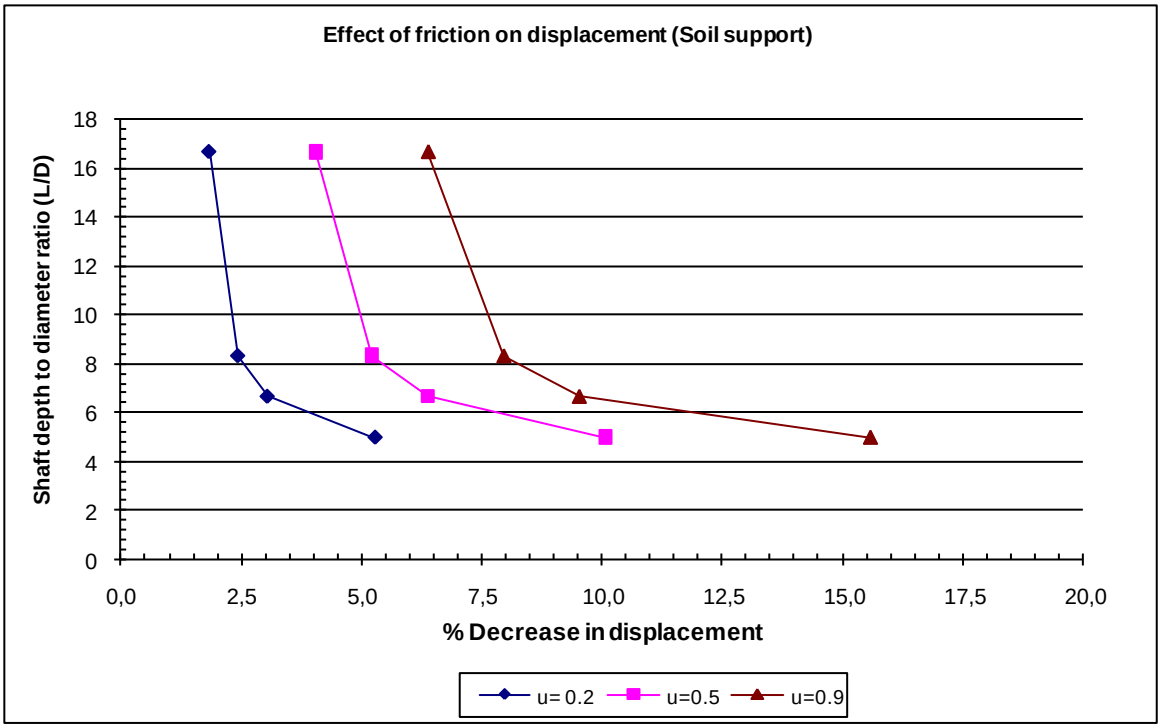

Figure 1.7 – Effect of friction on displacements for soil supported shafts.

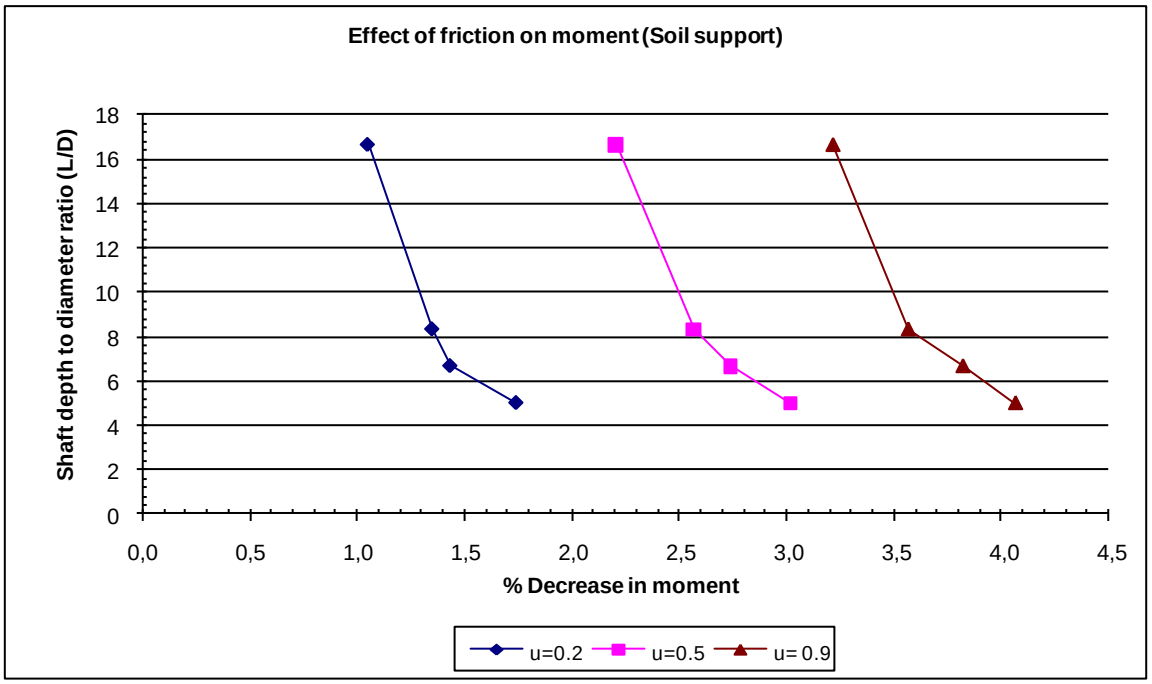

Figure 1.8 – Effect of friction on moment for soil supported shafts.

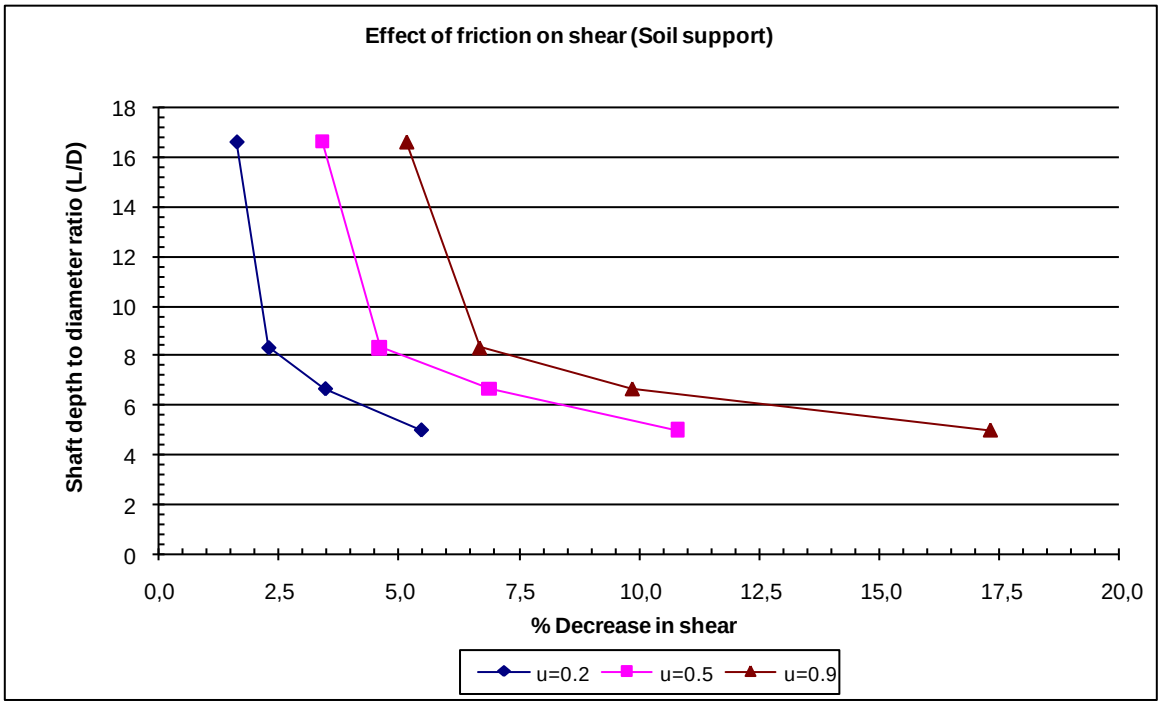

Figure 1.9 – Effect of friction on shear for soil supported shafts.

1.3 Effect of Poisson's Ratio of Soil

The lateral deformations of a material due to axial load is dependent on its Poissons ratio, which for elastic and isotropic materials is the ratio of lateral strain to applied axial strain. The value of Poissons ratio for most soil types is between 0.1 and 0.3. The maximum value is 0.5, which is valid for most natural rubbers and elastomeric materials.

Poisson's effects exhibited by materials causes no additional stresses unless the lateral strains are prevented. In deep foundations, the unconstrained free soil surface doesn't provide sufficient restraint; hence lateral deformations due to axial loading can freely take place. Thus, when a laterally loaded shaft is bearing against the soil, the soil close to the ground surface tends to *bulge* depending on the value of the poissons ratio of the soil. For low values of Poissons ratio, the amount of this bulge is low and for higher values the amount is high. It is expected that for a given soil type, its Poissons ratio will have an effect on the shaft response under lateral loads such that the lateral load capacity of the SSI system is higher for lower values of Poissons ratio. To investigate the shaft response under the influence of varying Poissons ratios, a 6 ft diameter shaft with 20ft column height and shaft depths of 100ft, 50ft, 40ft, and 30ft, were analyzed under a lateral load of 50kip. The shafts had fixed supports. The following values were selected for Poissons ratio ν: 0, 0.2 and 0.4.

Figure 1.10 shows the displacements along the shafts. The variations of the displacement with increasing Poisson's ratio for different depth to diameter ratios of the shaft are summarized in figure 1.13 along with a discussion.

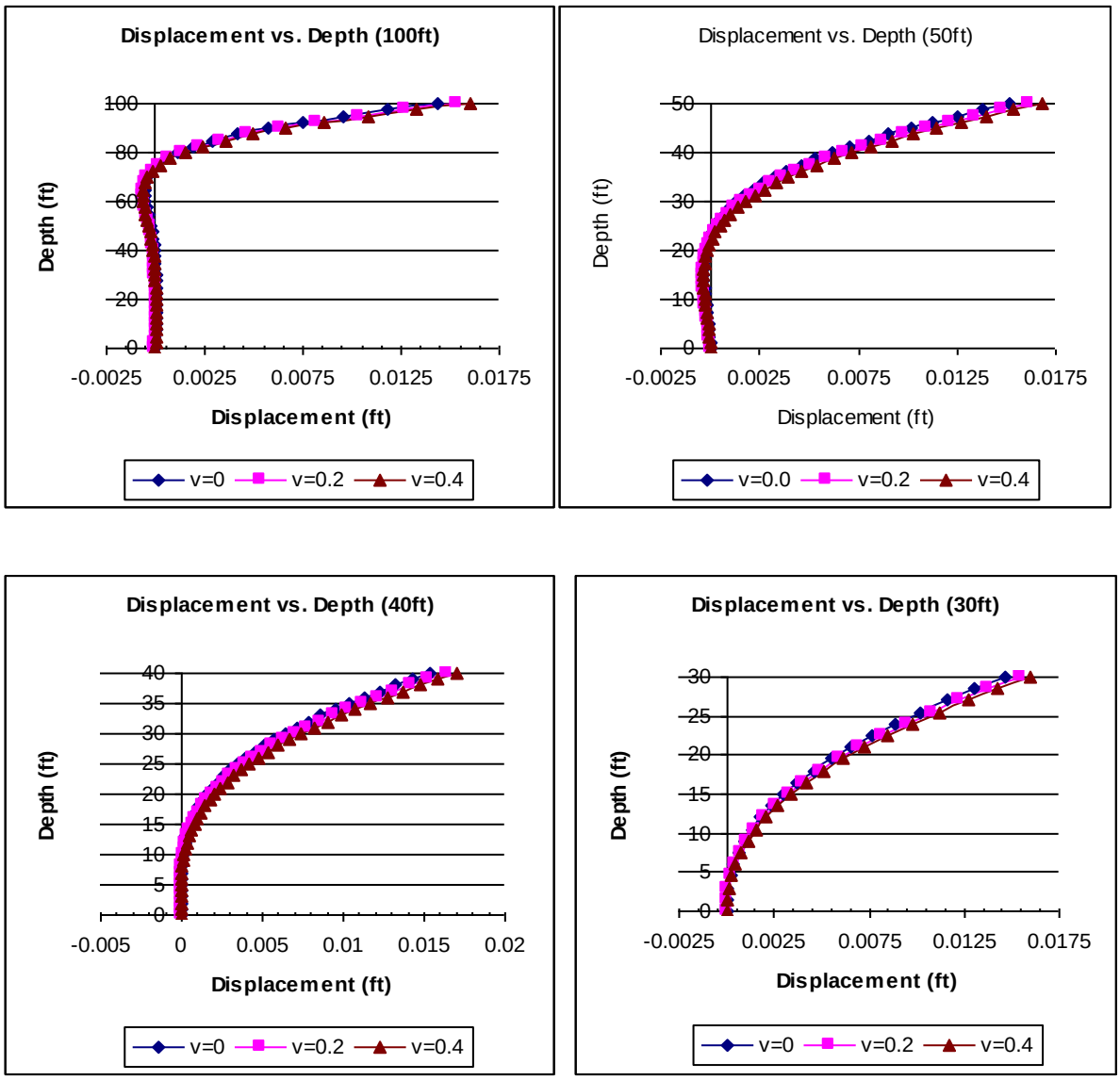

Figure 1.10 – Variation of shaft displacement for various Poissons ratios.

Figure 1.11 and 1.12 shows the variation of moment and shear for the various depths of shafts considered in the FE analysis. The relative variations of the moment and shear with increasing Poisson's ratio for different shaft slenderness values will be summarized in figure 1.13 and figure 1.14 along with a discussion.

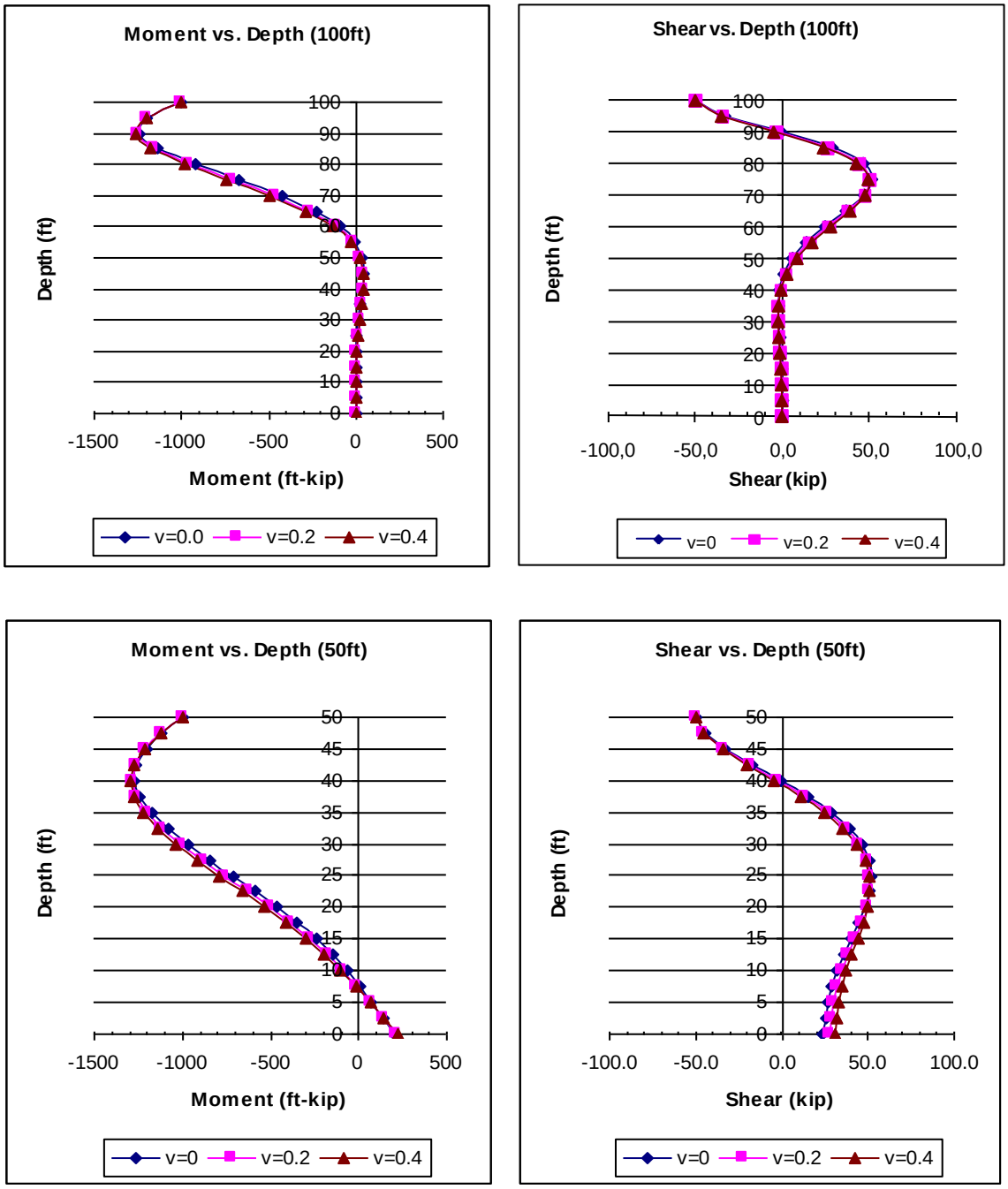

Figure 1.11 – Variation of shaft moments and shears for various Poissons ratios.

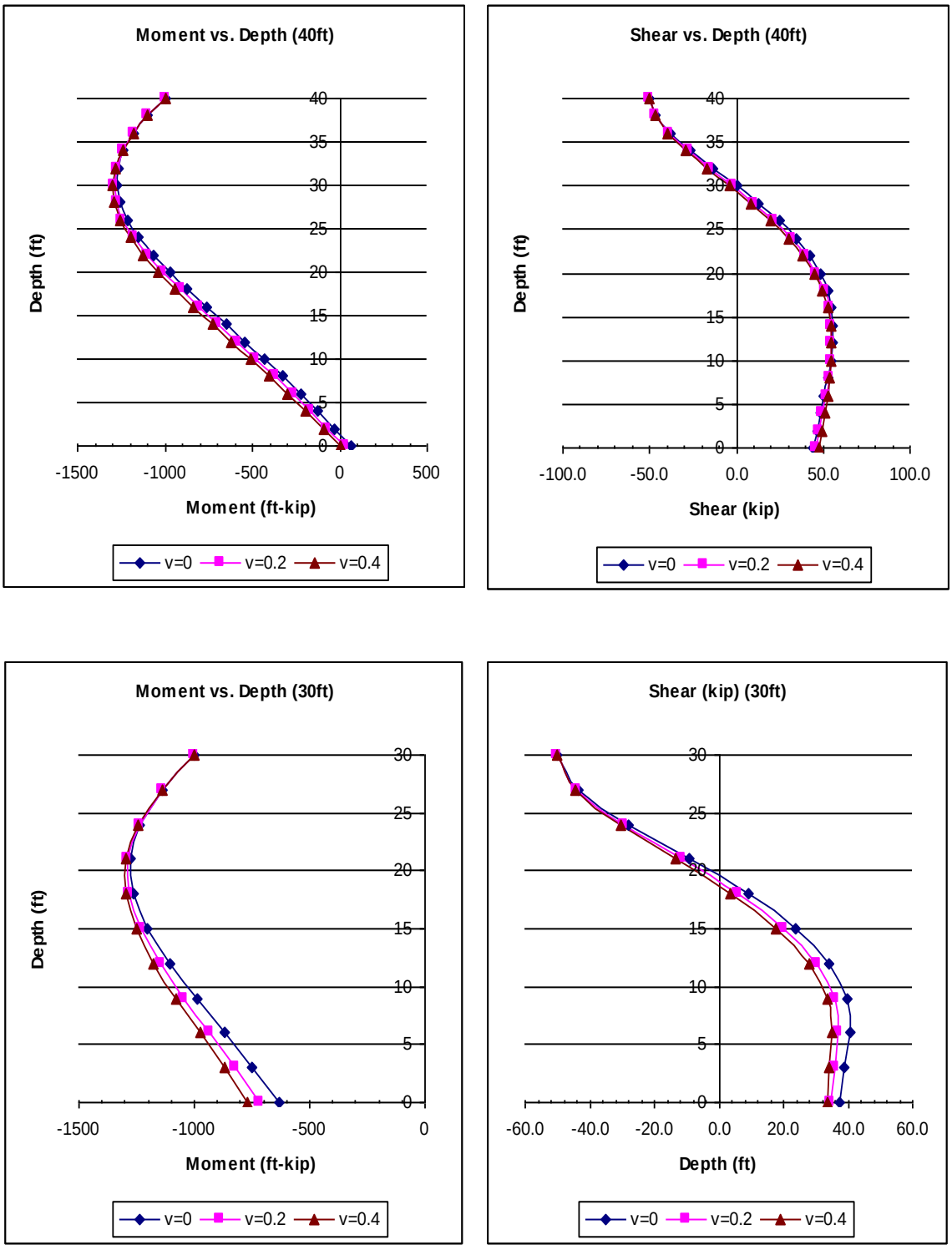

Figure 1.12 – Variation of shaft moments and shears for various Poissons ratios

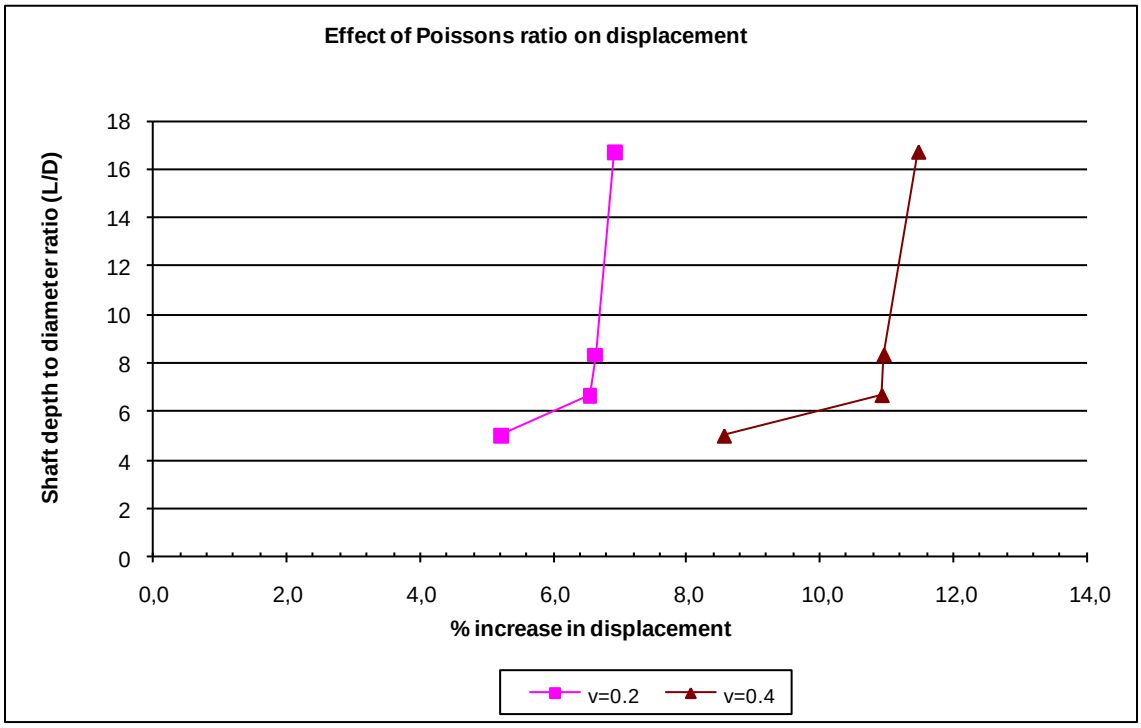

Figure 1.13 – Effect of Poissons ratio on displacements.

Figure 1.13 shows the percentage increase in maximum shaft displacement for Poisson's ratios of 0.2 and 0.4. As observed in the surface friction analysis, below a certain shaft depth to diameter ratio (in this case L/D≈7), the variation of Poisson's ratio does not have a significant effect on the response of the shaft. Note that for higher Poisson's ratio, the percentage increase in maximum shaft displacement is also higher. This behavior is attributed to the fact that higher soil Poisson's ratio indicates a higher tendency for the soil to bulge upward at the unconstrained soil surface at the ground level. Thus the higher the poissons ratio, the higher the soil moves upward at the ground surface under the bearing pressure between the shaft and the soil. This freedom to move upward reduces the bearing strength of the soil to lateral shaft movements thus resulting in higher shaft displacement.

Overall, a higher Poisson's ratio lowers the stiffness of the soil, increasing the relative stiffness between the shaft and the soil, thus increasing the burden on the shaft to resist the lateral loads. Figure 1.14 shows the effect of Poisson's ratio on maximum moment along the shaft. As Poisson's ratio increases, the maximum moment increases. However, the increase in maximum moment is less significant than that of the displacements.

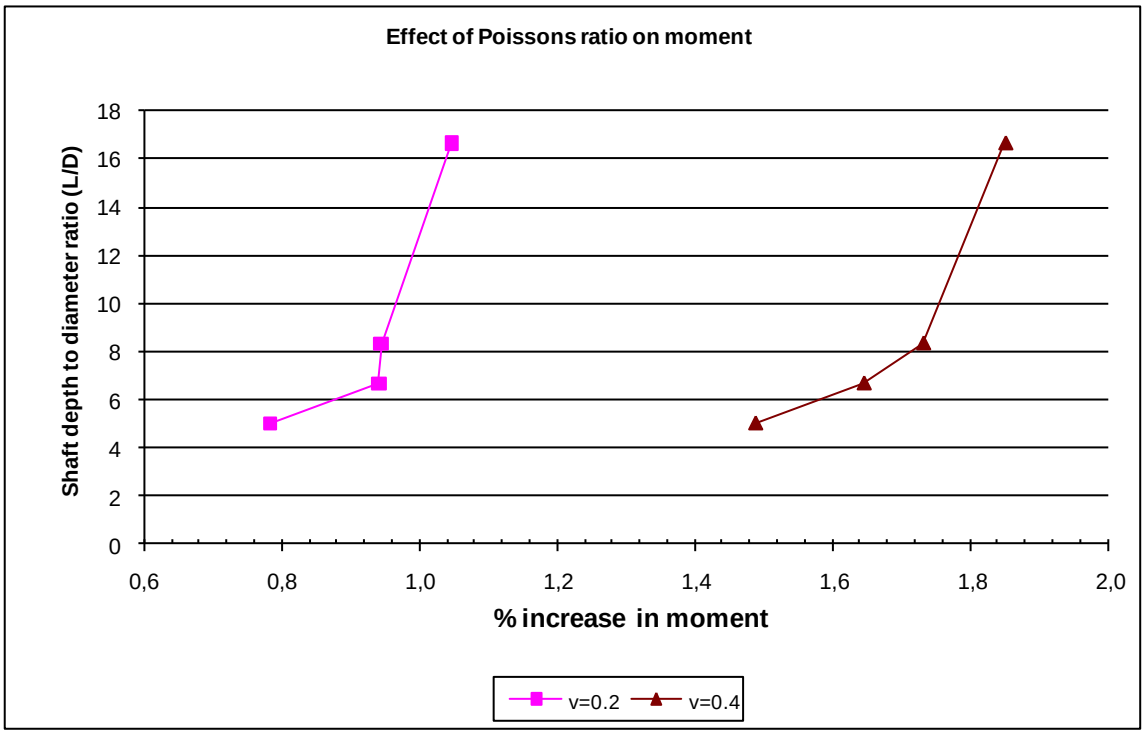

Figure 1.14 – Effect of Poisson's ratio on moment.

Figure 1.15 shows the variation of shear with slenderness. The maximum shear within the shaft decreases with increasing Poisson's ratio. The soil deformations are the contributing factor to the shears within the shaft. Since the soil stiffness is lower for higher values of Poisson's ratio, the forces generated by a unit displacement of soil is also lower, which is the primary reason for lower shear.

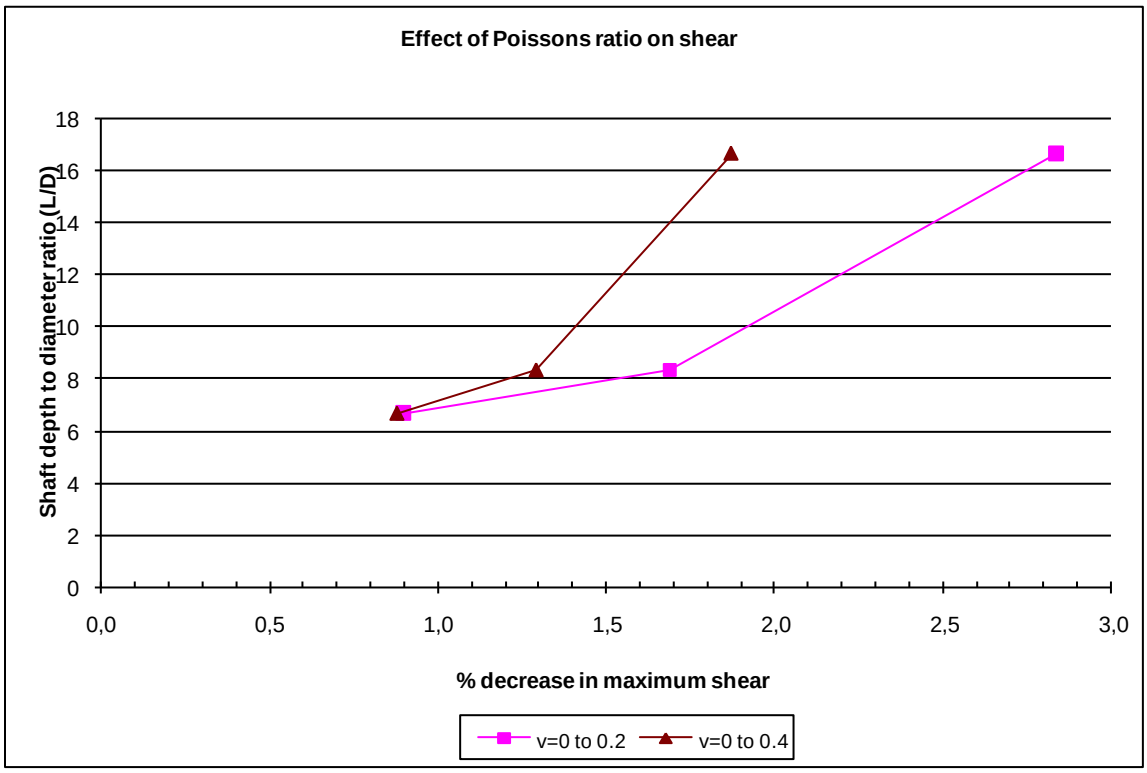

Figure 1.15 – Effect of Poissons ratio on shear

1.4 Effect of Soil Weight

The effect of soil weight on the response of drilled shafts under lateral load was investigated for two 6ft diameter shafts with shaft depths of 50ft and 100ft. The applied lateral load was 50 kips. The surrounding soil is cohesionless dense sand with unit weight equal to 120 pcf, and coefficient of subgrade reaction (n_h) equal to 50 pci. Shaft displacements, moments, and shears were compared with and without soil weight. Figure 1.16 shows the variation of displacement with depth. Inclusion of the selfweight in the FE analysis has increased the stiffness of the SSI system, which decreased the maximum displacement by about 25%.

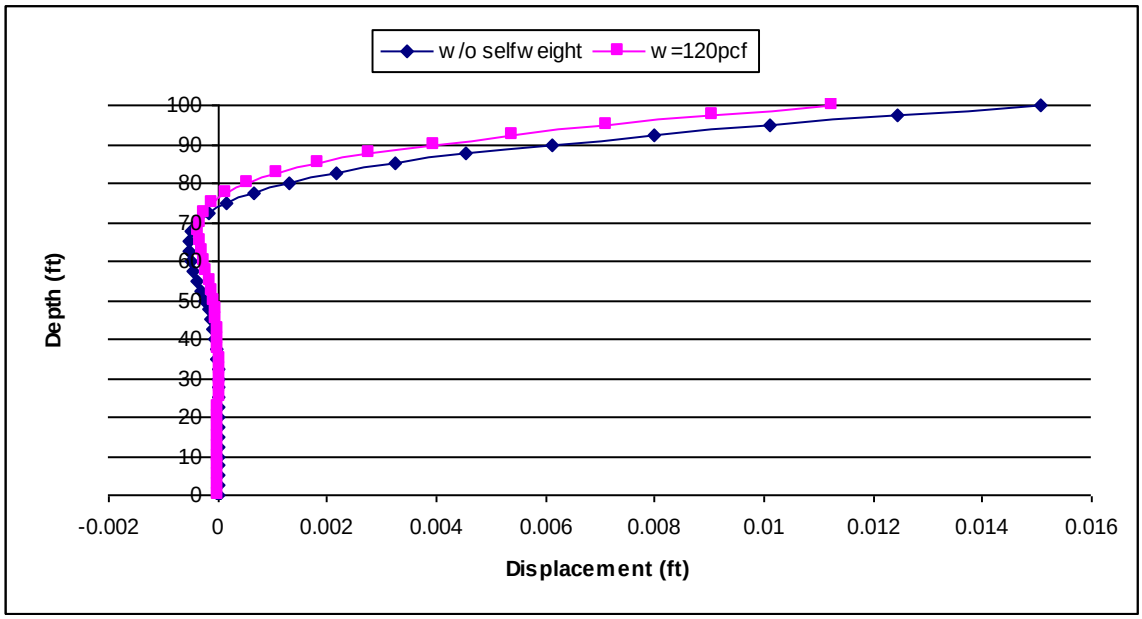

Figure 1.16 – Variation of displacement with and without soil selfweight for 100ft

Figure 1.17 shows the variation of the moment and shear along the shaft with and without soil selfweight. The shaft maximum moment occurred closer to the soil surface as the soil strength increased due to selfweight deformations. The decrease in the relative stiffness between the shaft and the soil reduces the portion of the lateral load resisted by the shaft alone. Also note the shift in the point of contraflexure as well as the 6% reduction in the maximum moment. Figure 1.17 also shows the effect of soil selfweight on shear along the shaft, where there is a 5% increase in the shear along the shaft. Overall, inclusion of the soil selfweight in the SSI model has resulted in lower response values. The effects of selfweight confinement for 50ft shaft have been observed to be slightly lower. Figure 1.18 shows that the reduction in displacement for the 50ft shaft is approximately 22.5%. The percentage decrease in maximum moment value is 3.7% and the percentage increase in maximum shear value is 2.5% as shown in figure 1.19.

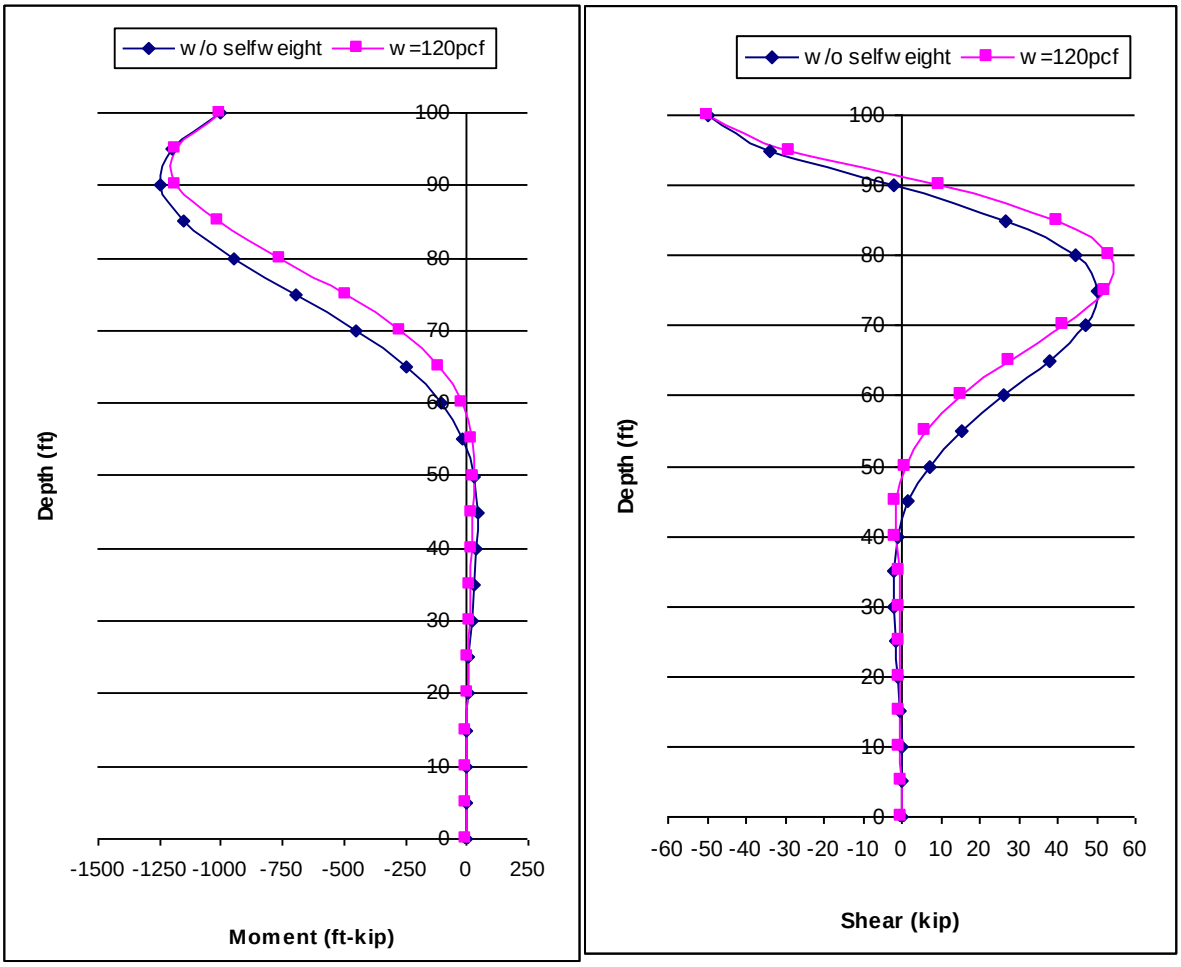

Figure 1.17 – Variation of moment and shear with and without soil weight for 100ft shaft.

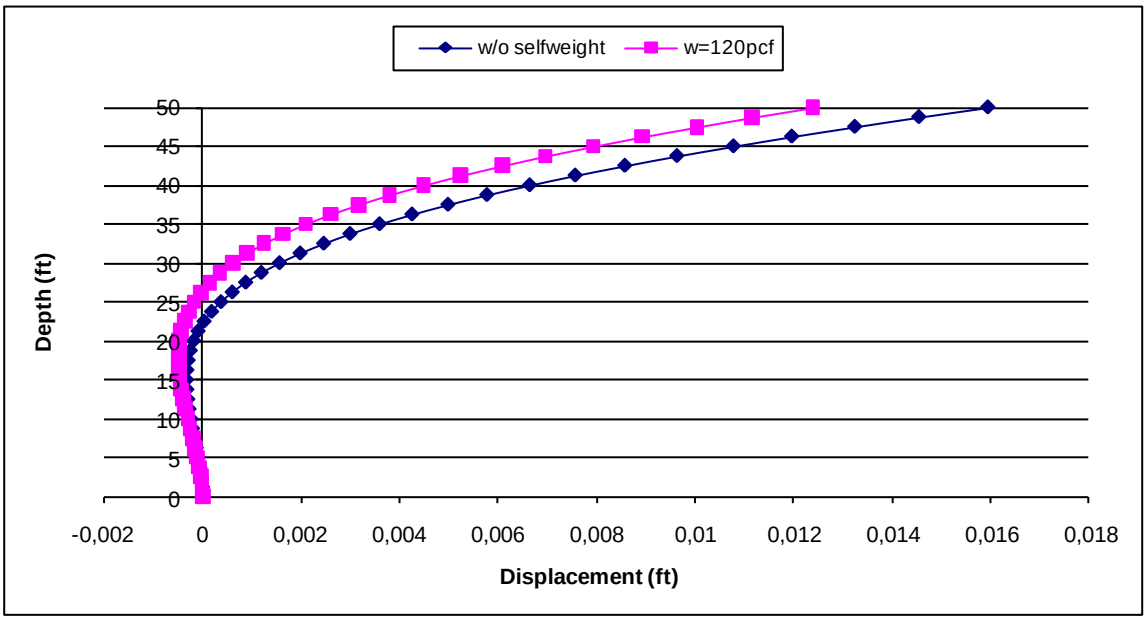

Figure 1.18 – Variation of displacement with and without soil selfweight for 50ft shaft.

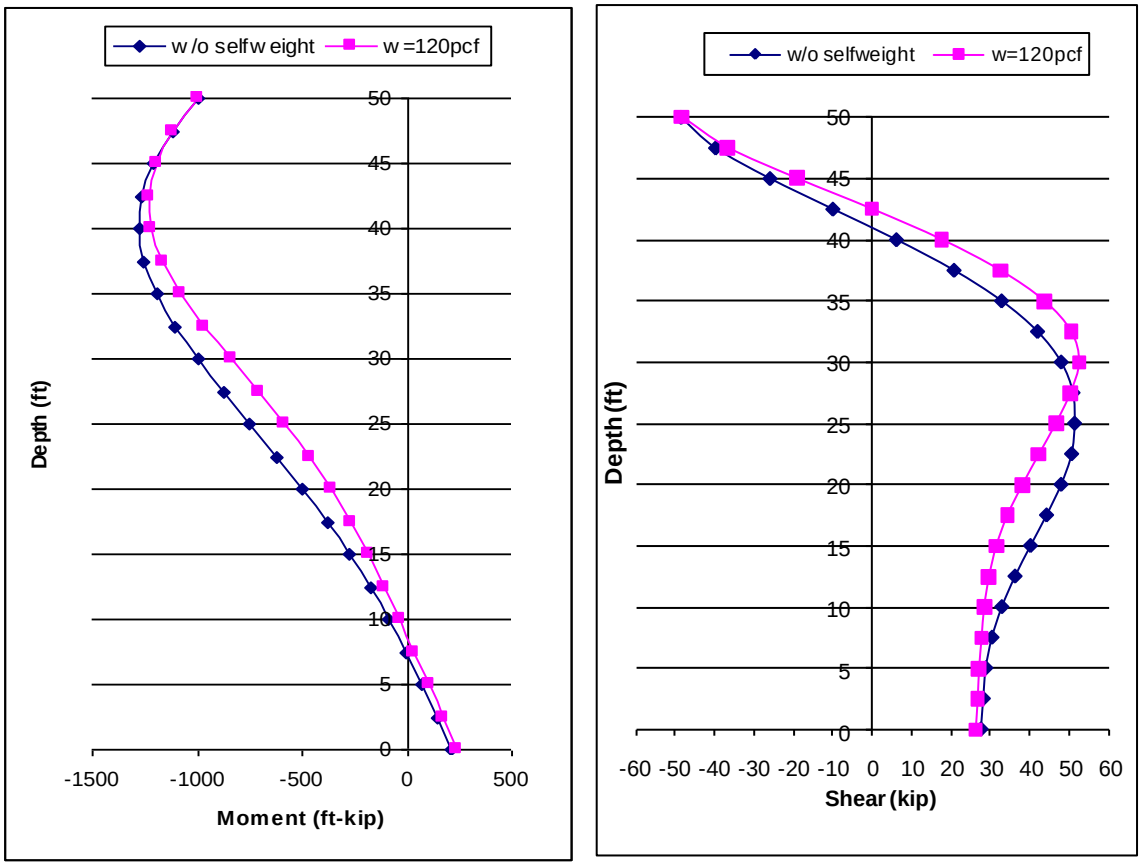

Figure 1.19 – Variation of moment and shear with and without soil weight for 50ft shaft.

1.5 Effect of Elastic Modulus of Soil

The elastic modulus of the soil is a stiffness property that influences the shaft response due to the indeterminate nature of the problem where the relative stiffness of shaft and soil become important. Maximum values of the response parameters such as displacements, moments, and shears are influenced by soil stiffness, which is dependent on the constant of horizontal subgrade reaction. The soil stiffness also affects the slenderness of the overall SSI system. To investigate the influence of varying soil stiffness, four 6ft diameter models with 20ft, 40ft, 50ft and 100ft shaft depths and 20ft column height were analyzed for an applied lateral load of 50 kip. The shafts were analyzed with fixed supports at the bottom. The surface friction constant was set as zero. The FE model used was Type-1 (Chapter three). The soil selfweight deformation effects and the surface friction effects have

been purposely excluded in order to isolate the effect of soil stiffness. The models were analyzed for three different cohesionless soil types which varied from loose sand, to dense sand with the following constant of subgrade modulus (n_h) values: 10 pci, 25pci, 50 pci. These values have been obtained from figure 1.12of the book "An Insight into the Theoretical Background of SSI" for angle of friction (ϕ) values of: 28°, 33° and 37°. The elastic modulus of the soil varied linearly with depth (E_y=y. n_h) where y is the depth from ground surface. Thus given the linear relation, an increase in n_h from 10 pci to 25 pci results in an increase in soil stiffness of 250%, and an increase from 10 pci to 50 pci results in an increase in soil stiffness of 500%. Figure 1.20 and 1.21 shows the effect of soil stiffness on displacements, moments and shears for the 100ft shaft. Note that the point of *zero-displacement* moves up as the soil becomes stiffer. Also the displacements become smaller. This can be attributed to the fact that the depth of the soil from the ground surface that has to be displaced and the amount that this depth of soil has to be displaced is smaller due to a higher soil stiffness value. The necessary soil resistance to lateral load can be developed by displacing a lesser amount of soil (higher location of shaft zero-displacement point) and a lower amount of soil deformation at the ground level (lower displacement). The maximum displacement decreases by 40% when soil stiffness increases from 10pci to 25pci and the decreases by 60% when the coefficient of subgrade reaction increases from 10pci to 50pci.

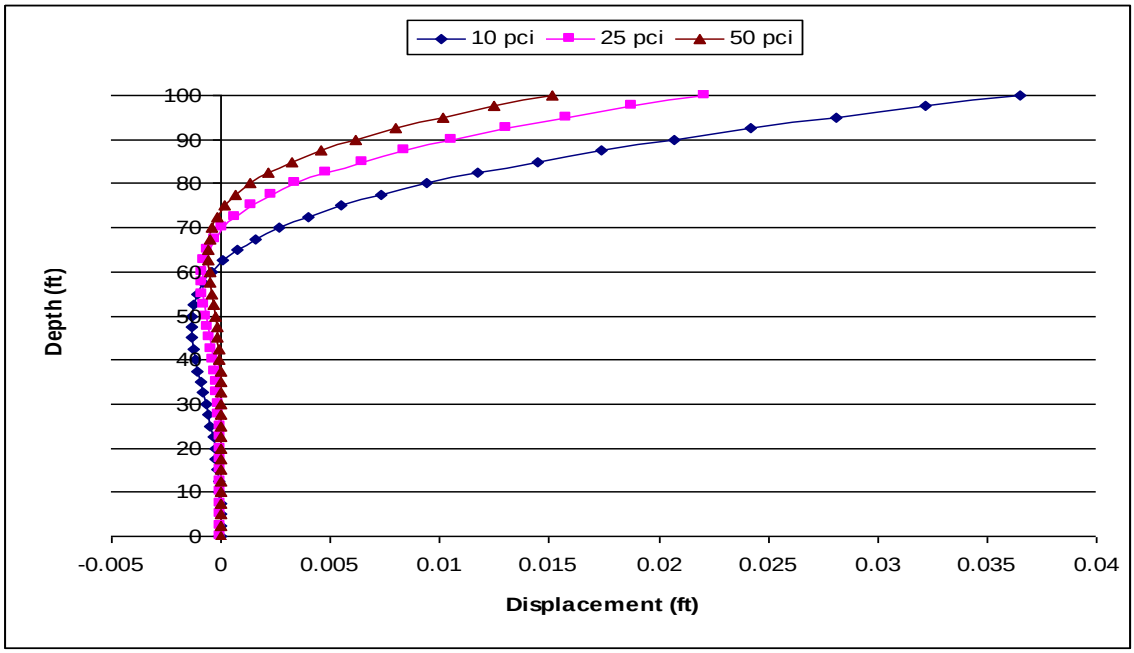

Figure 1.20 – Shaft displacements for various values of coefficient of subgrade reaction.

Figure 1.21 shows that the location of maximum moment moved down and its value increased with decreasing soil stiffness. As the soil stiffness decreases the portion of the lateral load resisted by the shaft increases thus the higher maximum value. The maximum moment decreased by about 8% when n_h increased from 10pci to 25pci and decreased by 13.5% when n_h increased from 10 to 50 is 13.5%. One interesting point in figure 1.21 is that for the weaker soil moments at the support were developed. Although the value is small compared to the maximum values, a support moment of approximately 50ft-kip is observed for soil with n_h=10pci. For other values of n_h, the support conditions did not have an effect. It is observed that the effect of support conditions is related to relative stiffness as well as the slenderness. Figure 1.21 also shows the variation of shear with soil stiffness. The point of maximum shear within the shaft shifts down, due to the increase in the amount of soil that has to be displaced to establish a state of equilibrium. The maximum shear value increases with increasing soil stiffness and the percentage

increase is about 13% when n_h increases from 10pci to 25pci is and 18% when n_h increases from 10pci to 50pci.

Similar analysis was conducted for 50 ft shaft for various values of n_h. However, the model was analyzed for two more n_h values (30pci, and 40pci).

Figures 1.22 show the displacement profile for the 50ft shaft. The percentage decrease in displacement was about 39% when n_h increased from 10pci to 25pci and about 58 % when n_h increased from 10pci to 50pci.

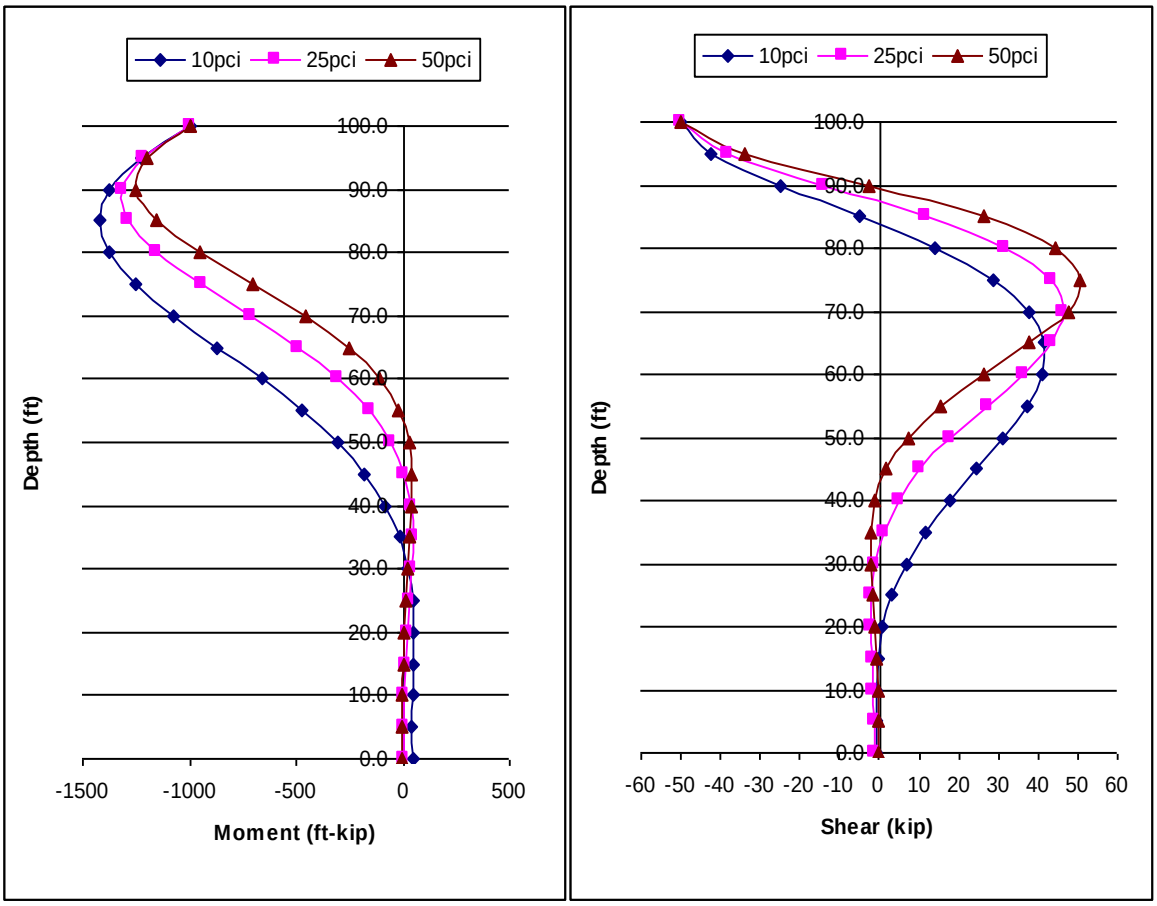

Figure 1.21 – Moment and shear variation along the shaft for various n_h.

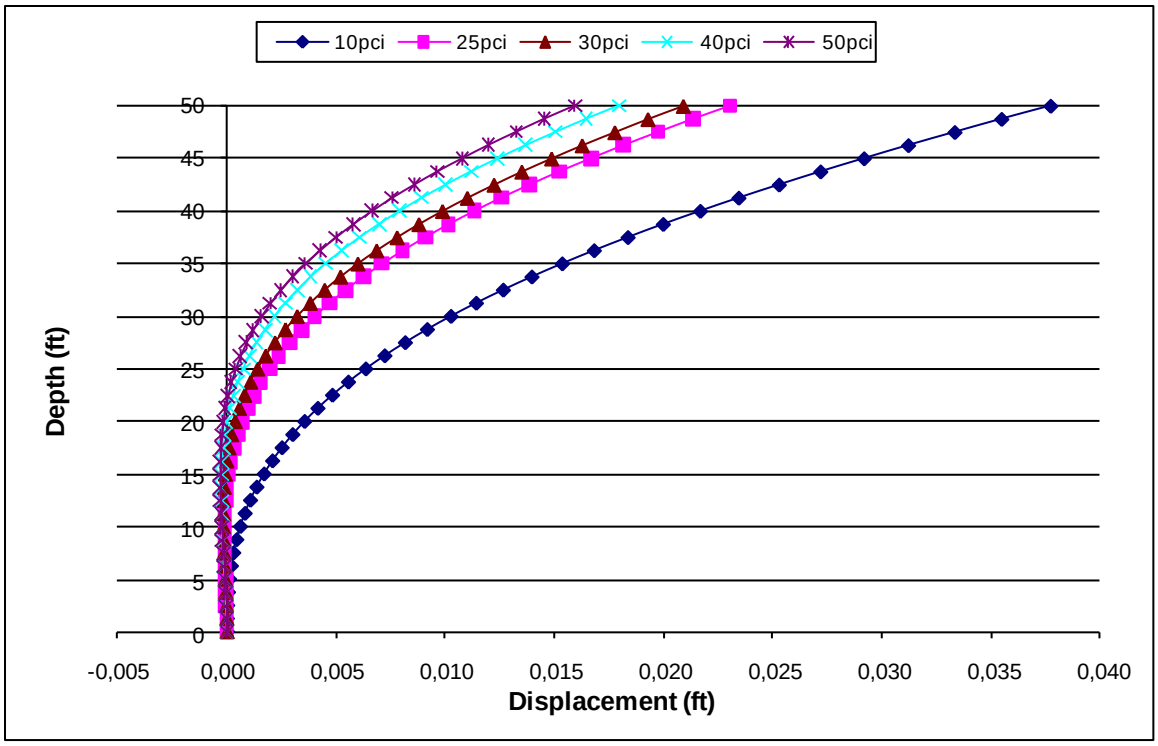

Figure 1.22 – Shaft displacements for various values of coefficient of subgrade reaction.

The decrease in moment for n_h values varying from 10 pci to 25 pci is about 8% and was about 13.4 % when n_h increased from 10pci to 50pci. Note the change in curvature in figure 1.23 as the soil stiffness increases. For n_h=10pci, the shaft has a single curvature and overtakes a greater portion of the lateral load resisting capacity of the SSI system. Figure 1.23 also shows the shear diagrams for the shafts with different soil stiffness. Note the behavior at the shaft base. As the soil stiffness increases, the variation of shear along the shaft approaches the behavior of a slender shaft, i.e. the base shear becomes closer to zero. For n_h=10 pci and n_h=25 pci this shift wasn't clear, after analyzes for n_h =30 pci and n_h=40 pci the shift became evident.

As in the case for 100ft deep shaft, the increase in the shear and the upward shift in the point of maximum shear are shown in figure 1.23. The higher the soil stiffness, the lower the amount of soil that needs to be mobilized. The increase in

shear was about 12.5% when n_h changed from 10pci to 25 pci is the increase was 14% when n_h changed from 10pci to 50 pci .

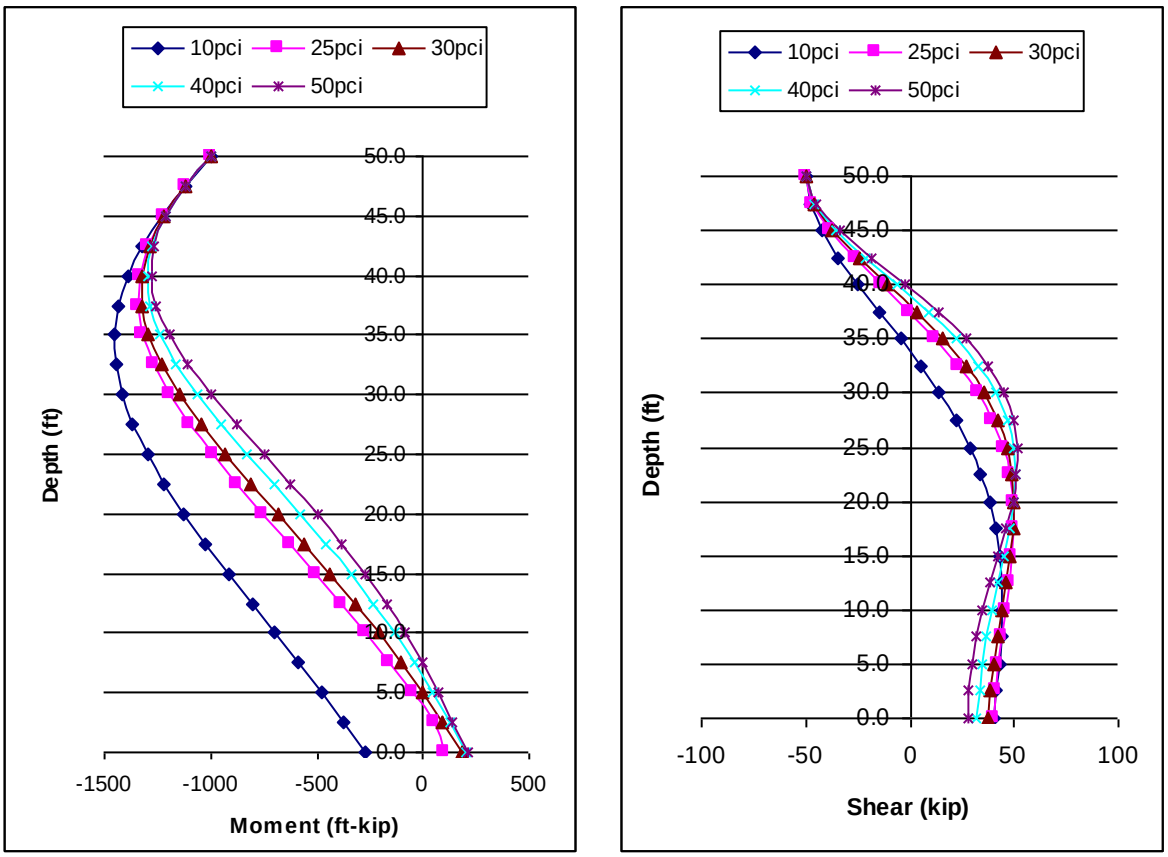

Figure 1.23 – Moment and shear variations along the shaft for various n_h.

As the shaft depth becomes smaller (40ft) due to a lower depth to diameter ratio (L/D) shaft stiffness starts to dominate the overall SSI system stiffness. Figure 1.24 shows the variation of displacements of the 40ft shaft. The percentage decrease in maximum displacement for a change in n_h from 10pci to 25pci is about 35% and from 10 pci to 50 pci is 55 %.

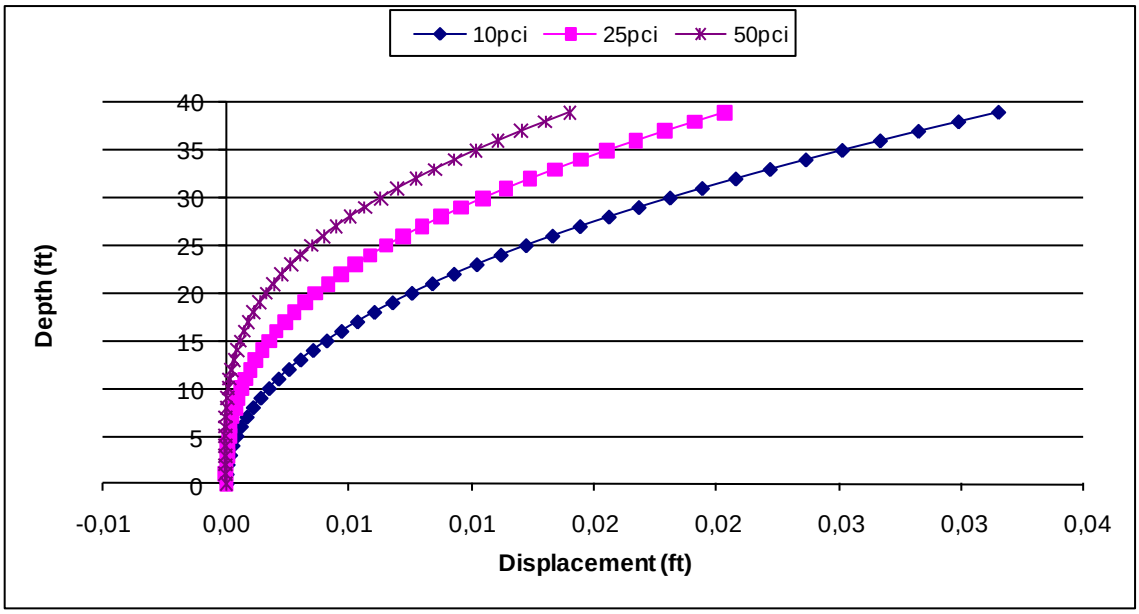

Figure 1.24 – Shaft displacements for various values of coefficient of subgrade reaction

Figure 1.25 shows the variation of moments and shears for the 40ft shaft. Note that all the contraflexure points have diminished and the shaft has a single curvature. For the 50ft shaft moments shown in figure 1.23, all shafts had a contraflexure point accept the shaft within the soil having n_h=10pci. This indicates the 50ft shaft is more slender as expected. The decrease in moment for a change in n_h from 10pci to 25pci is about 6% and from 10pci to 50pci is about 14 %. The increase in shear for a change in n_h from 10pci to 25 pci is about 43% and from 10pci to 50pci is 57 %.

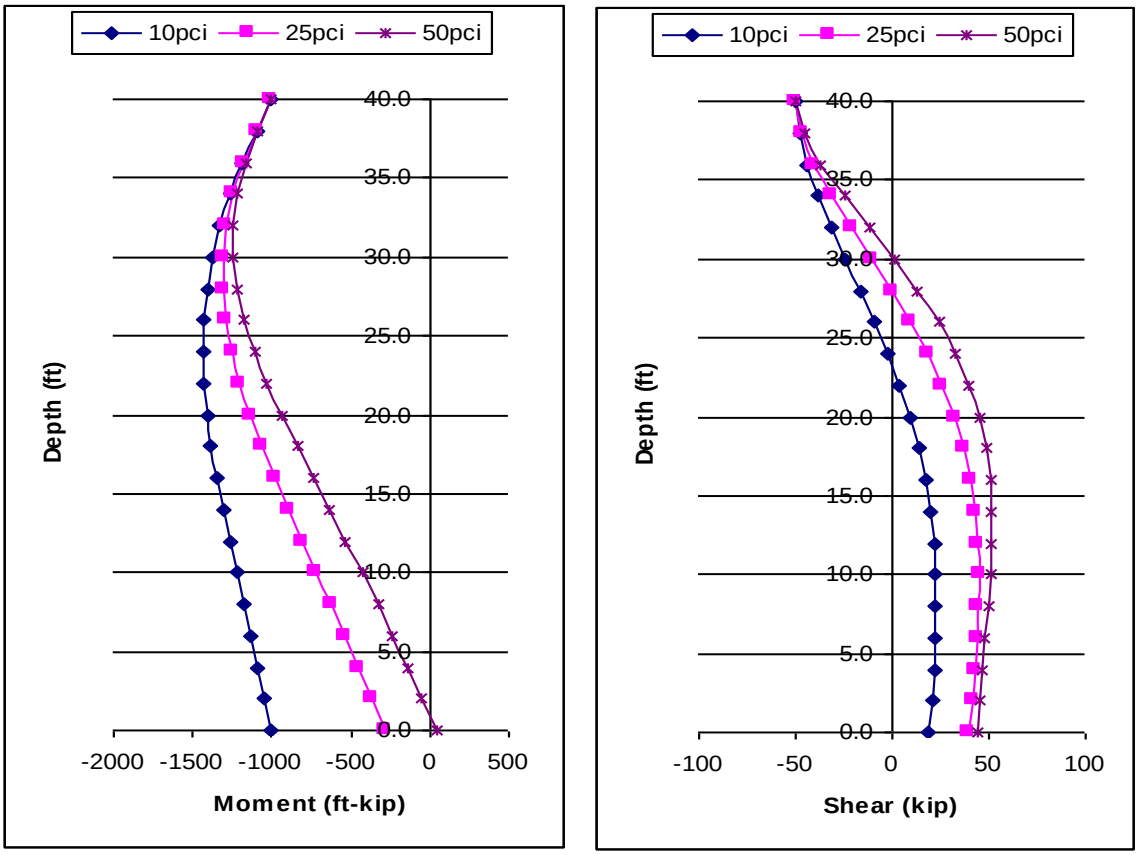

Figure 1.25 – Moment and shear variations along the shaft for various n_h.

Finally, a 20ft deep shaft was analyzed with the different soil stiffness values. At such a low depth-to-diameter ratio, the shaft was not sensitive to changes in soil stiffness compared to the 100ft and 50ft deep shafts. Figure 1.26 shows the variation in displacements along the shafts. The decrease in displacement for a change in n_h from 10pci to 25pci is about 4.5% from 10pci to 50pci is about 12 %.

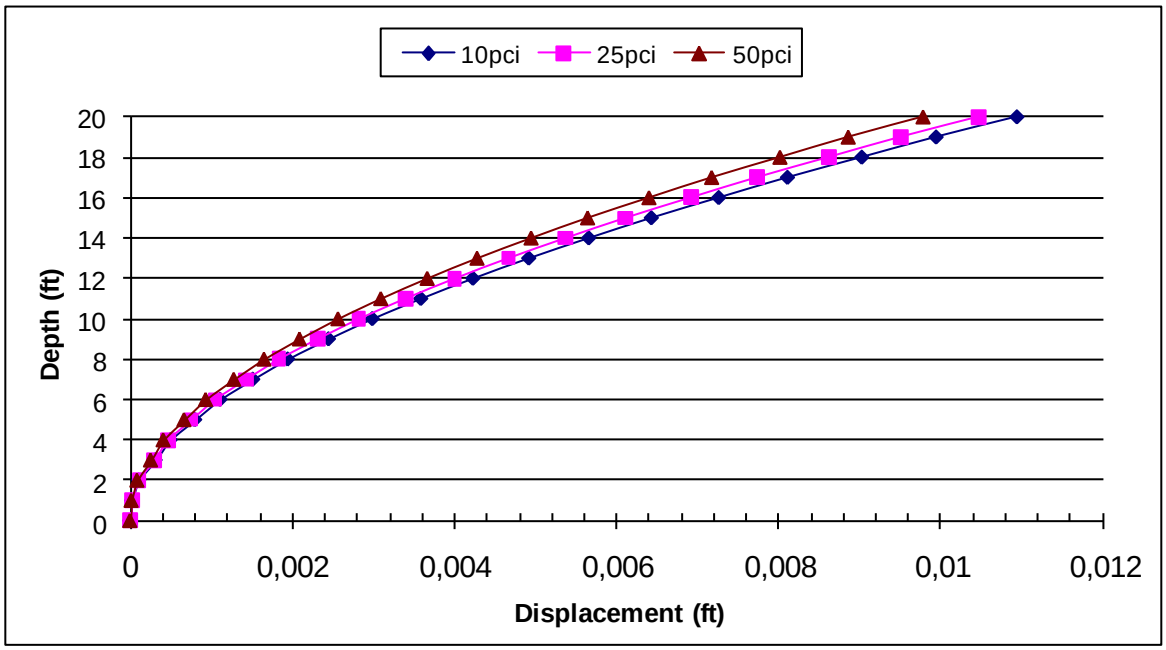

Figure 1.26 – Shaft displacements for various values of coefficient of subgrade reaction.

Figure 1.27 shows the moment profiles of the shafts. The decrease in maximum momentfor a change in n_h from 10pci to 25pci is about 6.5% and from 10pci to 50 pci is about 16%. Note that for n_h =10pci, the slenderness of the shaft-soil system is almost independent of the soil, i.e. the soil is weak and the shaft is resisting lateral loads as a cantilever. Increasing soil stiffness modifies the slenderness of the shaft and the moment at the base decreases. Figure 1.27 also shows the shear variation along the shaft. The decrease in the shear for a change in n_h from 10pci to 25pci is about 22% and from 10pci to 50pci is about 52 %. Note that as the soil stiffness decreases, the shear diagram approaches that of a cantilever with a concentrated load at the tip.

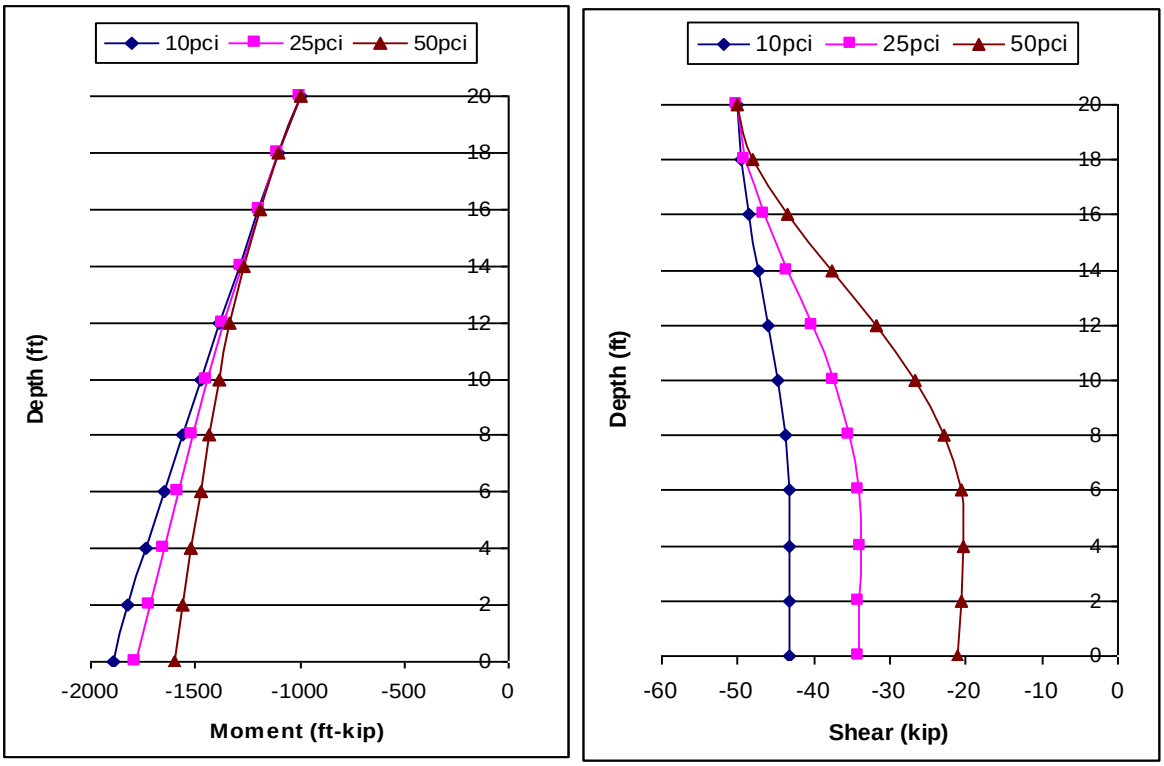

Figure 1.27 – Shaft displacements for various values of coefficient of subgrade reaction.

Figure 1.28 and 1.29 shows the variation of maximum displacements and maximum moments values with the coefficient of subgrade reaction of the soil, for various slenderness ratios. Figure 1.28 shows that for shaft slenderness higher than 8.33, the influence of change in soil stiffness on the lateral shaft response is the same and the response of the shaft is affected by this change. As the shaft slenderness decreases, the shaft flexural stiffness becomes more dominant on the overall SSI system stiffness and the soil stiffness will have less effect on the lateral shaft response. Figure clearly shows the difference between the plots for depth to diameter ratios of 6.67 and 3.33. For the stout shaft with depth to diameter ratio of 3.33, the influence of the change in coefficient of subgrade reaction is almost negligible, as the shaft stiffness almost unilaterally defines the stiffness of the system. The variation of the moments is similar. As the soil stiffness is increased, the relative effect of shaft stiffness on the overall SSI stiffness decreases.

Although the change in displacement is low for smaller slenderness values, due to high flexural stiffness associated with them, the change in moment is highly influenced. Thus the variation in moment values is similar for all slenderness values.

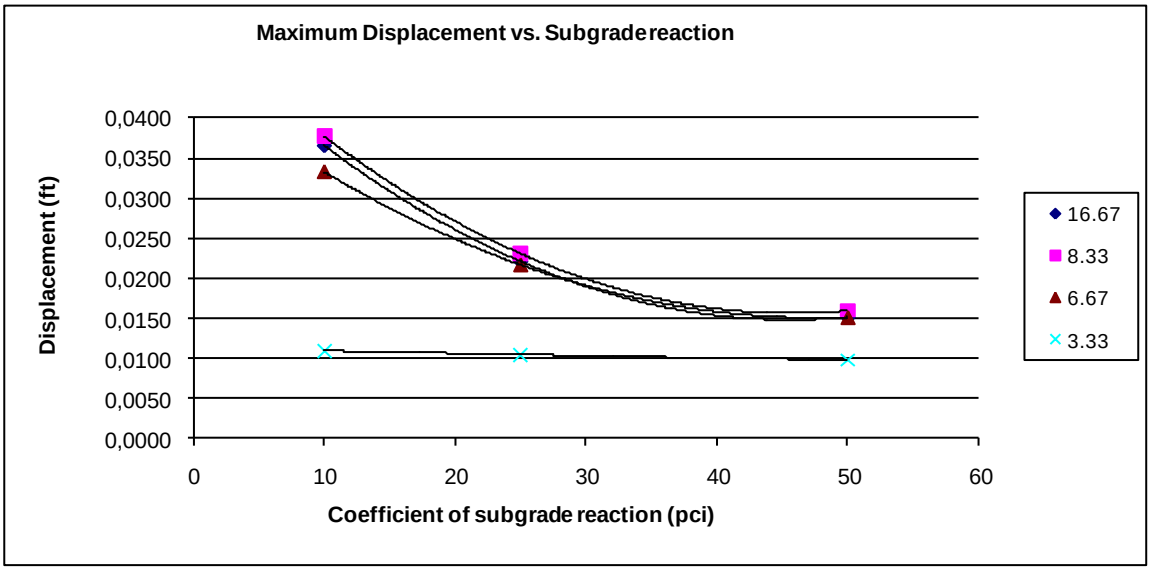

Figure 1.28 – Variation of maximum displacement for different shaft slenderness

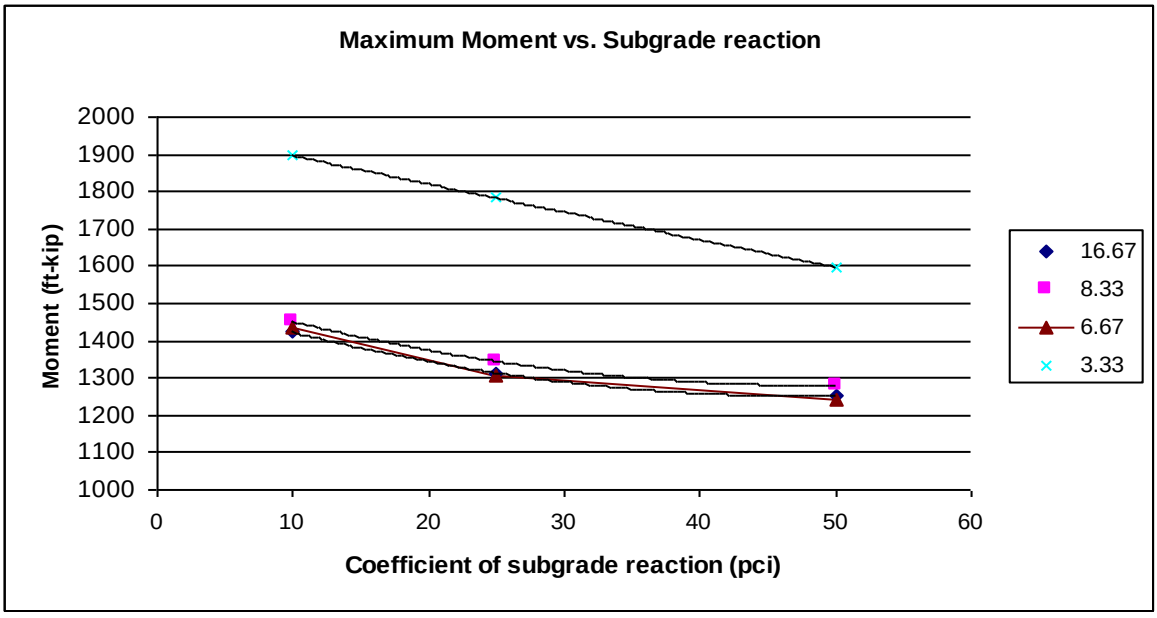

Figure 1.29 –Variation of maximum moment values for different shaft slenderness

1.6 Effect of Elastic Modulus of Concrete

The elastic modulus of the concrete used for the shaft is related to the concrete compressive strength and it is a determining factor in shaft rigidity. However, the rate of change of elastic modulus with compressive strength is not high. Thus the impact of concrete strength on the stiffness of the SSI system is not significant. A 6ft diameter and 100ft deep shaft with 20ft column in dense sand was analyzed under a lateral load of 50kip.The elastic modulus of the concrete was calculated based on ACI recommendation for normal-weight concretes: $E=57.000[f_c']^{(1/2)}$. The concrete strengths, f_c' used for the shaft were: 3.000psi, 4.000psi, and 5.000psi that results in elastic modulus E_c of: 450.000ksf, 520.000ksf and 580.000ksf respectively. The elastic modulus increases by 15% when the compressive strength is increased to 4.000psi, and increases by 29% when it is increased to 5.000psi. Figure 1.30 shows the displacements along the shafts for various moduli of concrete. The maximum displacements are reduced by about 6% when the compressive strength is increased from 3.000psi to 4.000psi, and reduced by 11% when the compressive strength is increased from 3.000psi to 5.000psi.

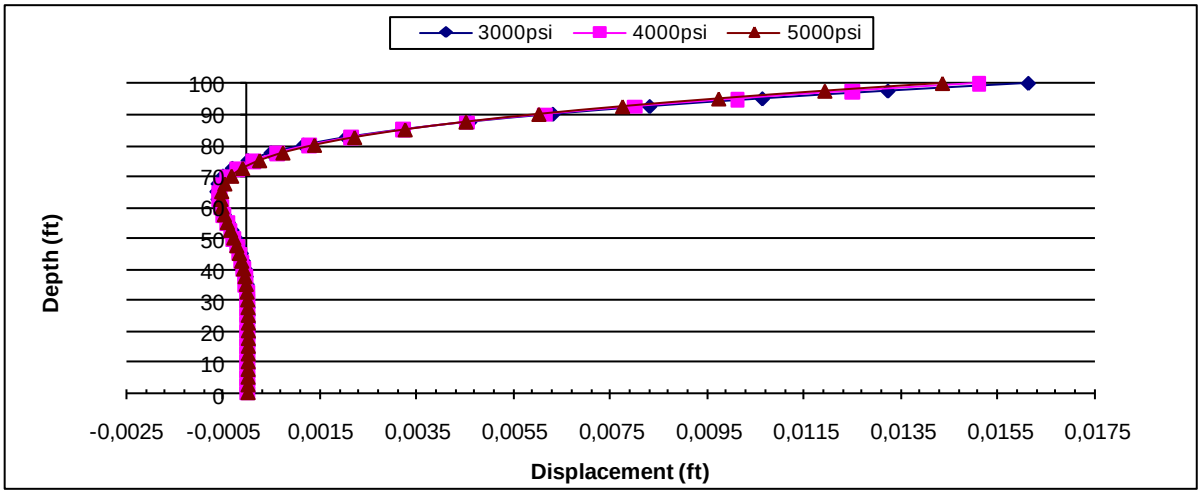

Figure 1.30 – Shaft displacements for different concrete strengths.

Figure 1.31 shows moment and shear variations along the shafts. There is a slight increase in moment with the increase in the elastic modulus. 2% increase in maximum moment is observed when the compressive strength is increased to from 3000psi to 5000psi. The corresponding decrease in shear due to lower displacements is about 3.5%.

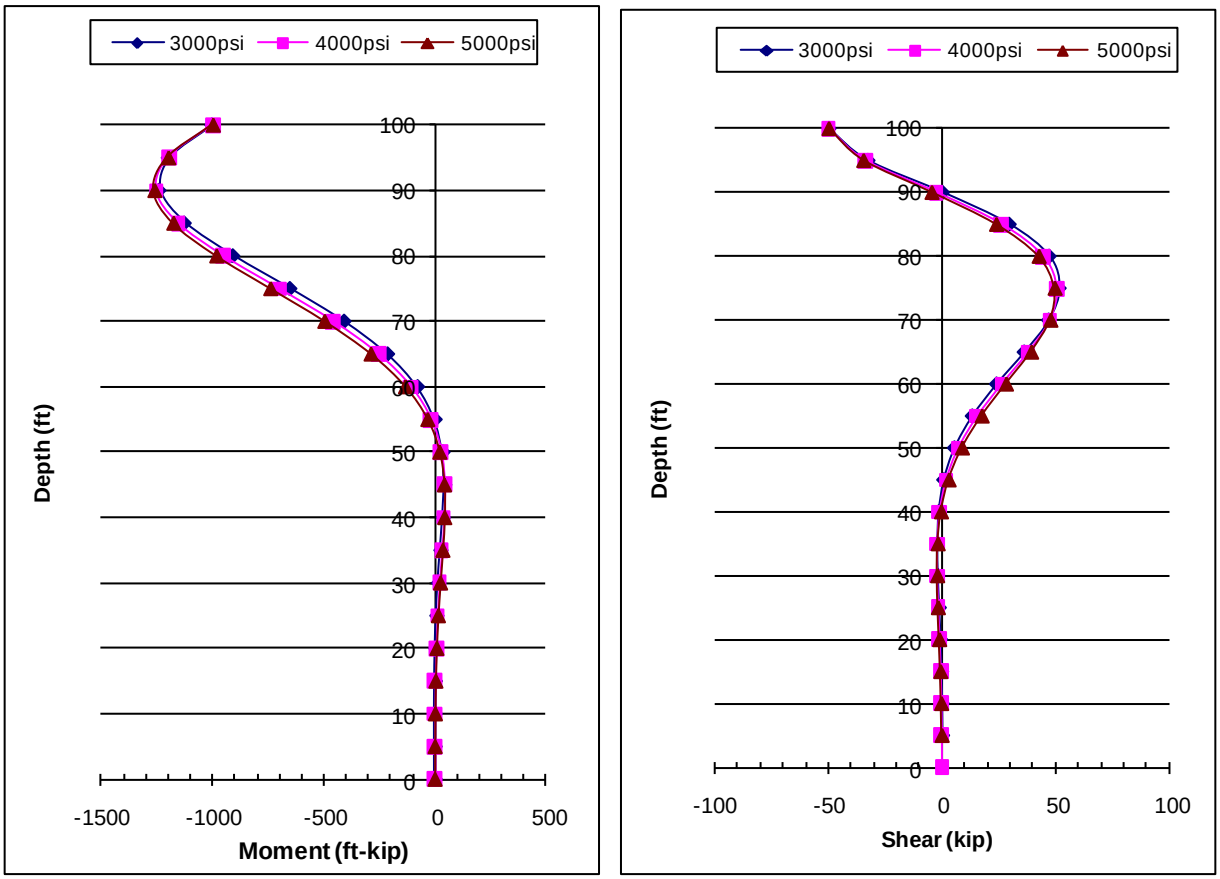

Figure 1.31 – Shaft moment and shear for different concrete strengths.

The effect of variation of concrete compressive strength on the shaft response was smaller than the effect of the variation of soil stiffness.

1.7 Effect of Shaft Diameter

The shaft diameter affects the moment of inertia of the shaft and it is a determining factor in the shaft rigidity, which affects the stiffness of the SSI system. Due to the indeterminate nature of the problem, distribution of the overall stiffness between the shaft and the soil, based on the individual stiffness values, affects the value and distribution of the displacements, moments, and shears along the shaft. In the previous chapter, the effect of variation in soil stiffness on the response of SSI system was analyzed. In this chapter the rigidity and the flexural stiffness of the shaft will be varied and the effects on the SSI system will be analyzed.

Rigidity of a prismatic shape is related to its elastic modulus and moment of inertia. Flexural stiffness of a prismatic shape is additionally related to the length. Thus by changing the diameter of the shaft, the rigidity and the flexural stiffness are changed.

100ft deep shaft with 20ft column with varying diameters were analyzed under a 50 kip load applied at the column tip. The shaft diameters (D) analyzed were: 6ft, 7ft, 8ft, 9ft, and 10ft which resulted in depth to diameter (L/D) ratios of: 16.7, 14.3, 12.5, 11.1, and 10. Increase in shaft diameter has a large impact on the rate of increase of shaft rigidity since the moment of inertia is directly related to the fourth power of the diameter. Taking the rigidity of the 6ft diameter shaft as 1, the rigidities of the remaining shafts normalized with respect to the 6 ft diameter are as follows: EI_1=1, EI_2=1.85, EI_3=3.16, EI_4=5.06, EI_5=7.72 assuming same E. The soil is dense sand with n_h=50pci. Figure 1.32 shows the variation of displacements along the shaft depth. Note the curvature change as the flexibility of the shaft decreases.

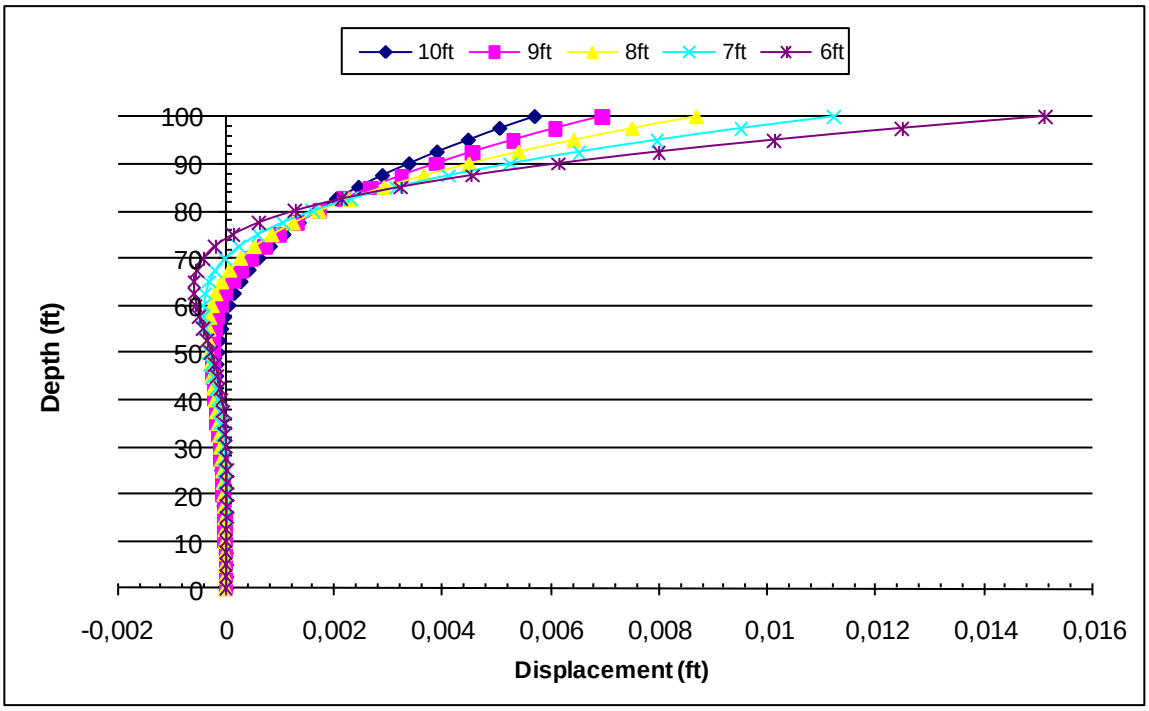

Figure 1.32 – Displacements for 100ft shaft with varying diameters.

If these results are normalized with respect to the 6 ft diameter shaft, the percentage decrease in the displacements with increasing diameter is as shown in figure 1.33.

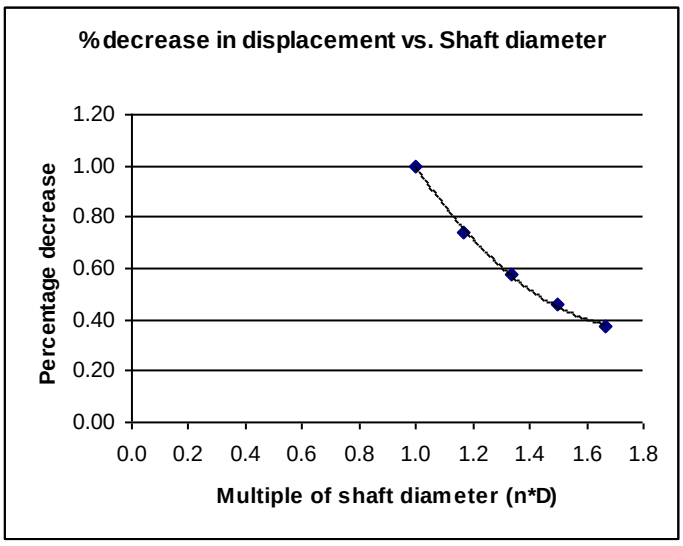

Figure 1.33 – Percentage decrease in displacements normalized with respect to 6ft shaft.

Figure 1.34 shows the variation of shears and moments along the shaft depth. As the shaft diameter increases, the flexural stiffness of the shaft increases. Higher stiffness causes higher moments and as the relative stiffness between the shaft and the soil increases, the maximum moment occurs at deeper locations along the shaft. The variation of the moment at the base of the shaft is also dependent on the stiffness of the SSI system although its value is small. As the stiffness of the shaft and the relative stiffness of the shaft with respect to soil increases, the moments at the fixed support are developed, indicating that the shaft starts to play a larger role in resisting lateral loads. The shaft displacements for higher shaft diameters are lower, which results in lower soil resistance. Therefore the shear decreases with increasing shaft diameter.

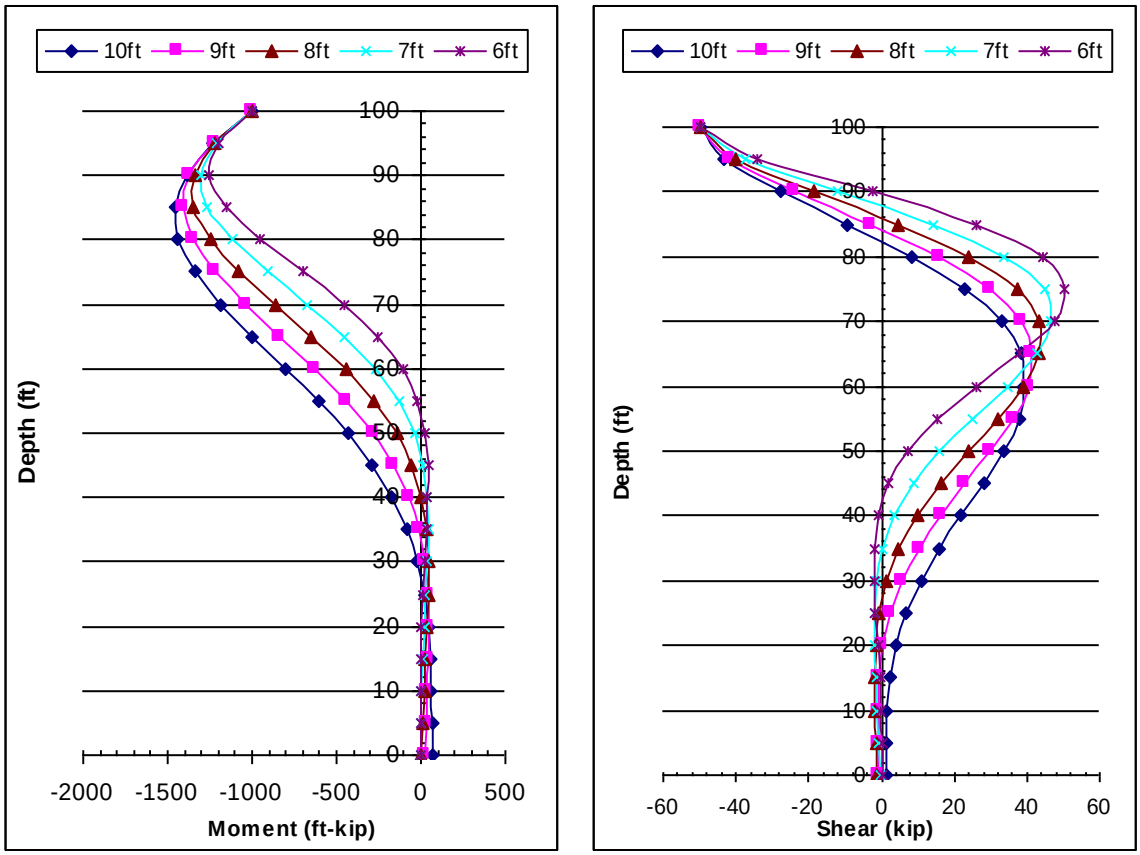

Figure 1.34 – Moment and shear variation along the 100ft shaft depth.

Figure 1.35 shows variations of the shears and moments, normalized with respect to 6 ft diameter shaft. This figure shows that moments increase and the shears decrease with increasing shaft diameter.

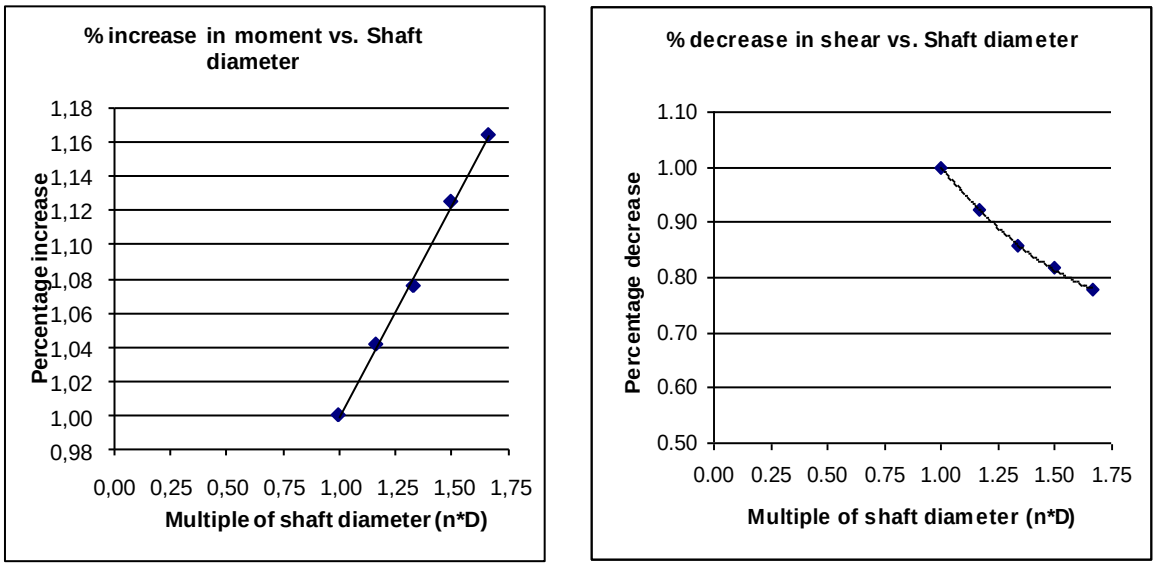

Figure 1.35 – Variations in moments and shears with diameter normalized with respect to 6ft shaft.

1.8 Effect of Column Height

A moment and an equivalent shearing force at the ground level can replace the lateral load applied at the column tip. The applied moment on the top of the shaft depends on the lateral load as well as the height of the column. Thus the same load applied at different column heights creates different moments. A change of the column height also modifies the slenderness and the flexural stiffness of the column. Thus, both the change in the moment and the shaft stiffness results in different displacements and related variables along the shaft. To investigate the effect of column height on the shaft response, a 6 ft diameter and 100ft deep shaft with L/D=16.67 was analyzed under a lateral load of 50 kips for the following column heights (H): 20ft, 30ft, 40ft, 50ft, 60ft, 70ft, 80ft, 90ft, and 100ft. To observe the effect of varying column heights on shafts with different depth to diameter

ratios, an 80ft shaft with L/D=15 and with column heights of: 16ft, 32ft, 48ft, 64ft, 80ft and a 50ft deep shaft with L/D=8.33 with column heights of: 10ft, 20ft, 30ft, 40ft, 50ft was also analyzed.

Figure 1.36 shows the shaft displacement at the ground level for different column heights. As the moment at the ground level is increases, the displacements also increase.

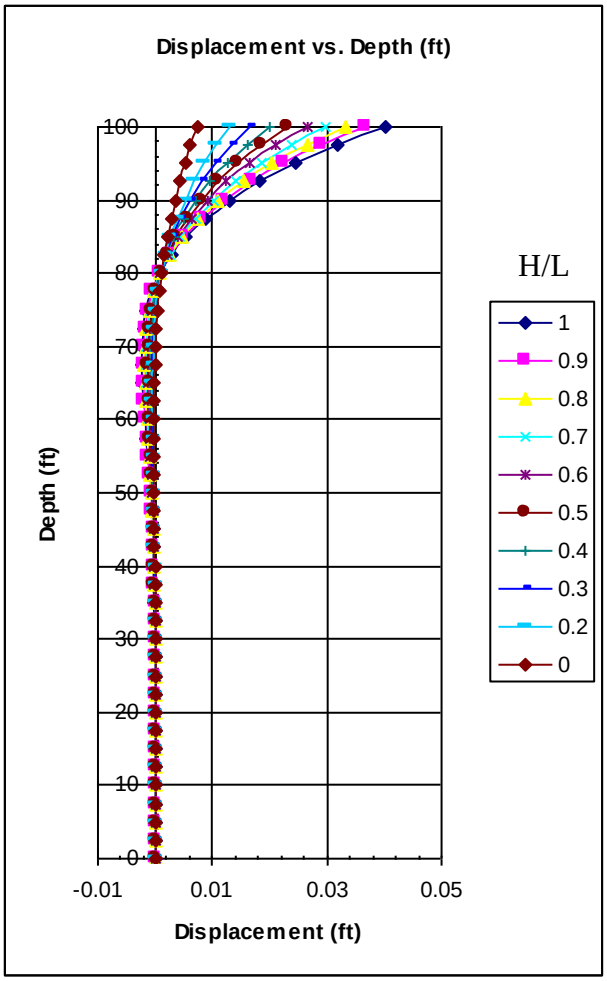

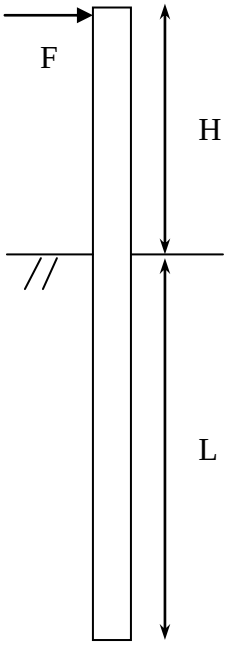

Figure 1.36 – Variation of shaft displacement for various column heights.

The variations of moments and shears are shown in figure 1.37. As the column height increases, the ground level moments become higher and the ratio of maximum moment to ground surface level moment approaches one. Thus the whole region between the point of maximum moment and the ground surface become an equally stressed region. The flexural stresses within the shaft are caused by the ground surface shear; which is equal to the lateral load and the

ground surface moment; which is dependent on the lateral load and the column height. When the column height becomes equal to the shaft depth i.e. H/L=1, the surface moment has the effect of creating a region of constant moment close to the ground surface. This region of maximum moment is also the highest stressed region, which is to display non-linear behavior and plasticity and eventual failure.

If there was no column and only a lateral load was applied at the ground surface of the shaft, the ground surface moment would be zero thus for H/L=0, moment ratio=∞. Thus it can be concluded that the point of maximum moment is dependent on the value of the lateral load as expected. However, the distribution of the moment between this point and the ground surface is dependent on the moment generated at the ground surface level. Figure 1.38 shows the variation of moment ratio and shear ratio with H/L.

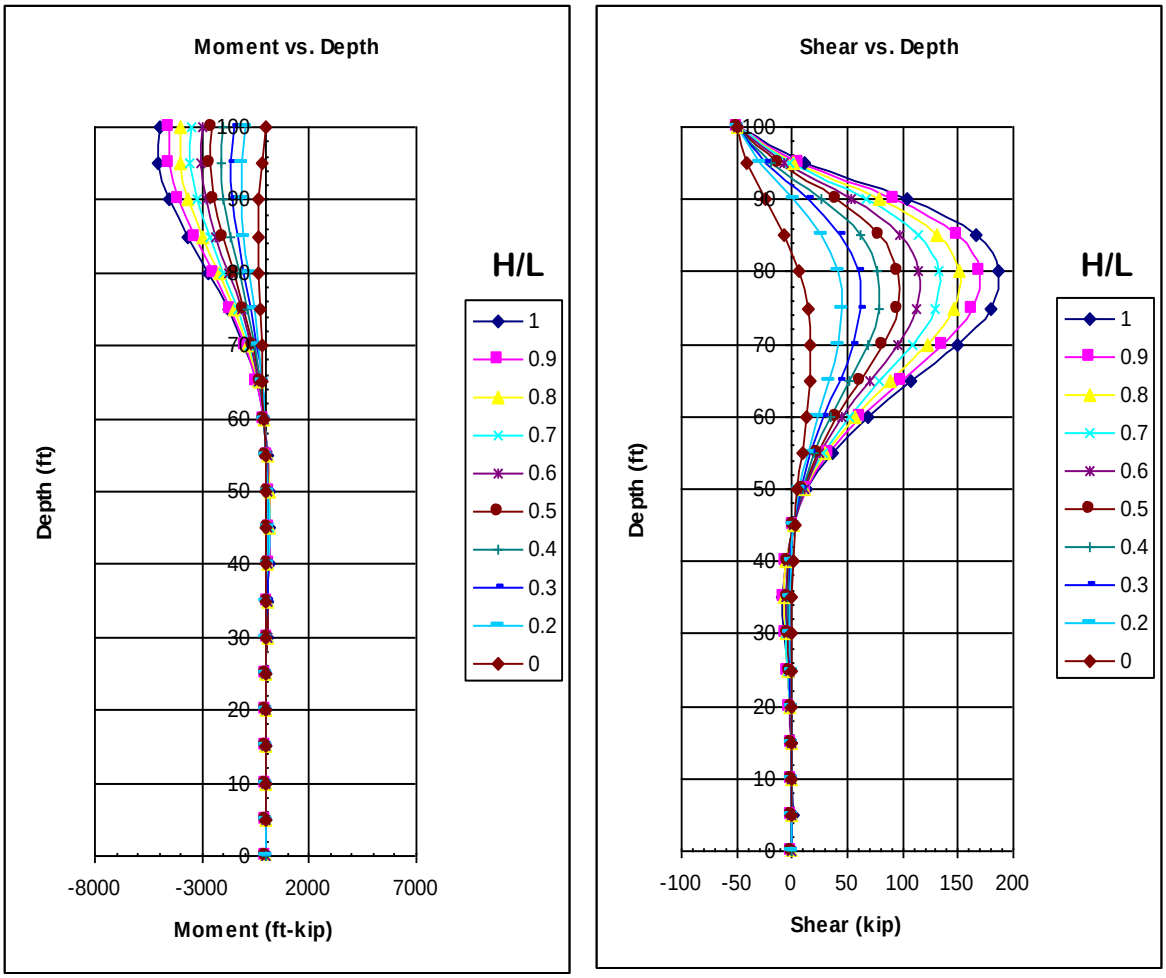

Figure 1.37 – Variation of moment and shear along the shaft various column height.

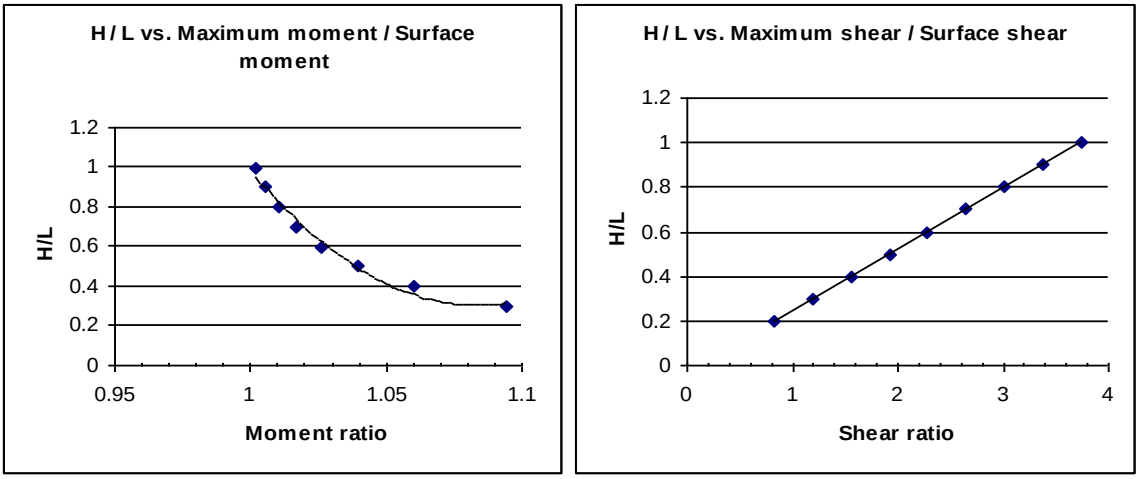

Figure 1.38 – Variations of maximum moment and shear with H/L.

Higher columns result in increased moments that cause higher shears in the shaft. The shear value at the surface is equal to the applied lateral load. However, the distribution of shear along the shaft depth is modified by the displacements caused by the lateral load and the displacements caused by the applied moment. Figure 1.39 shows the variation of soil stresses with depth for various column height to shaft depth ratios. As the column height is increased, the shaft displacements due to higher surface moments are also increased, resulting in higher soil stresses. Soil stresses reach the plastic region at the top layers and the plastic region extends below the surface as the shaft displacements increase.

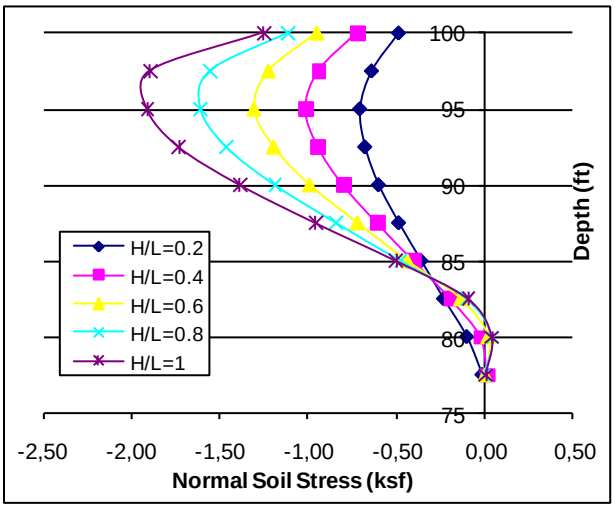

Figure 1.39 – Variation of soil stresses with depth for various H/L

Figure 1.40 shows the displacements for the 80ft shaft with different column heights.

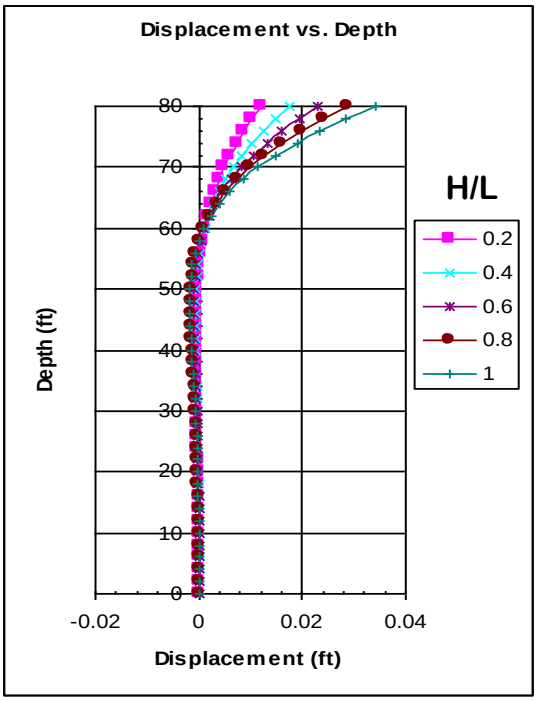

Figure 1.40 – Variation of shaft displacement for various column heights.

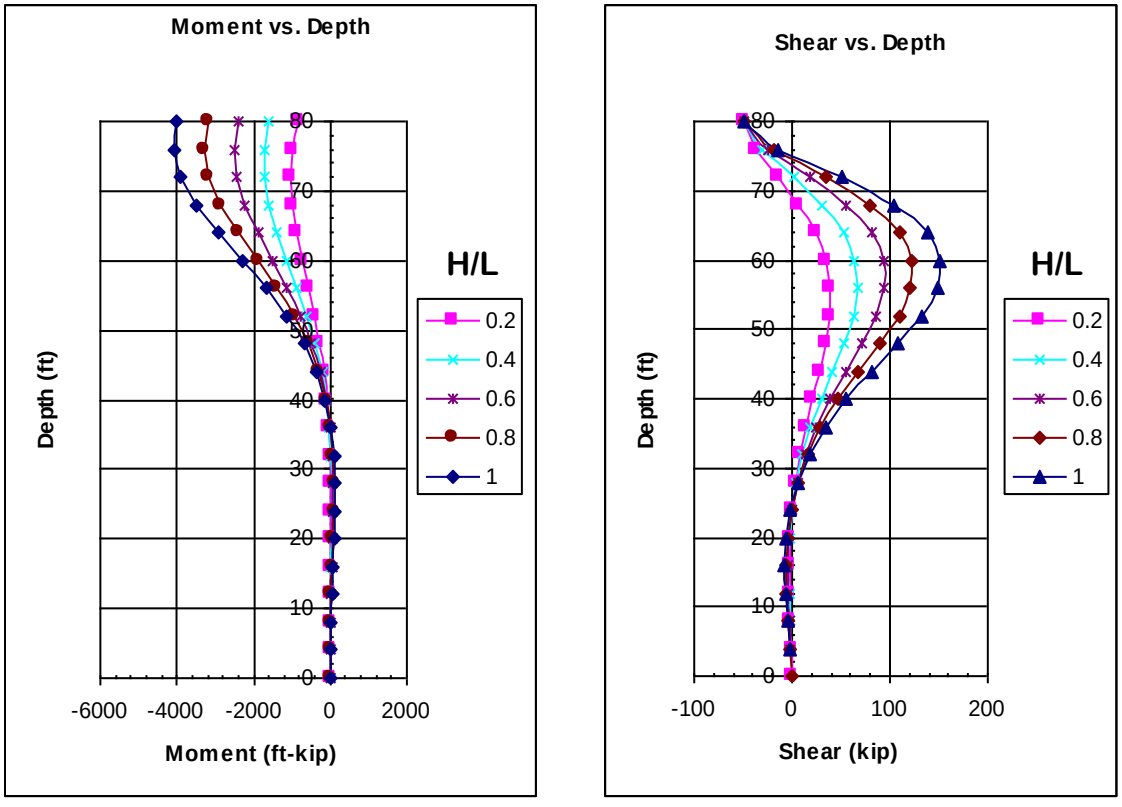

Figure 1.41 – Variation of moment and shear along the shaft various column height.

Variations of moment and shear are shown in Figure 1.41. Figure 1.42 shows the variation of the displacement and figure 1.43 shows the variation of moment and shear for the 50ft shaft. The displacements and moments for different shaft depth to diameter ratio values are combined in figures 1.44, 1.45, 1.46, and 1.47, to summarize the effect of column height on the shaft lateral response to lateral loads.

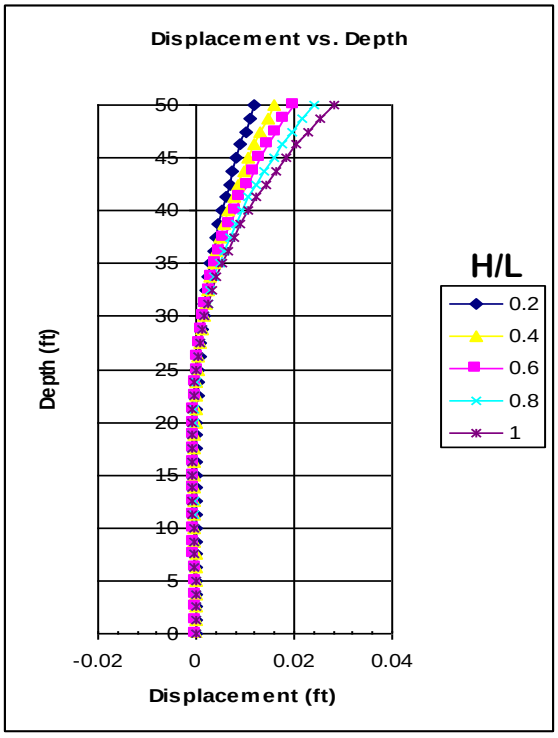

Figure 1.42 – Variation of shaft displacement for various column heights.

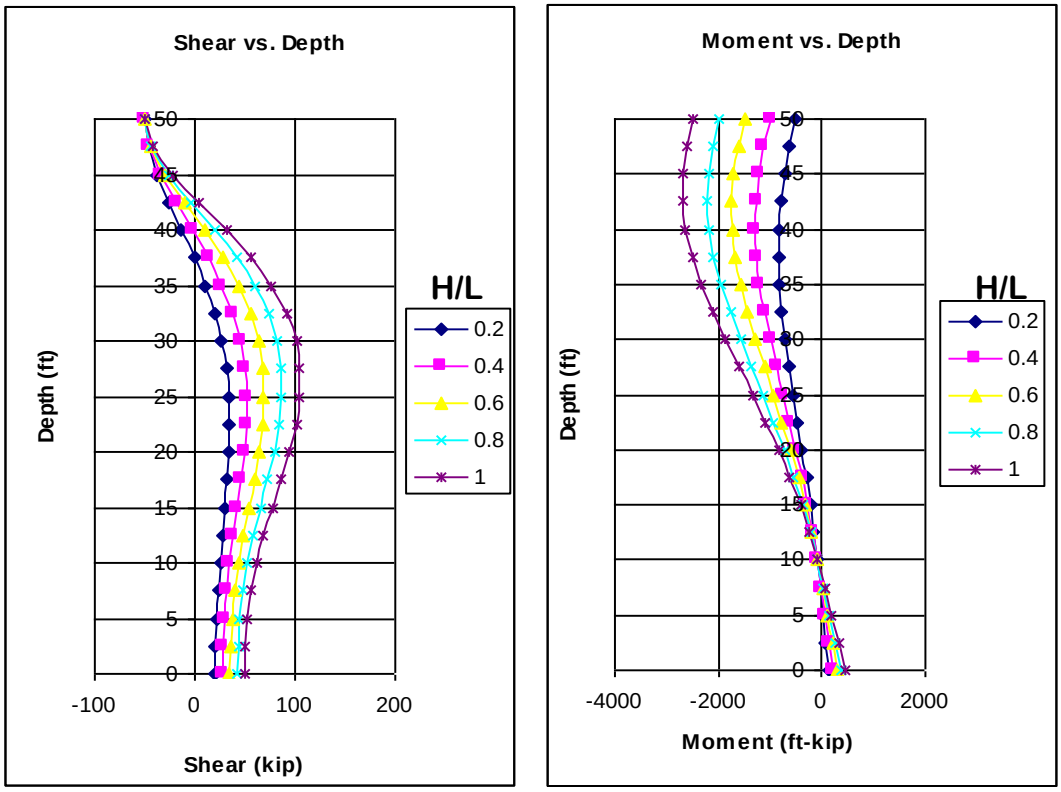

Figure 1.43 – Variation of moment and shear along the shaft for various column heights.

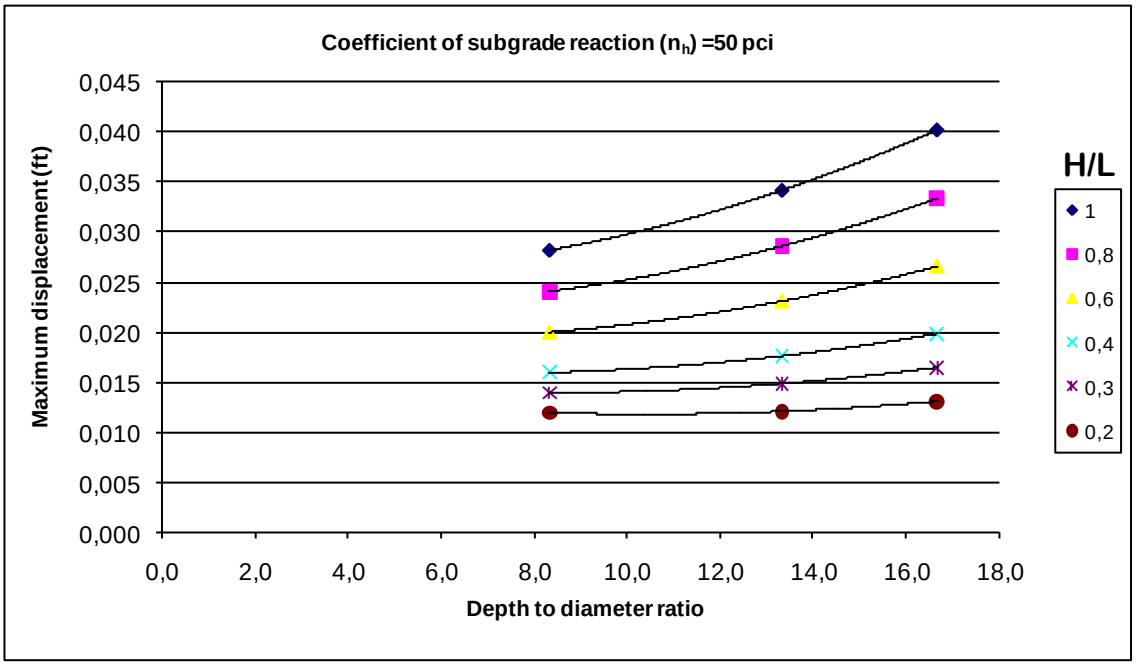

Figure 1.44 – Variation of maximum shaft displacement with shaft slenderness for different column heights

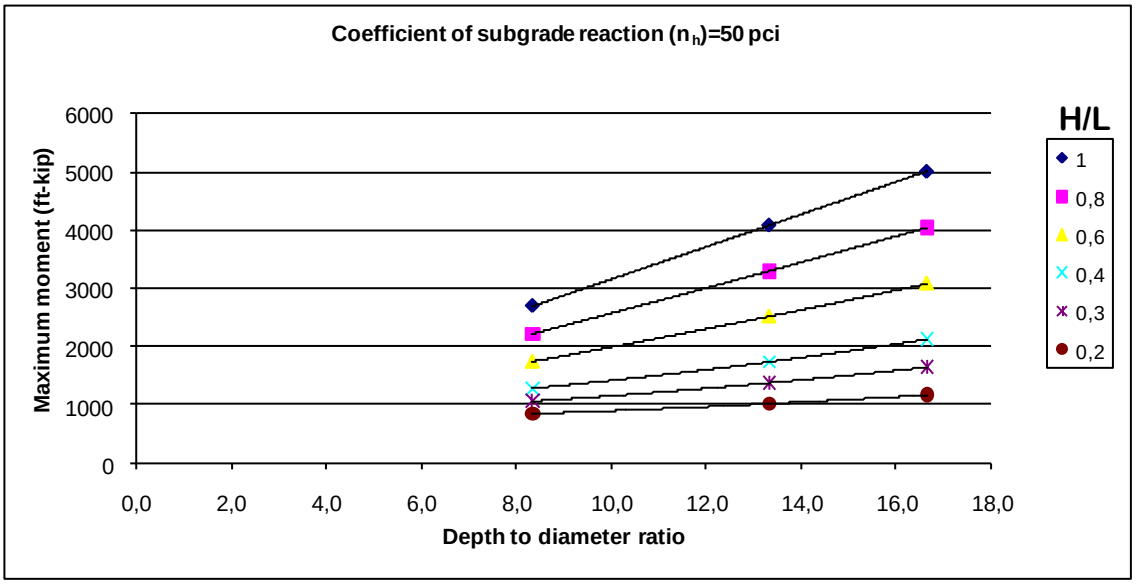

Figure 1.45 – Variation of maximum shaft moment with shaft slenderness for different column heights.

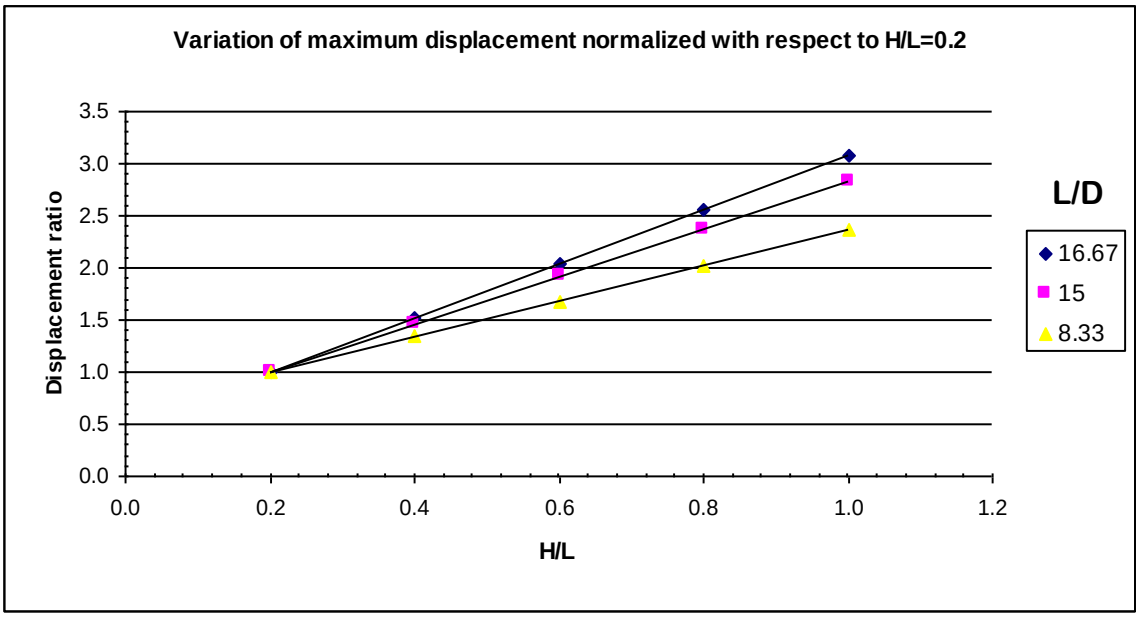

Figure 1.46 – Variation of the maximum displacements normalized with respect to H/L=0.2 with varying column heights.

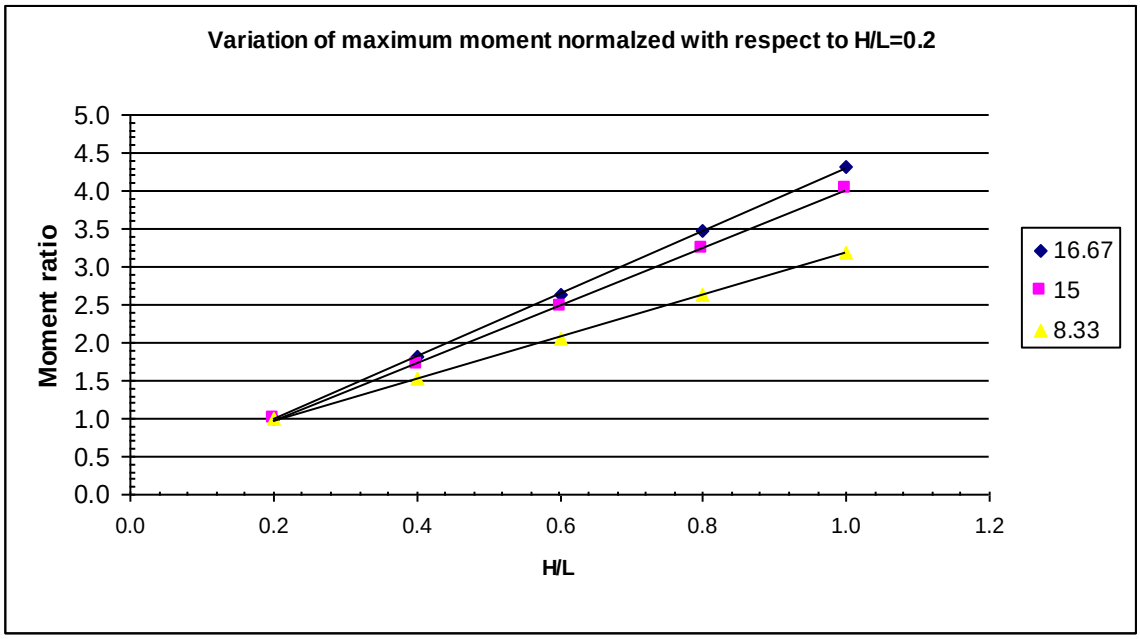

Figure 1.47 – Variation of the maximum moments normalized with respect to H/L=0.2 with varying column heights.

Figures 1.44 and 1.45 show that an increase in column height; increases the maximum displacements and moments. The maximum displacements and moments are normalized with respect to the results obtained for the shaft with H/L=0.2 and plotted in Figures 1.46 and 1.47, which shows that the rate of increase of these parameters is smaller for shorter shafts. The effect of column height on maximum displacements and moments is more significant for slender shafts.

1.9 Effects of Disturbed Soil Adjacent to the Shaft

The soil layers in close proximity to the shaft are disturbed due to drilling and construction. This disturbance weakens the soil along the perimeter of the drilled hole, resulting in lower stiffness values than other surrounding soils. Soil parameters such as elastic modulus in soils adjacent to the shaft are typically smaller. In many cases the design parameters do not reflect the changes that occur during construction phase. The developed FE model of SSI can take into

account such changes in soil properties and their impact on lateral response of the shaft.

A Type-1 model for a 6 ft diameter shaft with 100ft depth and 20ft column height was analyzed with a *weakened zone* around the perimeter of the shaft. Two variables were considered: 1) The extension of the weak layer beyond shaft design diameter, 2) The reduction of elastic modulus within this diameter. Figure 1.48 shows the weakened soil layer around the shaft.

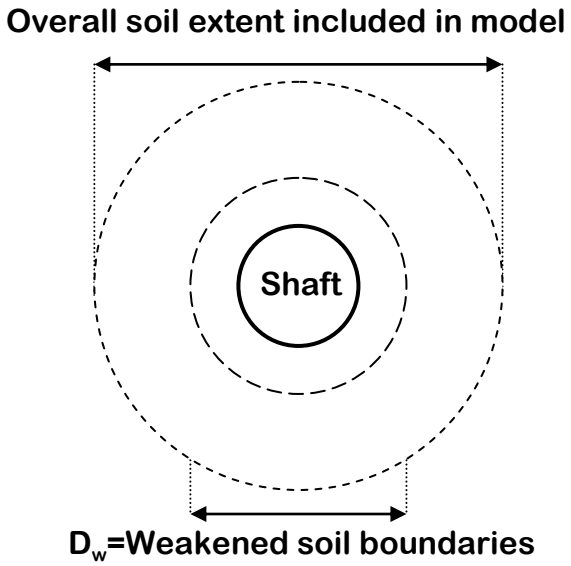

Figure 1.48 – Plan view of shaft and surrounding soil.

Four models were considered to model the extension of this weakened zone and the percentage reduction of elastic modulus within this zone. The weak soil extensions D_{w1} was: 7ft, and 7.5ft. Thus for a 6 ft shaft, 0.5ft and 0.75ft extension of weakened soil layer away from the shaft surface were considered. The percentage reduction in soil modulus within these layers was taken as 50% and 90% of the calculated elastic modulus. The following cases are evaluated:

Case 1: no reduction in elastic modulus (E) (No weak zone)

Case 2: 0.5ft extension with 90% reduction in E: 0.5ft-10%

Case 3: 0.5ft extension with 50% reduction in E: 0.5ft-50%

Case 4: 0.75ft extension with 90% reduction in E: 0.75ft-10%

Case 5: 0.75ft extension with 50% reduction in E: 0.75ft-50%

Figure 1.49 shows the variation in displacement for different cases. The weakest case is case 4 where both the extension and the modulus reduction are at the highest level. The percentage increase in displacements normalized with respect to case of *no reduction* is as follows: Case1: 1, Case2: 53%, Case3: 8%, Case4: 71%, Case5: 11%.

The increase in moment with reduction of soil strength is shown in figure 1.50. The percentage increase in moment with respect to case of *no reduction* is as follows: Case1: 1, Case2: 7%, Case3: 2%, Case4: 10%, Case5: 2%.

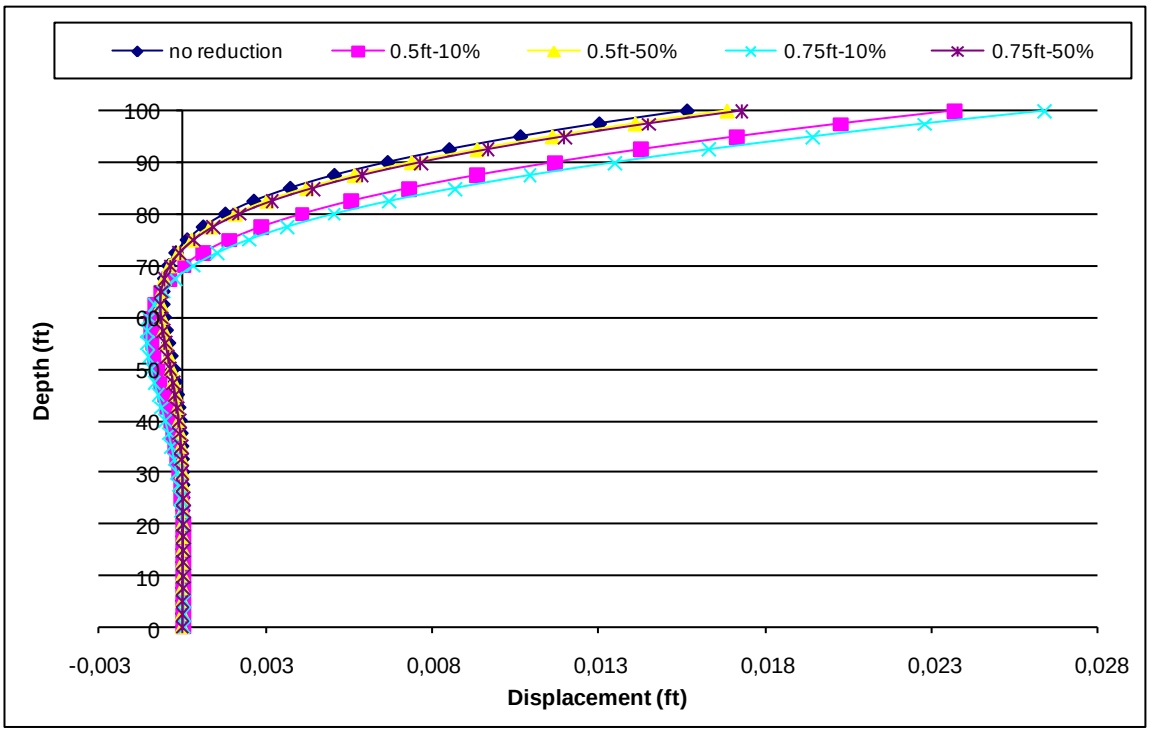

Figure 1.49 –Variation in shaft displacement for various cases of weak soil conditions around the shaft.

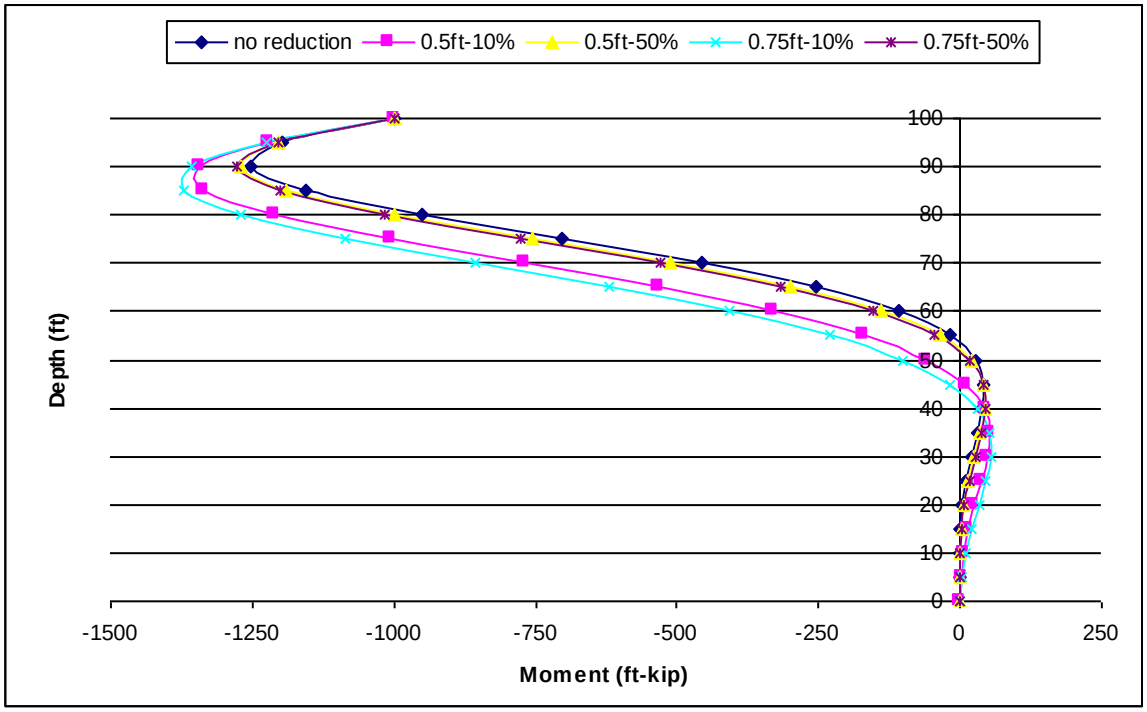

Figure 1.50 – Variation in shaft moments for various cases of weak soil conditions around the shaft.

The higher moment is due to larger displacements experienced by the shaft in weaker soils. Thus the shaft is sharing a larger portion of the overall lateral load resisting capacity of the SSI system.

The decrease in internal shear with reduction of soil strength is shown in figure 1.51. The percentage decrease in internal shear with respect to case of *no reduction* is as follows:

Case1: 1, Case2: 4%, Case3: 2%, Case4: 7%, Case5: 2%. The highest shear is the one corresponding to the undisturbed soil condition.

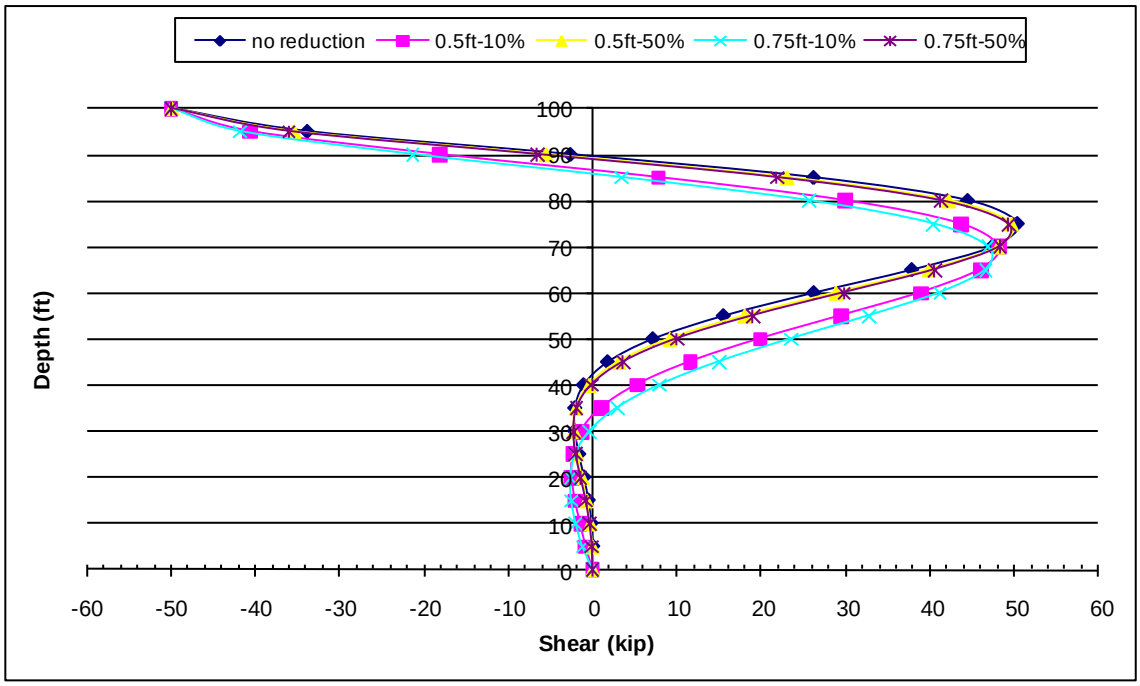

Figure 1.51 – Variation in shaft shears for various cases of weak soil conditions around the shaft.

1.10 Effects of Separation at the Soil-Shaft Interface

Design capacity of a deep-foundation can change with time due to many factors. One reason for strength reduction in lateral capacity of shafts is the separation at the interface due to cyclic loads. After repetitive lateral displacement with time cohesive soils tend to push away and compact the soil close to the shaft surface thus creating a separation at the previously contacting surfaces. Such a surface separation increases the length of the column. The previously calculated column length for lateral loads from the ground level now extends beneath the ground, thus increasing the displacements, moments and shears. To investigate the effects of surface separation, a 6ft diameter and 100ft deep shaft was analyzed under a lateral load of 50 kips with the immediate soil close to the shaft surface being removed at 2.5 ft increments from the ground surface down to a depth of 15 ft. Figure 1.52 shows the variation of displacement for varying depths of surface separation. As expected, deeper surface separation results in larger displacements.

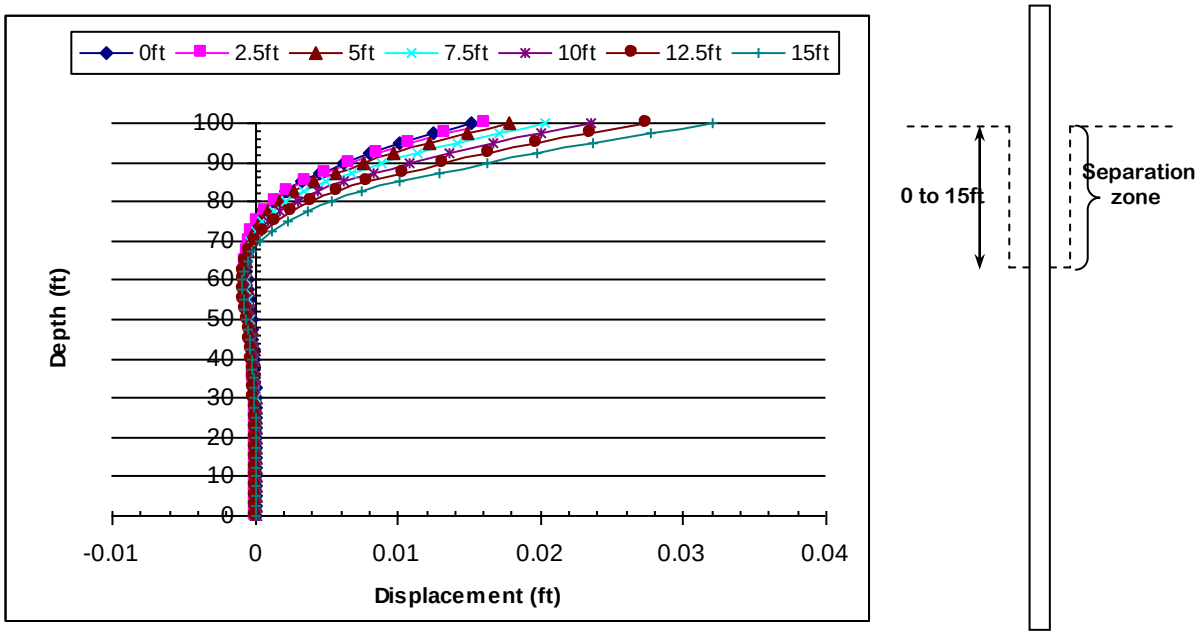

Figure 1.52 – Displacement variation along the shaft for varying surface separations.

The variation of shear and moment is shown in figure 1.53. Loss of soil support results in higher moments and shear along the shaft. The percentage increase in maximum displacements, shears and moments is tabulated in table 1.1.

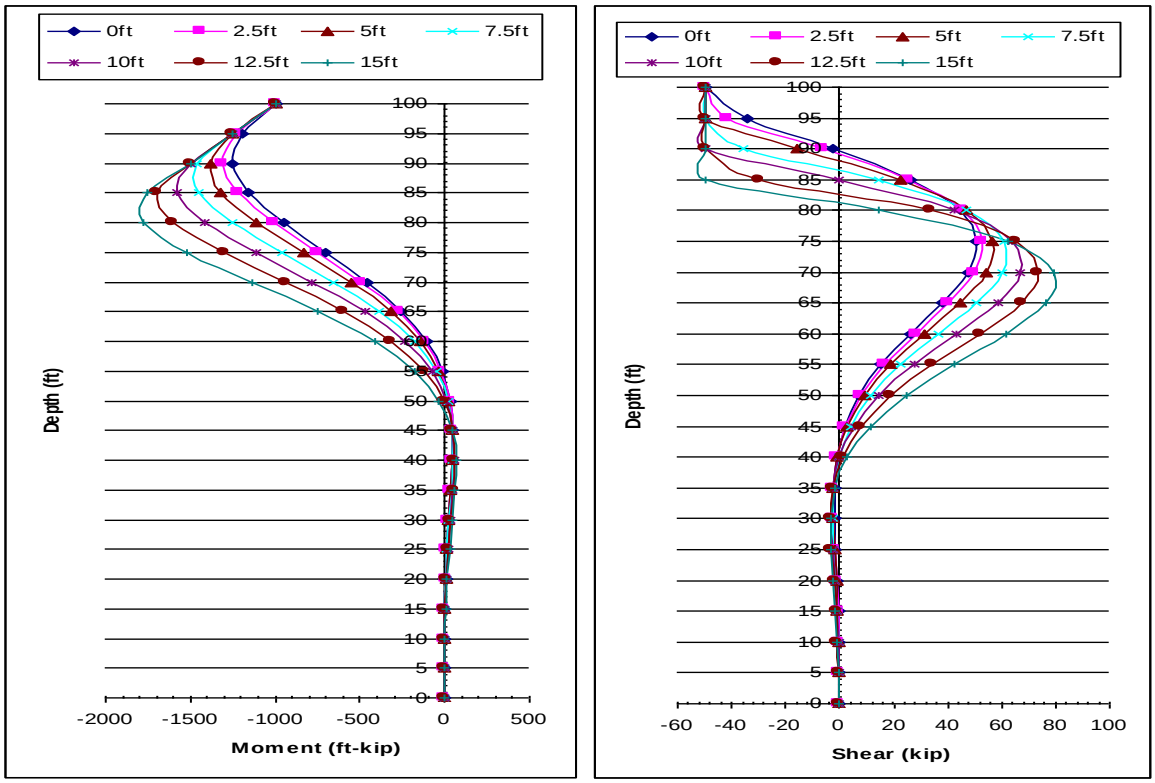

Figure 1.53 – Variation of shear and moment along the depth for varying surface separation

Table 1.1 – Variation in displacement, moment and shears values with separation.

	Separation Depth (ft)					
% increase	2.5	5	7.5	10	12.5	15
Displacement	4.8	13.2	24.5	38.5	54.9	73.7
Moment	4.2	10.6	16.9	26.4	35.8	42.3
Shear	4.3	10.6	16.7	24.5	31.2	36.2

1.11 Displacement and Moment Diagrams of Laterally Loaded Shafts.

Behavior of shafts with different sizes under increasing loads was analyzed in this section. Five shafts with varying depths (L) of: 100ft, 80ft, 60ft, 50ft, and 20ft with 6 ft diameter and 20ft column height were analyzed in dense sand with n_h=50pci. The applied lateral loads (F) at the column tip were: 50kip, 100kip, 150kip, 200kip, 250kip and 300kip. The load-displacement behavior of the soil and the column was assumed to be elastic perfectly plastic behavior. Analyzes was conducted for free head shafts.

The variations of displacements, moments and the shears along the shaft depth from the FE analysis were based on many interactions and many structural properties typically not considered by simple methods such as the spring model. The variation of the moments as well as the maximum value and the locations of maximum moment and the contraflexure points are dependent on the stiffness of the soil and the shaft as well as their material properties. Multiple FEA was conducted to demonstrate the effectiveness of the developed FE model in the modeling soil-shaft system. Figures 1.54 through 1.59 show the variation of displacements, moments and shears along the shafts for different depths under variable lateral loads. A discussion will be provided following these figures.

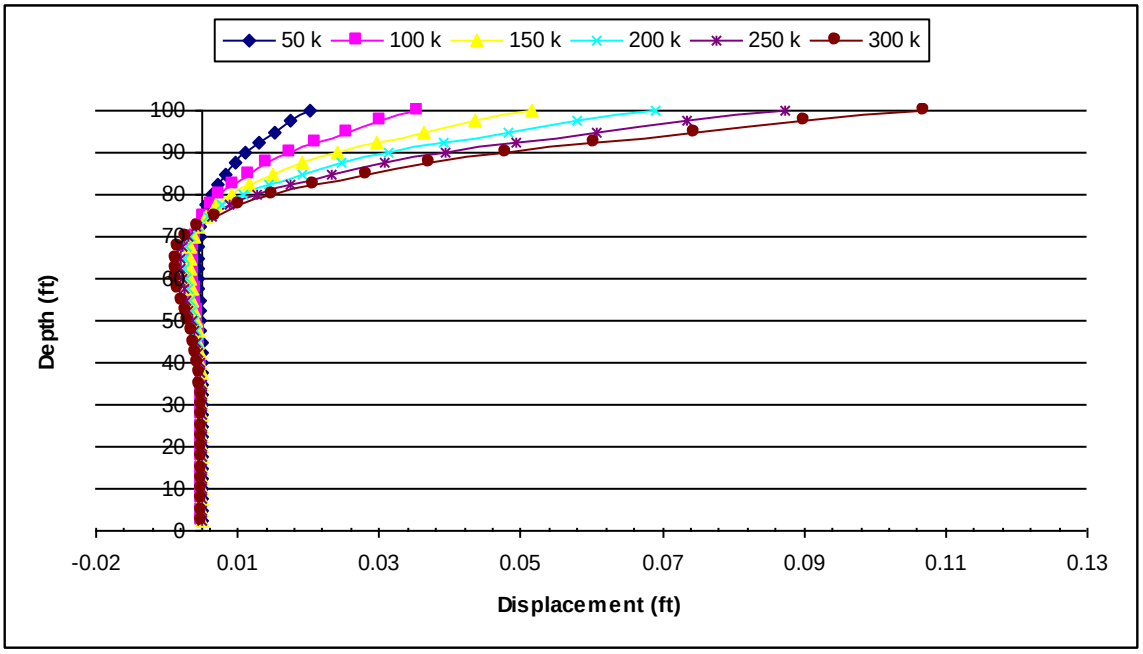

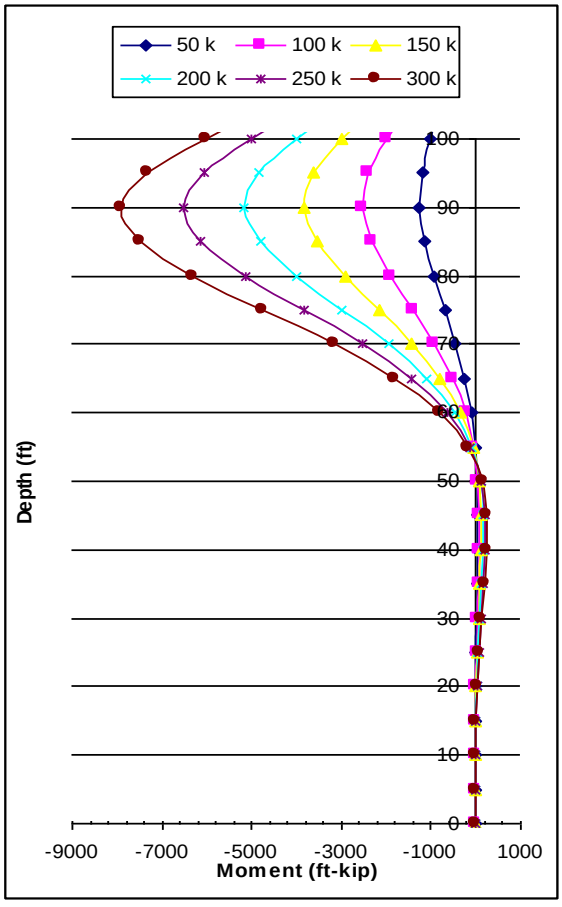

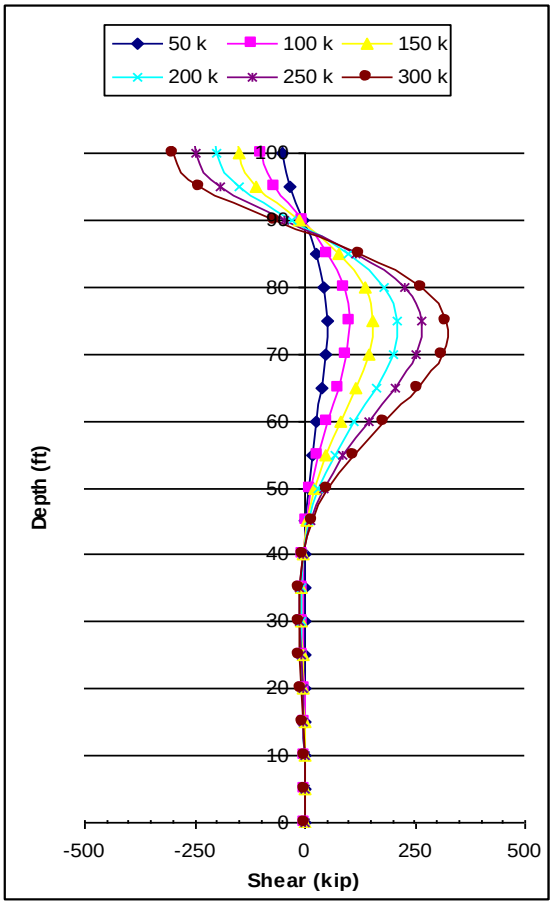

Figure 1.54 – Displacement, moment and shear diagrams for 100ft deep shaft.

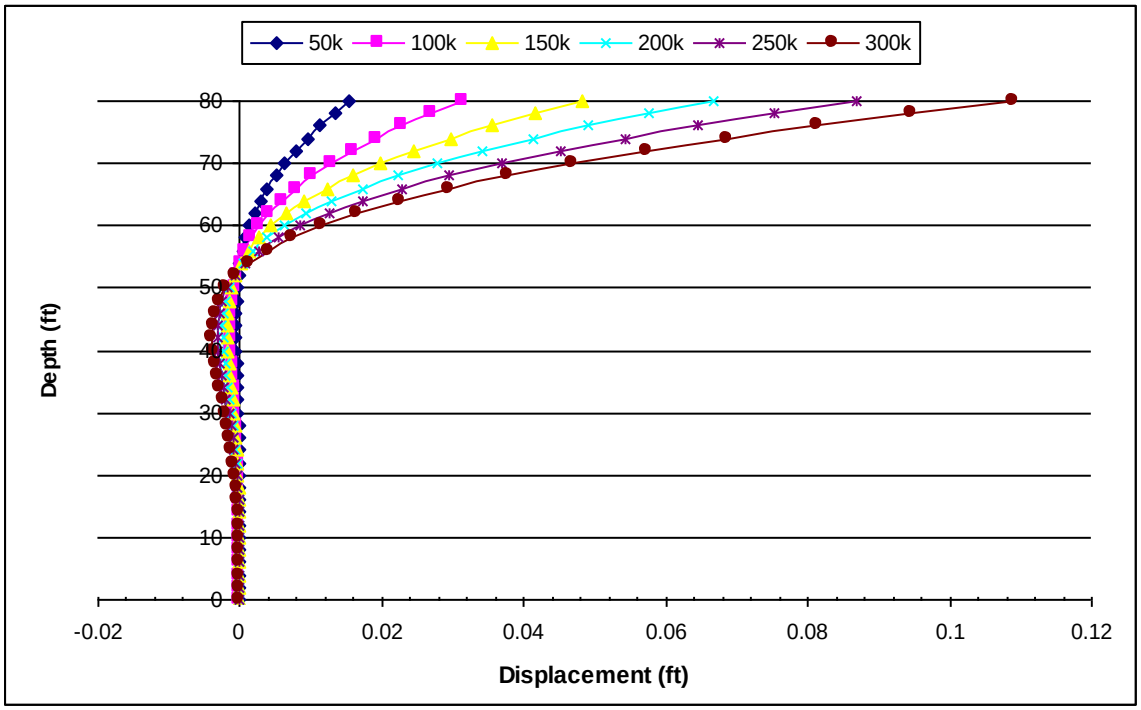

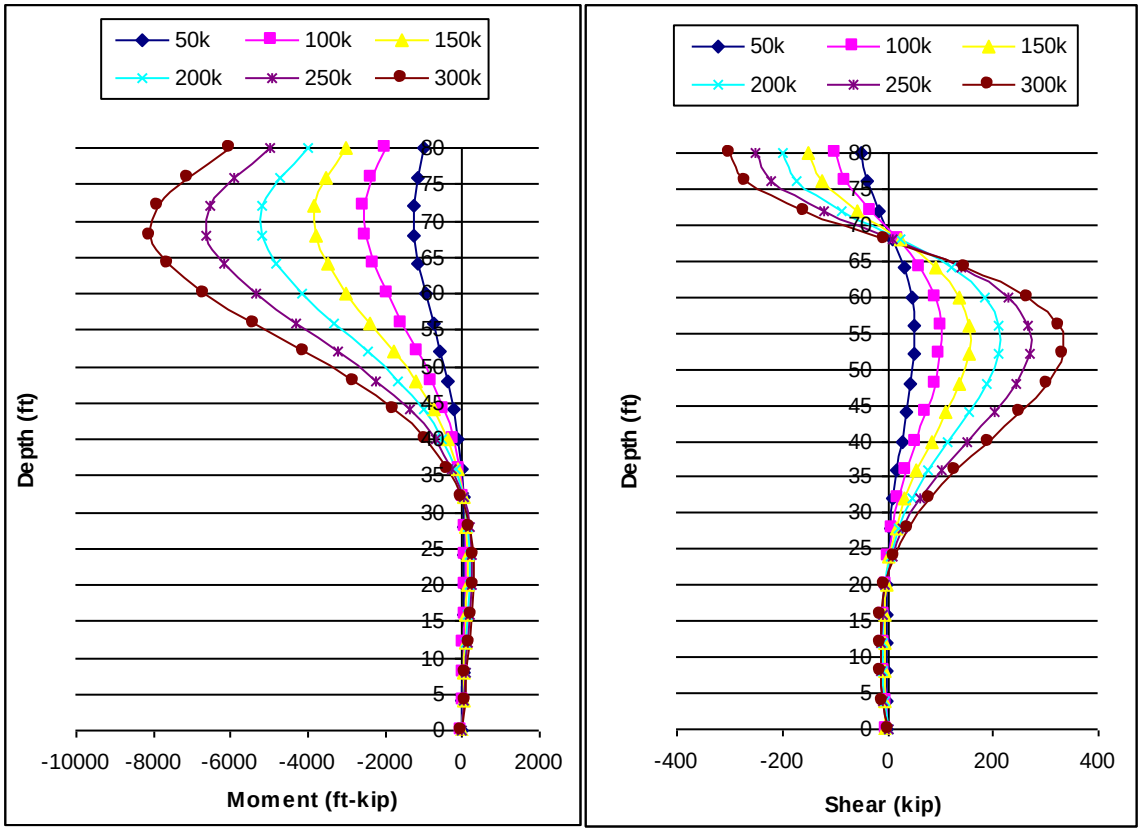

Figure 1.55 – Displacement, moment and shear diagrams for 80ft deep shaft.

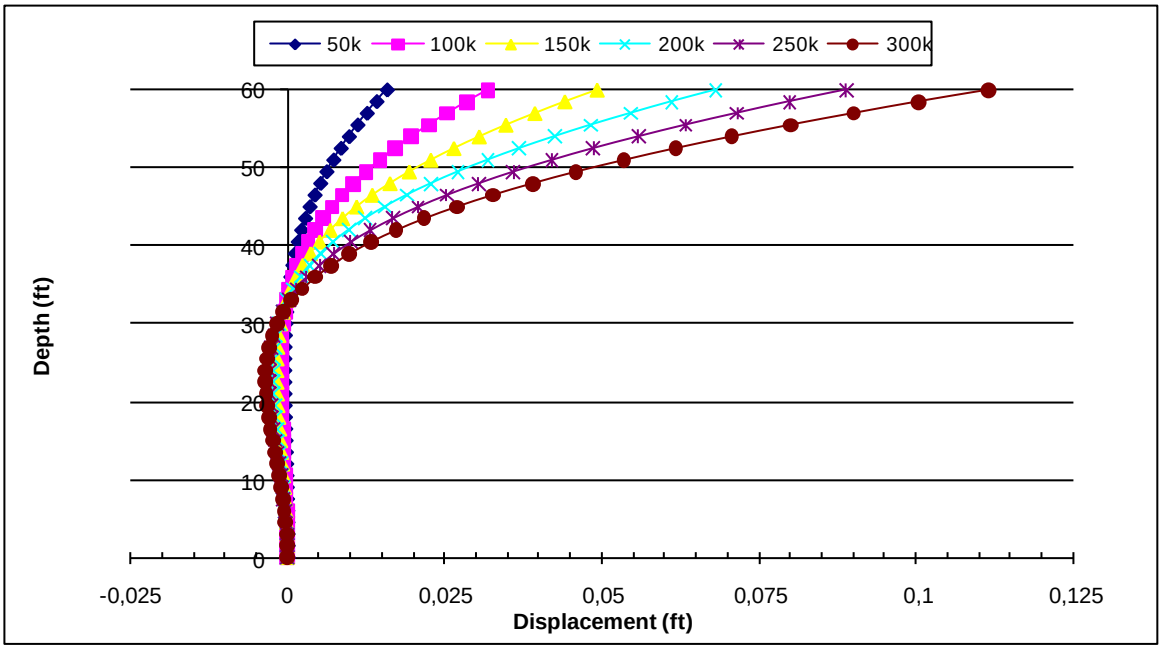

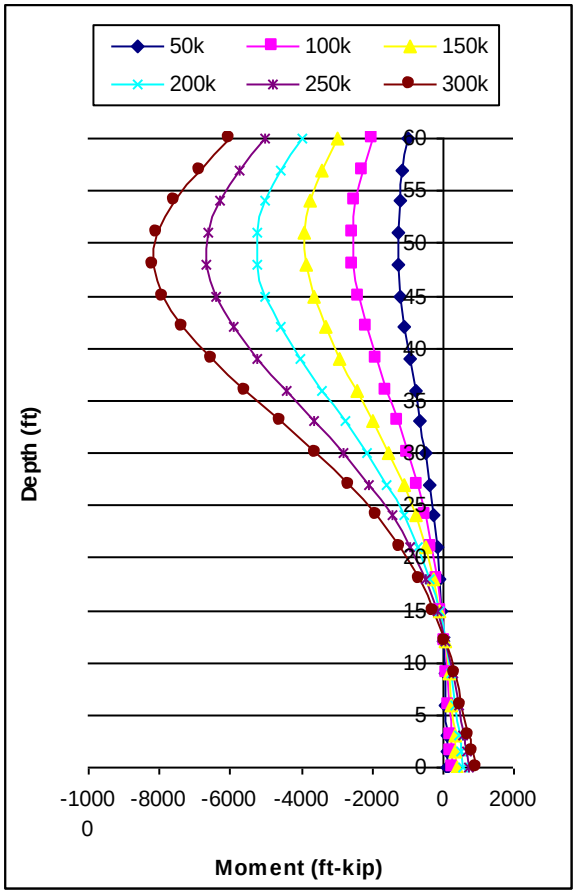

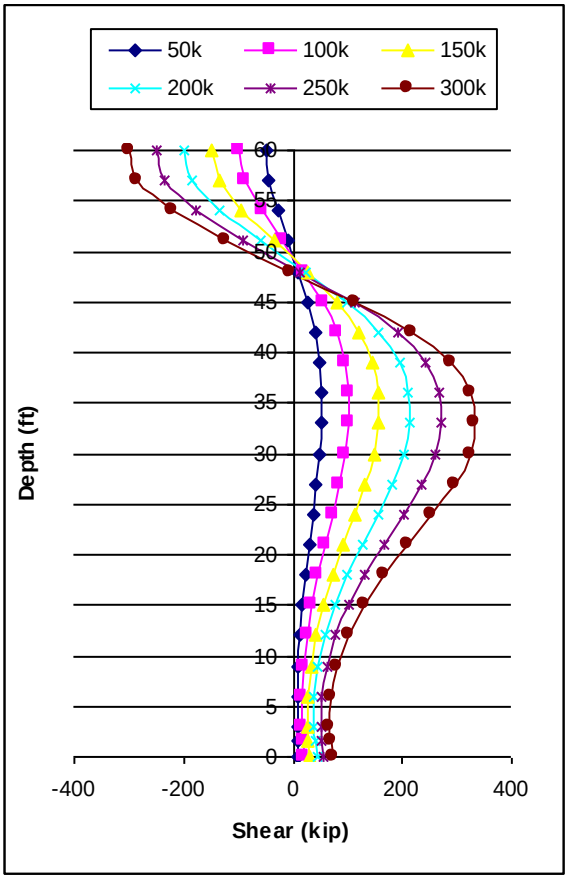

Figure 1.56 – Displacement, moment and shear diagrams for 60ft deep shaft.

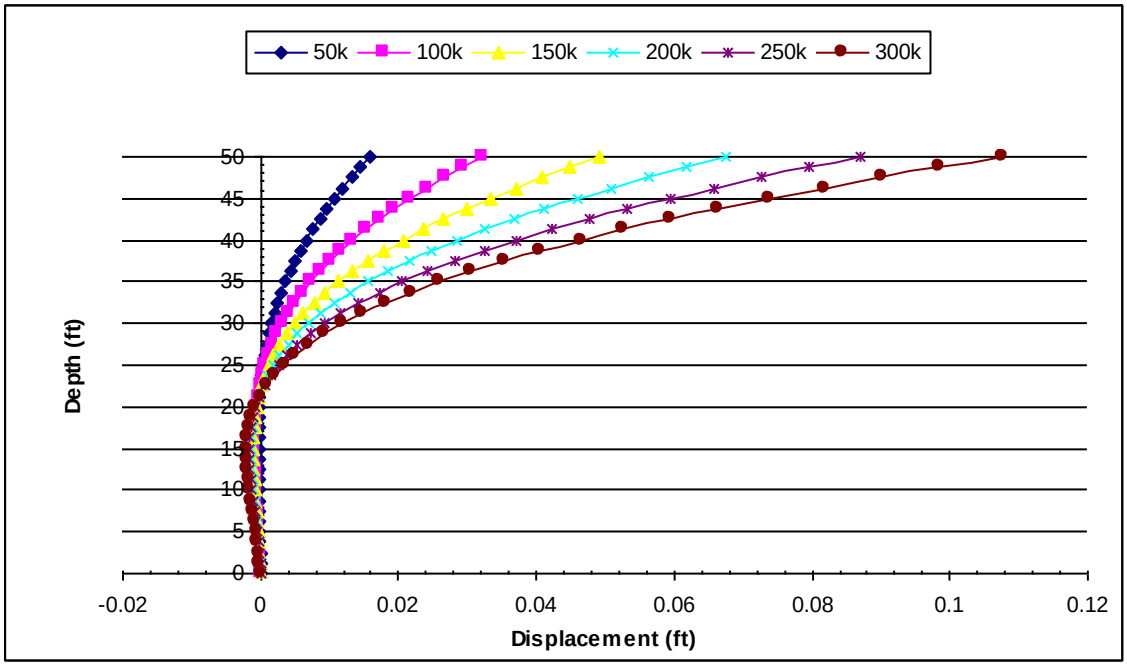

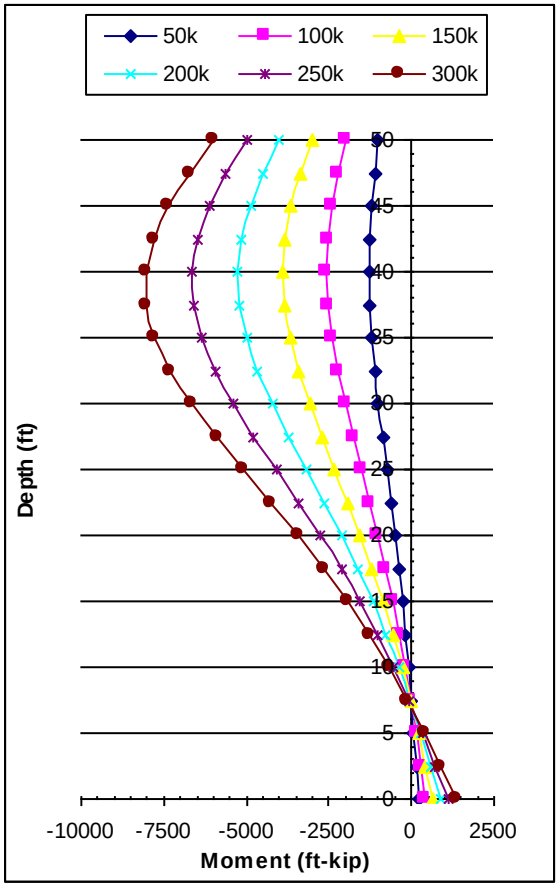

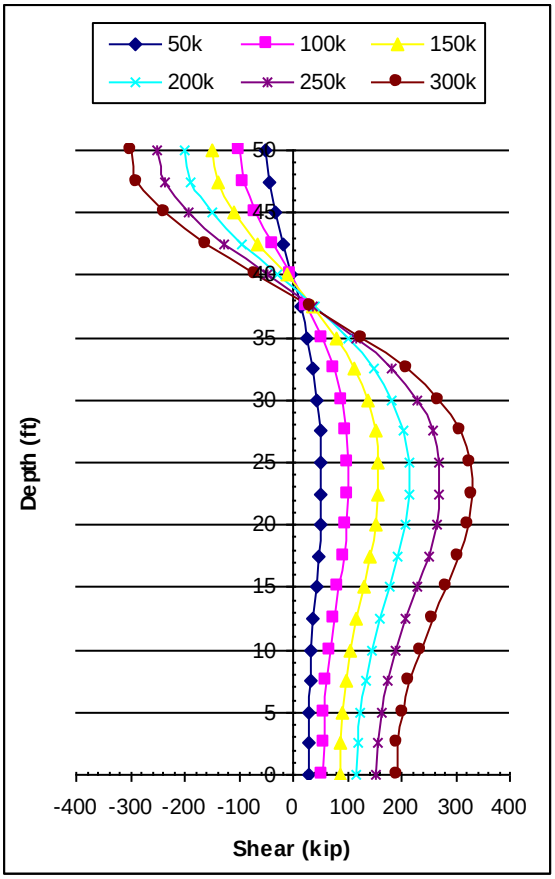

Figure 1.57 – Displacement, moment and shear diagrams for 50ft deep shaft.

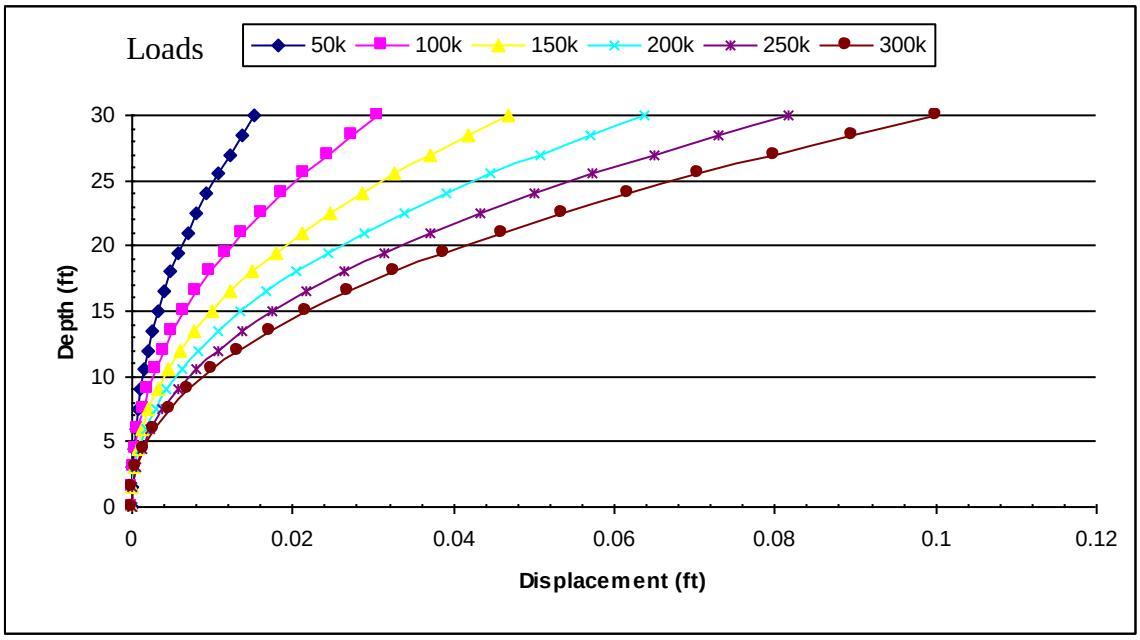

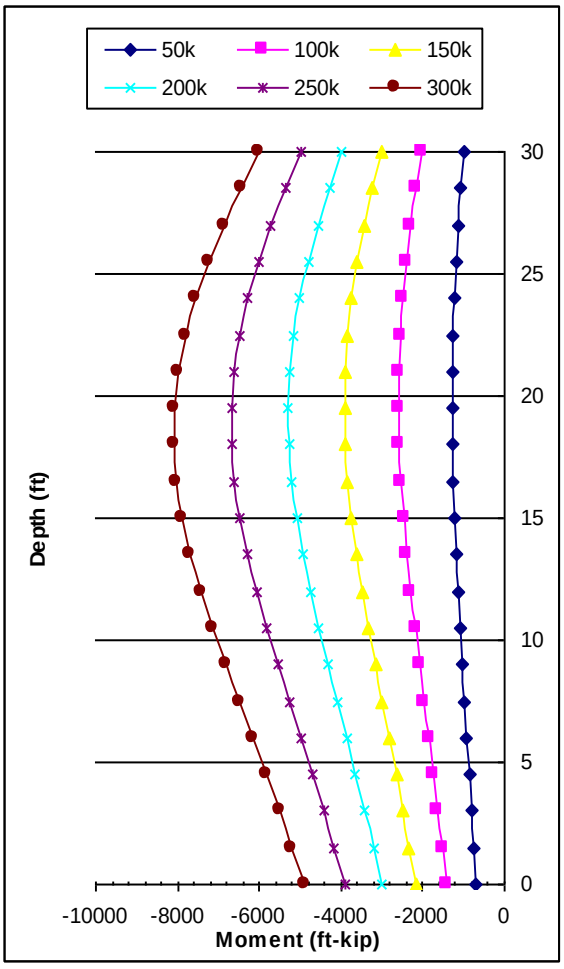

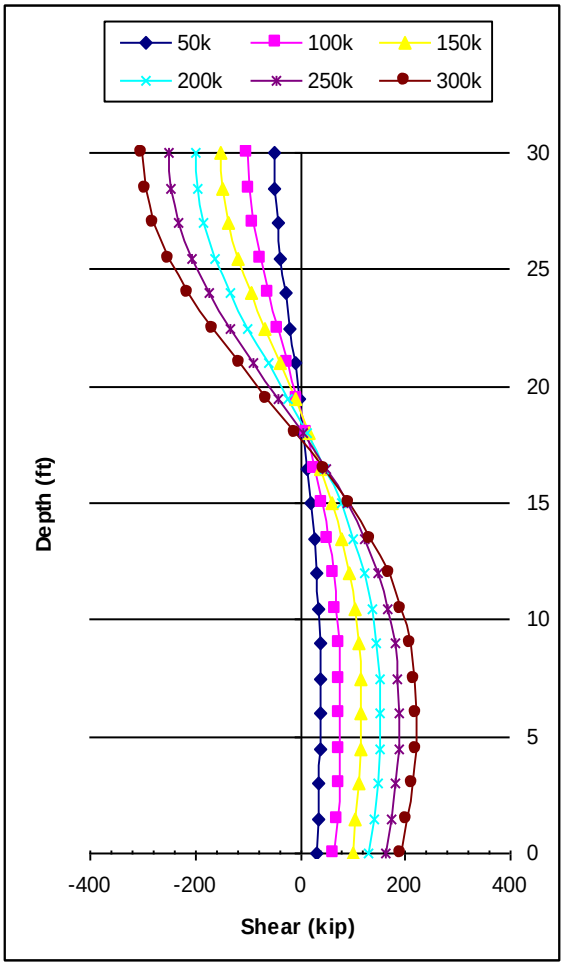

Figure 1.58 – Displacement, moment and shear diagrams for 30ft deep shaft.

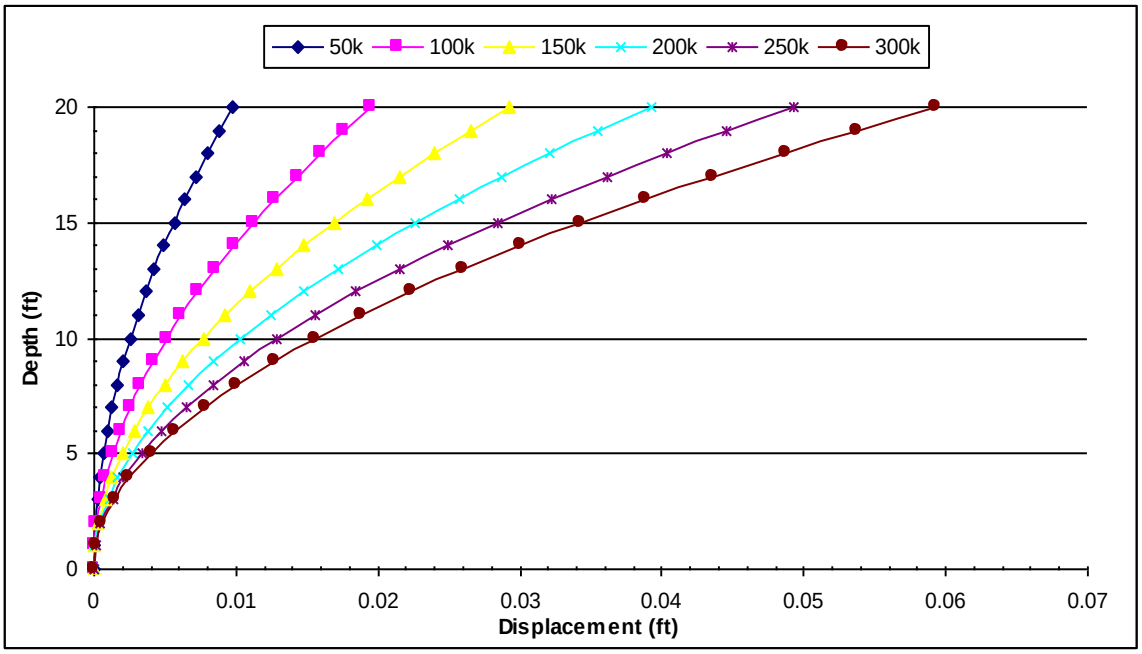

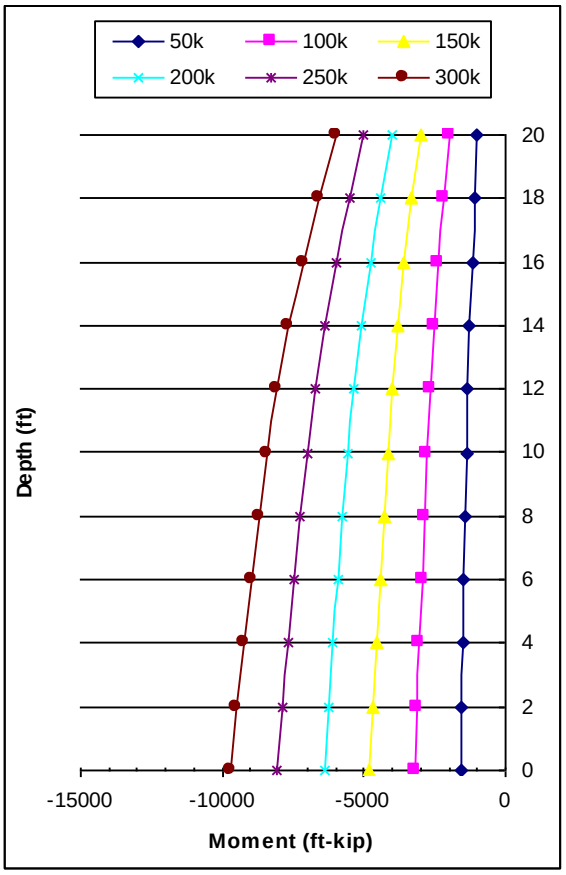

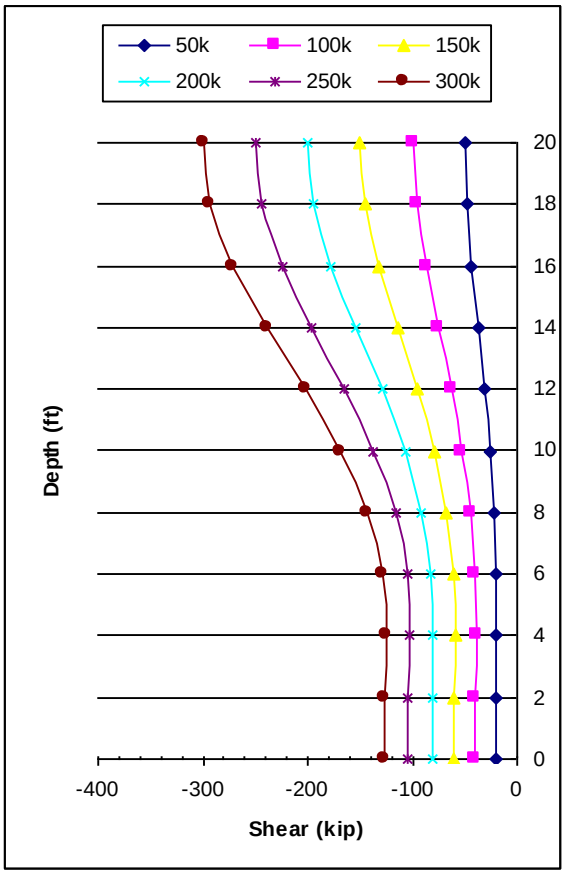

Figure 1.59 – Displacement, moment and shear diagrams for 20ft deep shaft.

FEA gives information about the distribution of displacement, moment and shear along the shaft depth. These values are dependent on many parameters that were considered so far in this chapter. Approximate methods have been used to estimate the response of the shaft and to simplify analysis of deep foundations. One such method is the use of the concept of *length of fixity* to determine the location and magnitude of the maximum moments, which is related to the stiffness values of the shaft and the soil. This concept removes the surrounding soil around the shaft and assumes that the shaft is fixed at a certain length below the ground.

The *equivalent cantilever behavior* is a procedure for deep foundations, where the foundation is replaced by cantilever with an equivalent depth to fixity. In this method the shaft is modeled as a freestanding cantilever or a built in beam. Table 1.2 compares the depth of fixity for moments calculated using the approximate method and those obtained using the FE model. The depth of fixity from the equivalent cantilever method is found as follows: The relative stiffness factor (T) is calculated for the cohesionless soils from equation (36) in the book "An Insight into the Theoretical Background of SSI". [$(T=(EI/n_h)^{1/5}$]. Where the E is the elastic modulus and I is the moment of inertia of the shaft and n_h is the coefficient of subgrade reaction of the soil. The approximate method is applicable for slender shafts such that L/T > 5. The depth of fixity (L_m) for free-headed shafts to find the maximum moment is: $L_m=0.8T$.

Unlike the cantilever method; the FE analysis considers the flexural stiffness, the plasticity of the materials, and the support conditions. Note the change in the location of maximum moment from FEA results, where the depth of fixity is constant according to the equivalent cantilever method.

For slender foundations, the differences in the results from the FEA and the equivalent cantilever method become significant. For shaft with L/D=15 and L/D=10

the estimated location of maximum moments are off by approximately 15% to 25%. For stout shafts, the method is not applicable

Table 1.2 is tabulated for various shaft heights with the following parameters: E=3.600.000psi, I=1.320.000in^4 and n_h=50pci, which resulted in T=156.87in.

Table 1.2 – Equivalent depth of fixity of 6 ft diameter shafts by equivalent cantilever method and location of maximum moment through FEA.

		L_m from FEM						L_m from equivalent cantilever method
		Load (kip)						
L (ft)	L/T	50	100	150	200	250	300	
100	7.6	*10*	*10*	*10*	*10*	*10*	*10*	*10.5*
80	6.1	*8*	*8*	*8*	*12*	*12*	*12*	*10.5*
60	4.6	*9*	*9*	*9*	*9*	*12*	*12*	*10.5*
50	3.8	*10*	*10*	*10*	*10*	*10*	*10*	*N/A*
20	1.5	*20*	*20*	*20*	*20*	*20*	*20*	*N/A*

Another observation is that, as the depth to diameter ratio of the shaft decreases, the moments at the support become significant. The ratio of the support moment to the maximum moment versus the depth to diameter ratio of the shaft is shown in figure 1.60. For slender shafts (L/D>15), the effect of the support at the bottom of the shaft on the moments is insignificant for a wide range of soil strengths. However, for shafts less than 60ft deep (L/D=10), the support moments are significant and are about 13% of the maximum moment. For lower depths such as the 50ft shaft (L/D=8.3), the support moment becomes approximately 22% of the maximum moment. For 30ft shaft (L/D= 5), the support moment is approximately 75% of the maximum moment. For 20ft deep shaft (L/D=3.33), the support moment becomes the largest moment along the shaft.

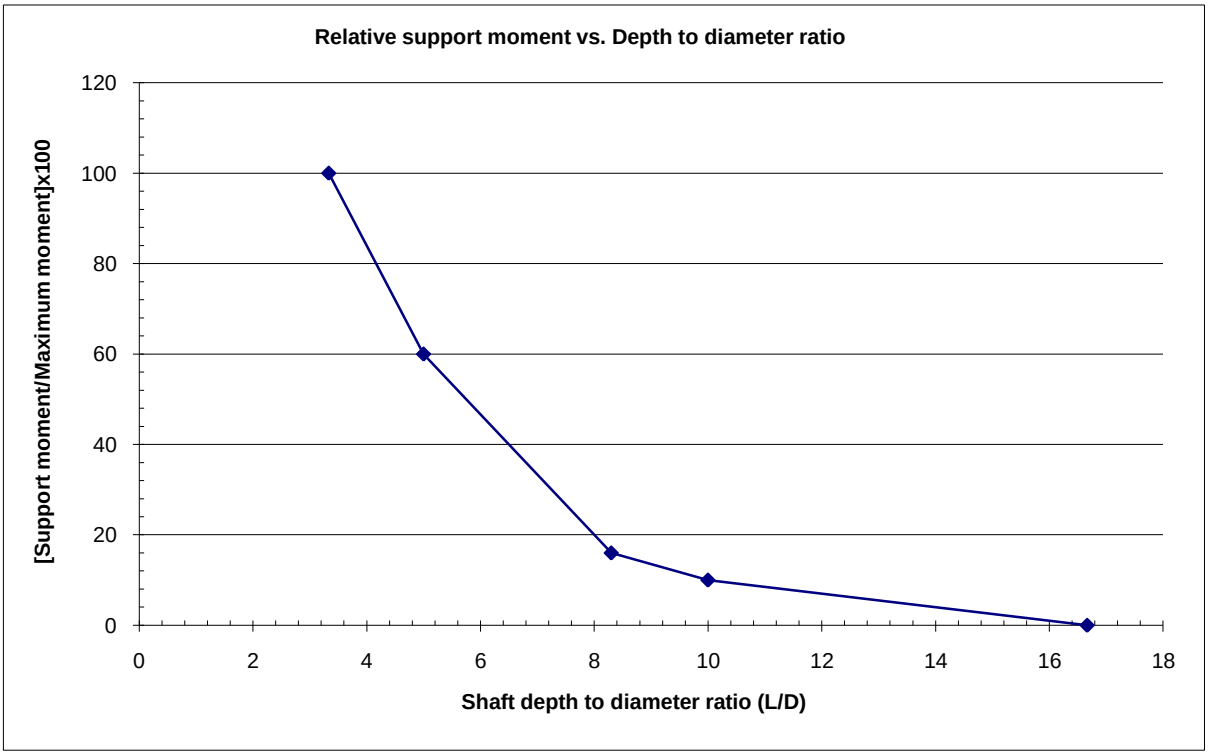

Figure 1.60 – Ratio of support moment to maximum moment versus shaft depth to diameter ratio.

REFERENCES

1. ABAQUS Standard/Explicit Manuals versions 6.3&6.4

2. Anderson, Townsend. (2002) "A Laterally Loaded Pile Database". Deep Foundations 2002: An International Perspective on Theory, Design, Construction, and Performance pp. 262-273

3. Baker (1993). "Use of Pressuremeter in Mixed Highrise Foundation Design". Design and Performance of Deep Foundations: Piles and Piers in Soil and Soft Rock pp. 1-13

4. Boulanger, Hutchinson, Chai, Idriss (2004). "Estimating Inelastic Displacements for Design: Extended Pile-Shaft-Supported Bridge Structures" Earthquake Spectra, Vol. 20, No. 4, pp. 1081-1094.

5. Bowles (1997). "Foundation Analysis and Design 5th Edition" MacGraw-Hill Companies

6. Briaud, Buchanan (2000) "Introduction to Soil Moduli".

7. Briaud, L.L., Smith, T.D. Tucker, L. (1985). "Pressuremeter Design Method for Laterally Loaded Piles," Proceedings of the XI International Conference on Soil Mechanics and Foundation Engineering, San Francisco, CA, U.S.A.,

8. Briaud, Johnson, Stroman (1984). "Lateral Load Test of an Aged Drilled Shaft" Laterally loaded deep foundations: Analysis and performance, STP 835 pp. 172-181

9. Britto, Gunn, (1987) Critical State Soil Mechanics Via Finite Elements Ellis Horwood Limited

10. Chen, Liu (1990). "Development in Geotechnical Engineering 52 -Limit Analysis and soil plasticity" -Elsevier Publishing

11. Chen, Mizuno (1990) "Developments in geotechnical engineering53 -Nonlinear Analysis in Soil Mechanics Theory and Implementation"- Elsevier Publishing

12. Chen (1975) "Development in Geotechnical Engineering 7 -Limit Analysis and soil plasticity"- Elsevier Publishing

13. Choi, Oh, Kwon, Kim. (2002) "A Numerical Analysis for Axial and Lateral Behavior of Instrumented Steel Pipe Piles". Deep Foundations 2002: An International Perspective on Theory, Design, Construction, and Performance pp. 289-304

14. Cook, Malkus, Plesha, Witt (2002). "Concepts and Applications of Finite Element Analysis 4th Edition" John Wiley and Sons Inc.

15. Dameron, Arzoumanidis, Bennett, Malik (1999). “Seismic Analysis and Displacement Based Evaluation of the Brooklyn-Queens Expressway”.

16. Das (1999) “Principles of Foundation Engineering 4th edition” PWS Publishing

17. Dessai, Abel (2002). “Introduction to Finite Element Modeling”. CBS Publishers & Distributers

18. Duggal, Bohinsky, Chu. (1989) “Comparative Performance of Two Pile Types” Foundation Engineering, pp. 943-956

19. Habigaghi, K. and Langer, J.A. (1984). “Horizontal Subgrade Modulus of Granular Soils”. Laterally loaded deep foundations: Analysis and performance, STP 835 pp. 21-34

20. Horvath, (1984). “Simplified Elastic Continuum Applied to the Laterally Loaded Pile Problem”. Laterally loaded deep foundations: Analysis and performance, Laterally loaded deep foundations: Analysis and performance, STP 835 pp. 229-238

21. Horvath J.S. (2002) “Soil-Structure Interaction Research Project:Basic SSI Concepts and Applications Overview” Report No. CGT-2002-2

22. Huang, Ye, Tang. (2002) “Dynamic Coupled Analysis for Earthquake Response of Pile Foundations”. Deep Foundations 2002: An International Perspective on Theory, Design, Construction, and Performance pp. 396-404

23. Kappos, Sextos (1999) “Effect of Foundation Type and Compliance on Seismic Response on RC Bridges”. Journal of bridge engineering, Vol.6, No.2, March 2001.

24. Kulhawy. (2002) “Observations on Some Shortcomings in Foundation Analysis and Design”. Deep Foundations 2002 (GSP 116), pp.1-5.

25. Kulhawy, Cushing.(2002) “Drained Elastic Behavior of Drilled Shafts in Cohesionless Soils”. Deep Foundations 2002: An International Perspective on Theory, Design, Construction pp. 22-36

26. Kulhawy, Agaiby, Trautmann (1996) "On large scale model testing of laterally loaded drilled shafts in sand " Geotechnical Testing Journal , vol.v19., no.n1., pp.pp32-40.

27. Kulhawy, F. H. (1991). “Drilled shaft foundations , Foundation engineering handbook”.

28. Kumar, Kort, Hosin, and Chong (2004) “Lateral Load Tests on Small Diameter Drilled Piers”

29. Kumar, Alizadeh (2002). “Lateral Load-Deflection Response of Single Piles in Sand”.

30. Kort, Kumar, Hosin, Ng (2002) "Lateral Load Tests on Small Diameter Drilled Piers".

31. Lin,Yang, Juang, Lee (2000). "Analysis of Laterally Loaded Piles in a Two-Layered Elastic Medium".

32. Lee, Kane, Bennett, Drumm (1989) "Investigation and Modeling of Soil-Structure Interface Properties"

33. Lee (1991) "Discrete Layer Analysis of Laterally Loaded Piles".

34. Long, Reese (1984). "Testing and Analysis of Two Offshore Drilled Shafts Subjected to Lateral Loads". Laterally loaded deep foundations: Analysis and performance, STP 835 pp. 215-228

35. Luna, Jadi (1998) "Determination of Dynamic Soil Properties Using Geophysical Methods".

36. Macklin, Nelson, Chou (1993) "A Lateral Load Test on Seven Foot Diameter Caissons".

37. Maharaj (1997)"Load-Deflection Response of Laterally LoadedSingle Pile by Nonlinear Finite Element Analysis".

38. Matlock, Reese, (1960). Generalized Solutions for laterally Loaded Piles, Journal of the Soil Mechanics and Foundations Division, ASCE, Vol.86, No SM5, Proc.Paper 2626, pp.63-91

39. Motan, Gabr. (1989) "A Flat-Dilatometer Study of Lateral Soil Response."

40. Neate (1983) "Augered Cast in Place Piles".

41. Neely (1979) "Bearing pressure-SPT Correlations for Expanded Base Piles in Sand".

42. Olson, Clifford, Wright (1983) "Nondestructive Testing of Deep Foundation with Sonic Methods".

43. Petek, Felice, Holtz. "Capacity Analysis of Drilled Shafts with Defects".

44. Pise, P. J. (1983), Lateral Response of Free-Head Pile, Journal of Geotechnical Engineering, ASCE, Vol. 109, No.8 pp. 1126-1131.

45. Popov (1998) "Engineering Mechanics of Solids 2nd Edition" Prentice Hall Publishing.

46. Prakash, Sharma (1990) "Pile Foundations in Engineering Practice". John Wiley and Sons Inc.

47. Puppala, Moalim (1986) "Evaluation of Driven Pile Load Capacity Using CPT Based LCPC and European Interpretation Methods".

48. Pyle, R. and Beikae, M. (1984). “A New Solution for the Resistance of Single Piles to Lateral Loading” Laterally Loaded Deep Foundations: Analysis and Performance, STP 835 835 pp. 3-20

49. Reese, Wright, Aurora (1984). “Analysis of a Pile Group Under Lateral Loading”. Laterally loaded deep foundations: Analysis and performance, STP 835 pp. 56-71

50. Reese, L.C., and Matlock, H., (1956). “Non-Dimensional Solutions for Laterally Loaded Piles with Soil Modulus Assumed Proportional to Depth”, Proceedings, Eighth Texas Conference on Soil Mechanics and Foundation Engineering,

51. Roberston, Hughes (1984). “Design of Laterally Loaded Displacement Piles Using a Driven Pressuremeter”. Laterally loaded deep foundations: Analysis and performance, STP 835 pp. 229-238

52. Sogge (1984). “Microcomputer Analysis of Laterally Loaded Piles”. Laterally Loaded Deep Foundations: Analysis and Performance, STP 835 pp. 35-48.

53. Smith, T.D., (1989) "Fact or Friction: A Review of Soil Response to a Laterally Moving Pile", Proceedings of the Foundation Engineering Congress, Northwestern University, Evanston, Illinois, pp. 588-598

54. Smith, T.D., Slyh, R. (1986) "Side Friction Mobilization Rates for Laterally Loaded Piles from the Pressuremeter, “ Proceedings of the Second International Symposium, The Pressuremeter and its Marine Application”, Texas A&M, May ASTM STP 950, pp. 478-491

55. Taciroglu, Rha, Stewart, Wallace, (1999). “Robust Numerical Models for Cyclic Response of Columns Embedded in Soil”.

56. Vennalaganti, Endley, Rao (1992) “Lateral Loads on Long piles and piers in granular soils”.

57. Wang, Rinne (1999) “Pile Foundation Construction Practice in Stiff Clays with Dense Granular Layers”.

58. Woodward, Gardner, Greer. (1972) “Drilled Pier Foundations” McGraw Hill Publishing

59. Zhang, Tulla, Grismala (1977) “Ultimate Resistance of Laterally Loaded Piles in Cohesionless Soils”.

60. Zafir (1986) “Seismic Foundation Stiffness for Bridges”.